STARCH HYDROLASE INHIBITORS FROM TROPICAL BOTANICALS: METHODOLOGY, HIGH THROUGHPUT SCREENING, AND SYNERGY

WONG IK CHIAN

NATIONAL UNIVERSITY OF SINGAPORE

2014

Thesis declaration

I hereby declare that this thesis is my original work and it has been written by me in its entirety, under the supervision of Associate Professor Huang Dejian (in the laboratory S13-05-02) at Food Science and Technology Programme, C/O Chemistry Department, National University of Singapore between August 2010 and July 2014.

I have duly acknowledged all the sources of information which have been used in this thesis.

This thesis has also not been submitted for any degree in any university previously.

The content of the thesis has been partly published in:

1. Wong, A.I.C., Huang, D.J. Chapter 38: Tea and starch digestibility. Tea in Health and Disease, edited by Victor R. Preedy, Academic Press, 2013, pages 457-467.

2. Wong, A.I.C., Huang, D.J. Assessment of the degree of interference from polyphenolic compounds on glucose oxidase/peroxidase assay, *Journal of Agricultural and Food Chemistry*, Vol. 62 (20), pp. 4571-4576.

Name	Signature	Date

Acknowledgements

First and foremost, I would like to express my utmost gratitude to my supervisor A/P Huang Dejian for his valuable guidance, advice, support and encouragement throughout my entire PhD research work. I feel extremely blessed to be a part of his team and to be able to learn from his profound knowledge and expertise. He is a constant source of encouragement and motivation to me, and I am deeply grateful for his kindness and patience in seeing me through the completion of my research project and thesis.

I would like to express my sincere thanks to all the FST staff for their excellent technical support, advice and help throughout the project. Also, I would like to extend my appreciation towards all my former and current fellow lab mates for their advice, technical assistance and moral support rendered throughout the project. My special thanks to Dr Zhang Dawei and Mr Yip Yew Mun for their help with the molecular docking studies.

I wish to acknowledge and thank the Singapore International Graduate Award (SINGA) for financial support of my research project.

My deepest love and appreciation also goes to my beloved parents and family members for their continuous moral and prayer support all these years. I thank all my friends for their helping hand and friendship, which has made everything more interesting and colourful.

Above all, I thank God for His constant guidance and grace.

Table of contents

Chapter 2 Evaluation of the *p*-nitrophenyl α-D-glucopyranoside assay

Chapter 3 Assessment of the degree of interference from polyphenolic compounds on glucose oxidase/peroxidase assay

Chapter 4 Screening of medicinal plants from Singapore Botanic Gardens for starch hydrolase inhibitors

Chapter 5 Characterization of proanthocyanidins from torch ginger flower (*Etlingera elatior)* as strong starch hydrolase inhibitors

Summary

The number of diabetes cases are on the rise worldwide. To address this issue, various high-throughput screening (HTS) assays (e.g. *p*-nitrophenyl-α-D-glucopyranoside (*p*NPG) and glucose oxidase/peroxidase (GOP) assays) have been applied but not properly evaluated in their application to the screening of starch hydrolase inhibitors in botanicals.

The *p*NPG assay uses a synthetic substrate, contrary to the GOP assay, which applies the natural substrate maltose. The impact of substrates on inhibitor potency was assessed by determining the K_i and K_i' of acarbose and 1-Deoxynojirimycin (1-DNJ). Application of *p*NPG resulted in consistently higher K_i for both inhibitors compared to maltose. Larger K_i translates to larger IC_{50} (i.e. lower potency). The mode of inhibition, however, remained the same despite the change in substrate. The importance of applying natural substrates is warranted in order for the results to be representative and applicable.

The GOP assay was developed initially to quantitate the amount of D-glucose in human fluids but its application has since been expanded to screen for starch hydrolase inhibitors in botanicals. It was illustrated that the majority of polyphenolic compounds found within the plant kingdom caused significant interference to the GOP assay, which makes it not useful in measuring the α-glucosidase inhibition activity of botanical extracts. More specifically, compounds which possess many hydroxyl groups, particularly in the *ortho* position of the B-ring in flavonoids, tend to produce higher interference.

Medicinal plants are biochemically diverse and provide an important resource for plant-based medicinal therapy. However, an estimation of less than 10 % of these plant species has been investigated chemically. As such, the WHO recommended (in a 1991 report on diabetes) that intensive research on the beneficial effects of medicinal plants be performed. In line with this, collaborative work with the Singapore Botanic Gardens (healing garden) was carried out to screen a total of 298 medicinal plants for α-amylase and α-glucosidase inhibition activity. This screening lays the groundwork for future in-depth studies of isolation and characterization of inhibitors. A further step was taken to apply assay-guided fractionation and separation of polyphenolic compounds from the ginger flower (*Etlingera elatior*). Results indicate that potent α-amylase inhibitory activity of *E. elatior* extract was largely attributed to the presence of proanthocyanidins (PAC). It is possible that other inhibitors besides PAC are present in the aqueous phase.

Finally, a study was done on the synergistic effects of epigallocatechin gallate (EGCG) with acarbose and dracoflavan B (DFB) with the rationale of enhancing the effectiveness of conventional drugs through the use of commonly consumed foods like tea. Acarbose and DFB was shown to be able to work together synergistically with EGCG to inhibit α-amylase through "bliss independence" mechanism. The extent of synergy is dependent on the amount of EGCG in the system. This study provides new insight into the use of naturally occurring enzyme inhibitors in foods rich in EGCG (eg. green tea) as a supplement to aid in the treatment of diabetes.

List of tables

List of Figures

List of Abbreviations

AE	Acarbose equivalents
BDE	Bond dissociation enthalpy
CE	Capillary electrophoresis
CI	Combination index
CNP	2-chloro-4-nitrophenyl
DFB	Dracoflavan B
DMAC	4-dimethylaminocinnamaldehyde
1-DNJ	1-Deoxynojirinycin
DNSA	3, 5-Dinitrosalicylic acid
DPPH	2, 2-Diphenyl-1-picrylhydrazyl
EGCG	Epigallocatechin gallate
GAE	Gallic acid equivalents
Gal-G2-α-CNP	2-Chloro-4-nitrophenyl-4-O-β-D-galactopyranosyl-maltoside
GOP	Glucose oxidase/peroxidase
HTS	High-throughput screening
K_i	Inhibitor constant
MD	Molecular dynamics
MGAM	Maltase-glucoamylase complex
ntMGAM	N-terminal glycoside hydrolase maltase-glucoamylase
PAC	Proanthocyanidin
PAE	Proanthocyanidin equivalent
***p*NPG**	*p*-nitrophenyl α-D-glucopyranoside
PPHG	Postprandial hyperglycemia
SBS	Secondary binding site

SDS	Sodium dodecyl sulfate
SD	Standard deviation
SGLT1	Sodium-dependent glucose transporter
T2D	Type II diabetes
TCM	Traditional Chinese Medicine
TPC	Total Phenolic Content
WHO	World Health Organization

List of Publications and Presentations

Publications

1. Wong, A.I.C., Huang, D.J. Chapter 38: Tea and starch digestibility. Tea in Health and Disease, edited by Victor R. Preedy, Academic Press, 2013, pages 457-467.

2. Wong, A.I.C., Huang, D.J. Assessment of the degree of interference from polyphenolic compounds on glucose oxidase/peroxidase assay, *Journal of Agricultural and Food Chemistry*, 2014, Vol. 62 (20), pp. 4571-4576.

3. Wong, A.I.C., Mun, Y.Y., Sun, S., Zhang, D.W., Huang, D.J. Synergistic effect of Dracoflavan B and Acarbose with Epigallocatechin gallate on the inhibition of α-amylase. Manuscript in preparation.

4. Wong, A.I.C., Huang, D.J. Characterization of proanthocyanidins from Torch ginger flower (*Etlingera elatior*) as strong starch hydrolase inhibitors. Manuscript in preparation.

5. Wong, A.I.C., Huang, D.J. Screening of edible plants from Singapore Botanic Gardens for starch hydrolase inhibitors. Manuscript in preparation.

Presentations

1. Wong, A.I.C., Huang, D.J. Comparative study on α-glucosidase inhibition kinetics using synthetic and natural substrates, poster presentation, International Conference on Food Science and Nutrition (ICFSN) 2012, Sabah, Malaysia.

2. Wong, A.I.C., Huang, D.J. Assessment of the degree of interference from polyphenolic compounds on glucose oxidase/peroxidase assay, oral presentation, 5th Joint Symposium on Food Science and Technology between NUS and TUMSAT, 2012, Tokyo, Japan.

3. Wong, A.I.C., Huang, D.J. Screening of botanicals from Singapore Botanic Gardens for α-amylase and α-glucosidase inhibitors, oral presentation, 6th Joint symposium on Food Science and Technology between NUS and TUMSAT, 2013, Singapore.

4. Wong, A.I.C., Mun, Y.Y., Sun, S., Zhang, D.W., Huang, D.J. Synergistic effect of dracoflavan B and acarbose with epigallocatechin gallate on the inhibition of α-amylase, oral presentation, NUS Food Science and Technology Programme Lunchtime Seminar, 2014, Singapore.

Chapter 1

Literature review

1.1 Introduction

Diabetes is a progressive metabolic disorder of multiple etiologies characterized by an increase in blood glucose level, due to the disruption of the homeostasis of carbohydrate metabolism that results from defects in insulin secretion, insulin action, or both (*1*). The majority of diabetes cases fall into either of two broad etiopathogenetic categories: type I or type II diabetes (T2D). In type I diabetes, the patient has an absolute deficiency of insulin secretion, which is due primarily to the destruction of pancreatic islet β-cells, which are needed to produce insulin. This type of diabetes is linked to an autoimmune pathological process that occurs in the pancreatic islets and by genetic markers (*2*). In the other category, T2D, also being much more prevalent, is caused by a combination of insulin resistance as well as an inadequate compensatory insulin secretory response. Insulin resistance occurs when the beta cells are able to produce insulin but the body is unable to use it effectively due to a resistance of the body to the action of insulin (*2*).

Due to a defect in the production of insulin in diabetic patients, the degradation of starch by starch hydrolases proceeds rapidly and leads to elevated postprandial hyperglycaemia (PPHG), which is a key risk factor of the disease. The high blood glucose level in diabetic patients can lead to complications that include coronary heart disease, stroke, peripheral arterial disease, nephropathy, retinopathy, and possibly neuropathy and

cardiomyopathy (*3*). Since an increase in PPHG has been shown to correlate with the activity of human pancreatic α-amylase (*4*), the inhibition of intestinal α-glucosidase can retard the rate of carbohydrate digestion, thereby reducing PPHG. This also buys time for the beta cells to secrete more insulin and reduce glucose levels in the circulatory system (*5*).

The World Health Organization (WHO) suggests that the world is in a midst of a diabetes epidemic, and estimated that this disorder affects some 100 million people worldwide (*6, 7*). Furthermore, this number is predicted to reach 336 million people by year 2030, where people from South East Asia and the Western Pacific are considered most at risk (*8*). A serious and relevant problem caused by diabetes is its cost on society, which is estimated to be 5-10% of national health budgets, and this excludes additional costs of cardiovascular diseases, blindness, amputations and kidney failure that can be attributed to diabetes (*9, 10*). In view of this, there is an inherent need for a cure or a preventative control for hyperglycaemia, the main concern of diabetic patients. Numerous researches has been invested into this area of need but despite extensive diabetes research, there is a lack of effective and safe means in controlling PPHG through food consumption. An interesting concept to explore would be the use of everyday foods to control PPHG. In line with this, tea is a suitable candidate to fulfil this role, since, in most cultures, it is regularly consumed, and has been linked to health-promoting effects like anti-diabetes in epidemiological studies (*11*).

1.2 Anti-diabetic effects of tea catechins

Tea (*Camelia sinensis)* is believed to be the most widely consumed beverage in the world, as it has often been associated with longevity and the prevention of many diseases (*12-17*). Much interest has been generated in its potential health benefits, as animal models and *in vitro* studies have demonstrated its anti-oxidant, anti-mutagenic, anti-carcinogenic and anti-hypertensive properties (*18-21*). Teas may be largely categorized by its degree of fermentation: non-fermented (green tea), semi-fermented (oolong tea) and fermented (black tea), each giving very different chemical profiles. For example, the chemical composition of green tea is quite complex, comprising polysaccharides, polyphenols, amino acids and alkaloids. However, its health benefiting properties have been largely attributed to its rich catechin contents, which are comprised of (-)-catechin, (-)-epicatechin, (-)-gallocatechin, (-)-epicatechin gallate, (-)-epigallocatechin, (-)-gallocatechin and (-)-epigallocatechin gallate (EGCG) **(Figure 1)**. Among these catechins, EGCG is most abundant in green tea, and is thought to be a major contributor to the health benefits ascribed to tea.

Contrary to the findings of the potential health-benefiting properties of tea in human clinical trials, epidemiological studies on the effects of tea consumption on cancer and cardiovascular diseases have not been consistent (*22*). Nonetheless, epidemiological studies are complex and the inconsistencies among them could be attributed to many factors such as subject selection, test material, dietary substrate, intervention regimen and measurements (*22*).

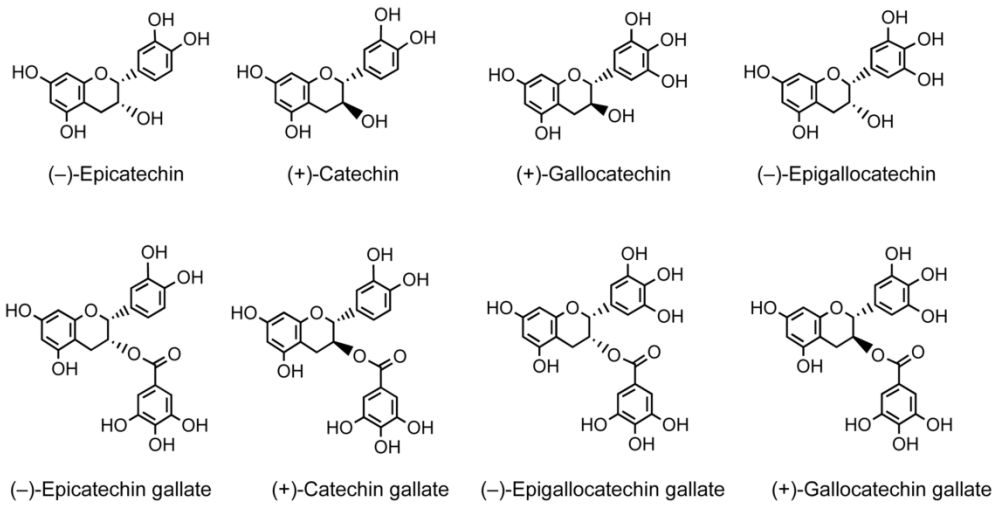

Figure 1. Chemical structures of green tea flavan-3-ols (Adapted from Stalmach et. al. 2009) (*23*).

In addition, it is also possible that these inconsistencies stem from the fact that the actual mechanisms of the anti-diabetic properties of tea could be highly complex, and due to potential multiple-action pathways and roles of different constituents in tea. Taking EGCG as an example, various studies showed the anti-diabetic effects of EGCG alone influences cellular interactions via different pathways and some of the proposed mechanisms are listed below and summarized in **Figure 2**.

a. Lowering appetite

An *in vivo* study demonstrated that when EGCG was injected into the intraperitoneum of mice, it resulted in a decrease in food intake, which may be related to changes in its appetite (*24*).

b. Increasing protection of diabetes-related cells

Due to its high antioxidant activity, EGCG is able to alter the redox status in many cells, and thus, give a protective effect on these cells (e.g. liver, β-pancreatic, nerve cells) from oxidative stress. For example, *in vitro* EGCG

treatment was shown to reduce the production of destructive nitric oxide, which in turn protects against interleukin-1 β and interferon γ cytotoxicity in RINm5F insulinoma cells (a pancreatic β-cell) (*25*).

c. Enhancing insulin sensitivity / Increasing insulin-like activity

In vitro, EGCG enhanced insulin sensitivity by inducing a greater insulin activity, 17-fold, using epididymal fat cell assay compared to the control (*26*). This was consistent with *in vivo* studies where 0.5 g of lyophilized green tea powder dissolved in 100 mL of deionized distilled water was able to stimulate insulin (1 nM)-induced glucose uptake by rat adipocytes (*27, 28*).

d. Enzyme inhibition

Green tea catechins have been shown to regulate the activity and/or expression of enzymes and proteins that are related to carbohydrate digestion, absorption, transport, synthesis and metabolism. For example, during dietary starch and sucrose digestion, tea catechins can inhibit intestinal glucose transporter type 2 and sodium-dependent glucose transporter (SGLT1), which is responsible for glucose uptake into cells (*29*). In addition, many *in vitro* studies have also demonstrated that tea catechins are able to inhibit starch hydrolases like α-amylase and α-glucosidase, which reduces the breakdown of complex carbohydrates to simple sugars and lengthens the digestion process, thereby modulating blood glucose levels (*30-34*). It is likely that the prime target of tea polyphenols (for its effects on glucose metabolism) is via this mechanism, since the gut lumen has the highest concentration of polyphenols, post-prandially, compared to any other site in the body (*35*).

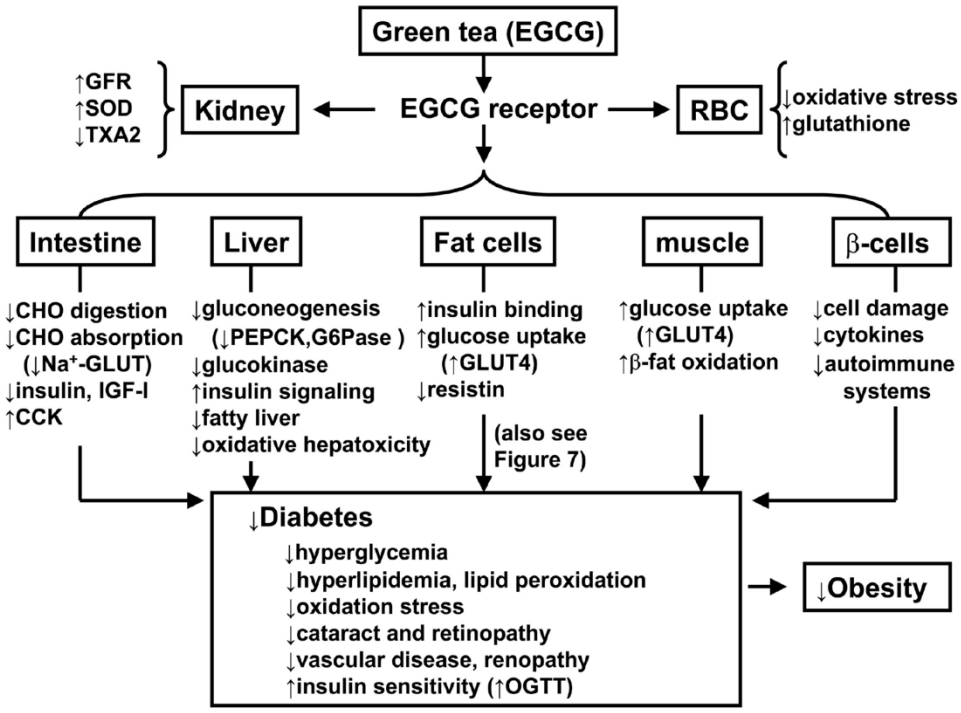

Figure 2. Proposed mechanisms of action of EGCG on diabetes prevention (Adapted from Kao et. al. 2006) (*36*).

1.3 Enzyme inhibition as a means for prevention of post-prandial hyperglycaemia.

In the digestive system, pancreatic enzymes like α-amylase and α-glucosidase are responsible for hydrolysing starch to maltose and finally to glucose.

Flavan-3-ols present in foods that are consumed pass through the oral cavity and are able to interact with salivary proteins that are rich in proline, forming polyphenol-protein complexes through hydrogen and hydrophobic interactions (*37*). However, due to the small amount of protein present within the oral cavity, the aggregates formed are not significant enough to alter the availabilities of polyphenolic compounds elsewhere in the body (*38*). In the stomach, polyphenolic compounds are then subjected to strong acidic conditions, which may influence its structural stability. Nonetheless,

experiments on catechins revealed that despite such a harsh acidic environment in the stomach, they are still stable (*39*). In the small intestine, flavan-3-ols are hydrolyzed by two active enzymes: lactase-phlorizin hydrolase and cytosolic β-glucosidase, which causes the sugar unit to be released and an aglycone formed. The lipophilicity of the released aglycone is able to enter epithelial cells via passive diffusion and polar glycosides are transferred into enterocytes via an active SGLT1 (*40*). Besides glycosylation, polyphenols also undergo glucuronidation and methylation, which is mediated by enzymes belonging to the uridine diphosphate glucutonosyltransferase and catechol-*O*-methyltransferases respectively (*41, 42*). The body transfers the polyphenolic compounds via the portal vein to the liver where main coupling reactions like sulfation, methylation and glucuronidation takes place. These coupling reactions facilitate their elimination in the bile and urine by increased solubility of the metabolites. In addition, phenolic compounds may also undergo oxidation, reduction, hydrolysis and hydration reactions which are catalyzed by phase 1 enzymes (*43*).

Despite the biochemical reactions that take place in the prior sections, the main site for polyphenol absorption occurs in the large intestine, where colonic microflora play a major role in the catabolism of these compounds. It was found that polyphenol concentrations in the gastrointestinal tract exceeded 1 mM (and possibly even higher) if the compounds are being administered in polymeric capsules that can be hydrolyzed by bacterial glycosidases (*44, 45*).

Hence, this highlights the importance of starch hydrolase inhibitors as a promising and potential solution to the prevention of hyperglycaemia since polyphenolic compounds are largely present within the gastrointestinal tract

where main starch hydrolases are present. Furthermore, this mechanism does not require the active compounds to be absorbed into the blood stream and pass through modifications by liver enzymes (*46*). In fact, some existing conventional pharmacological treatments for the control of T2D (like acarbose) act through this mode of action, but they are not without their limitations. Acarbose, a known α-glucosidase inhibitor, produces undesirable gastrointestinal side effects like diarrhoea, flatulence and abdominal pain when ingested, making it unpopular as an anti-diabetic drug (*47*).

The reason behind these side effects was suggested to be because of their non-specificity in targeting different glycosidases, resulting in abnormal bacterial fermentation of undigested carbohydrates in the colon (*48*). Therefore, this opens up a need to discover more specific and effective enzyme inhibitors, which continues to be an important area of investigation. Those inhibitors that can be found in foods (such as fruits and vegetables) and botanicals are of particular interest, because they are non-toxic and suitable for application as ingredients in starchy foods, having less regulatory concerns. It would be ideal to control hyperglycaemia through the development of functional foods or beverages that can slow down the speed of carbohydrate digestion and absorption.

1.4 High-throughput screening (HTS), a strategy to identify enzyme inhibitors

In the quest to identify promising leads on starch hydrolase inhibitors derived from natural sources, the use of HTS methods are typically applied. HTS has become an important and integral strategy in the path of drug

discovery. Some of the factors which contribute to good HTS methods are: automation, cost-effectiveness, and the use of substrates and enzymes that are physiologically relevant. Firstly, automation is important because it provides speed, repeatability and robustness. Secondly, the consideration of cost is vital, as the quantity of runs is expected to be high, in order to be able to find a good lead. Finally, the substrates and enzymes utilized in the assay should be natural and physiologically representative, and they should not interfere with the signal or response. Furthermore, it is vital that these assays would be validated and optimized so that it maintains fidelity to the chemical interactions occurring in the human body.

Within the literature, the reported inhibition potencies (i.e. IC_{50}) of pure compounds (e.g. EGCG and acarbose) against starch hydrolases were extremely scattered amongst different research groups **(Appendix 1)**. This may have been attributed in part to the choice of enzymes used from different origins. For instance, α-glucosidases have been isolated and purified from a variety of sources ranging from plants (*49*), bacteria (*50*), yeast (*51*), fungi (*52*) to animal origins (*53*). On the basis of the differences which exist in its primary structure, α-glucosidase may be largely divided into types I (e.g. baker's yeast) and II (e.g. mammals).

Acarbose, a frequently used positive control in inhibition studies, was shown to have varying IC_{50} values between different studies, which may be linked to the type of enzymes used. For example, several studies from different research groups utilized the 4-nitrophenyl α-D-glucopyranoside (*p*NPG) assay with yeast α-glucosidase (*54-57*), and their results gave IC_{50} values that were in the same order of magnitude, but varied significantly at

141, 242, 217, and 907.5 µM respectively. There was an exception, however: Choi *et. al.* 2010 (*58*) utilized the same *p*NPG assay with yeast α-glucosidase as its enzyme source, but their results gave a very deviant IC_{50} value (9110 µM) as compared to the other four studies.

In contrast, when rat intestinal α-glucosidase was used in the *p*NPG assay, it was observed that the IC_{50} of acarbose was lower by one or two orders of magnitude as compared to the IC_{50} values of *p*NPG assays with yeast α-glucosidase. For example, researches (*59, 60*) that utilized rat intestinal α-glucosidase in the *p*NPG assay reported lower IC_{50} values (0.18 and 63 µM, respectively). The use of bacterial (*61*), pig and rabbit (*60*) intestinal α-glucosidase also gave lower IC_{50} values of 3.25, 87 and 62 µM respectively, as compared to that of yeast α-glucosidase. Similarly, it was also shown that the inhibitory effect of various inhibitors against α-glucosidases from different origins gave varied results. For example, acarbose was shown to strongly inhibit mammalian α-glucosidases but no inhibition was observed in yeast α-glucosidases (*60*).

From these results, it is shown that the magnitude of α-glucosidase inhibition is greatly affected by its origin and that the selection of enzymes utilized is vital. It is thus essential to use α-glucosidases of animal origin, since it mirrors more closely the enzymes found in humans (*60*).

1.5 Structural features of human starch hydrolases

1.5.1 Structure of human maltase-glucoamylase (MGAM)

The MGAM (EC 3.2.1.20) is an enzyme that is localized in the brush border of the small intestine and belongs to glycoside hydrolase family 31. It

is composed of peptides with 1857 amino acids (molecular mass 209,702 Da) and contains five distinct domains: (a), a small cytosolic domain consisting of 26 amino acids; (b), a transmembrane domain of about 20 amino acids; (c), *o*-glycosylated linker of about 55 amino acids and two homologous catalytic domains each consisting of about 900 amino acids. The two catalytic subunits comprise an N-terminal subunit that is proximal to the membrane bound end and a C-terminal **(Figure 3)** (*62*).

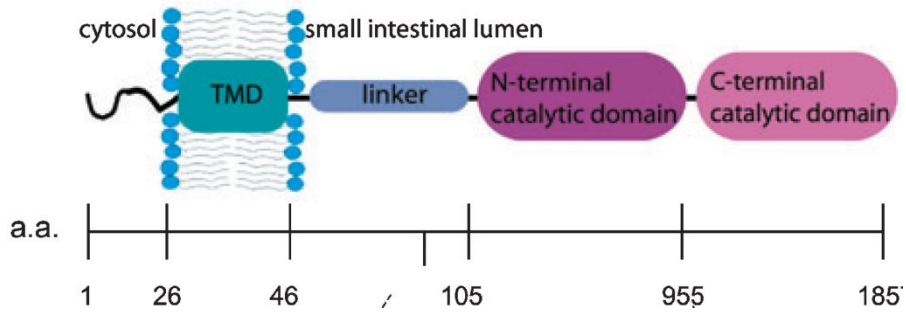

Figure 3. MGAM protein organization (Adapted from Rossi et. al. 2006) (*63*).

MGAM is an exoenzyme which catalyzes the release of glucose from the reducing ends of starch and hydrolyzes the α-(1, 6) glycosidic linkages (*64*). Its mechanism of bond cleavage is mediated by two catalytic carboxylic acid residues, and is proposed to proceed through a positively charged oxocarbenium-ion transition-state mechanism. In this mechanism, the function of the carboxylate group is proposed to promote the formation of the oxacarbenium ion and stabilize intermediates, whereas the carboxyl group attaches the oxygen of glucosidic linkage. Hence, they cooperatively undergo nucleophilic displacement, of the hydroxyl ion of water to the oxocarbenium ion, to finish the reaction (*65*).

There are high similarities between the amino acid sequences within MGAM family II and in particular, the catalytic amino acid residues are found to be conserved in all MGAMs. For example, some of the sources of MGAM family II, like those from human, rabbit and rat intestinal sources, are shown to only have regions 2 and 5 in their catalytic sites, with highly similar amino acid sequences (in contrast to MGAM family I, which has four conservative regions: 1, 2, 3, 4) (*64*). In addition, MGAM contains a catalytic site made up of amino acid sequence tryptophan-X-aspartate-methionine-asparagine-glutamate (WXDMNE), where X is the variable amino acid, and this sequence is found to be similar amongst MGAM family 31, which includes human, rabbit, rat, sugar beet, and barley sources (*66*).

1.5.2 Structure of α-amylase

α-amylase (α-1, 4 glucan-4-glucanohydrolase, EC 3.2.1.1) is an endoglycosidase and a member of glycosyl-hydrolase family 13, which is responsible for catalyzing the hydrolysis of α-(1, 4) glycosidic linkages of starch, while bypassing the α-(1-6) linkages of amylopectin components (*67*). Linear maltose oligosaccharides as well as branched isomaltose oligosaccharides are generated as a result of the α-amylase hydrolysis of starch. There are two types of isoenzymes for porcine pancreatic α-amylases (PPA): I and II (*68*). Although the two isoenzymes have slightly different amino acid compositions and isoelectric points, the overall conformations of their structural proteins are almost identical (*69*). X-ray crystallographic studies show that the PPA is made up of 496 amino acids on a single polypeptide chain. It is composed of three domains: Domain A, the largest

catalytic domain with a $(\beta/\alpha)_8$ barrel structure; Domain B, α-helix in structure with no definite topology; Domain C, with a Greek key motif (protein structure that consists of four adjacent antiparallel strands and their linking loops) (*70*). There are two secondary binding sites (SBS) present on the α-amylase – the first is located at the interface between domains A and C of the free enzyme (*70*) and the other is located close to the calcium binding site (*71*).

α-amylases are present in a range of different sources, for example fungus, plants and mammals, and there are significant structural differences amongst different species (*72*). On the contrary, the molecular structures of mammalian sources (eg. humans and porcines) were shown to be very similar. For example, studies on molecular models for the α-amylases from human pancreas (*73*) were described as being highly similar to that of the porcine pancreas (*74*). In addition, a comparison of the pancreatic and salivary α-amylases of humans and rats revealed that the corresponding cDNA nucleotide sequences were highly homologous (*75*).

1.6 Artificial vs. natural substrates

When measuring the enzyme inhibition activity, the substrates used would ideally be native or natural, and be physiologically relevant. Yet, artificial substrates are still often used as a substitute for natural ones due to its convenience in measuring enzyme kinetics. However, the artificial substrates do not always accurately mimic the structure and property of the native substrate (such as those found in foods like starch and maltose) and may be a contributing factor leading to false conclusions.

This is because the structural motif and binding sites, as well as the affinity of various substrates to the enzymes, vary considerably from one another; in addition, the substrate's specificity and susceptibility to inhibitors may also vary significantly and therefore affect kinetic parameters like the Michaelis constant (K_m), catalytic rate of an enzyme (k_{cat}), and inhibitor constant (K_i) (*76*). For example, the N-terminal of glycoside hydrolase maltase-glucoamylase (ntMGAM) was shown to display a clear preference for maltose substrates compared to *p*NPG, with a k_{cat}/K_m value of 26 ± 8 $s^{-1}mM^{-1}$ versus 1.4 ± 0.1 $s^{-1}mM^{-1}$ respectively (*77*). In addition, it was also demonstrated that the use of different substrates (maltose, maltotriose, maltotetraose and maltoheptaose) impact the K_i for glucoamylase-maltase with 1-Deoxynojirimycin (1-DNJ) and acarbose. Their results showed that when maltose was used as the substrate, the K_i values of 1-DNJ (0.76 μM) and of acarbose (0.84 μM) were about 100 times higher than the corresponding values for hydrolysis as compared to when maltooligosaccharides were used (*77, 78*).

In addition, the use of synthetic substrates over natural ones would also affect the pH optima of the enzymes. A change in pH will most likely affect the conformational structure of the enzyme, which will in turn affect the binding interaction of ligands (inhibitors or substrates) to the enzyme. It was shown that the pH optima of α- and β-amylases was higher with synthetic, as opposed to natural, substrates (*79*).

In another study, the effect of the nature and concentration of the substrate on β-glucosidase activity value was determined. A natural substrate,

cellobiose, and synthetic substrates, salicin and β-nitrophenyl-β-D-glucoside, were used to measure β-glucosidase activity. It was found that significant variations in values were observed, and it was cautioned that the use of synthetic substrates should not be assumed to be representative of an organism's ability to hydrolyze natural substrates (*80*). Furthermore, another study of enzyme analysis for Pompe disease in leucocytes also noted that the use of artificial substrate (4-methylumbelliferyl-α-D-glucoside) is a poor alternative to the use of natural substrate (glycogen), as it insufficiently distinguishes between affected and unaffected individuals (*81*). Taken together, the evidence demonstrates that the use of most synthetic substrates rather than natural ones may generate misleading results, and not be reflective of the biochemical reactions occurring in the body. Hence, proper validation must be first administered when using synthetic substrates in assays, and the results should be interpreted with care.

1.7 Assays for determining starch hydrolase activity

1.7.1 Assays to determine α-amylase activity

One of the popular methods for determining hydrolase activity is based on the analysis of reducing sugars formed as a result of glycosidic bond cleavage between two carbohydrates, or between a carbohydrate and a non-carbohydrate moiety. Reducing sugars are sugars with an aldehyde group that can act as a reducing agent. Under alkaline conditions, ketoses may behave as weak reducing sugars as they are able to isomerise to aldoses. The following details several colourimetric methods used to measure reducing sugars. The more popular methods are the 3, 5-dinitrosalicylic acid (DNSA) assay and the

Nelson-Somogyi assay. The lesser used colourisation reaction is the mixture of two reagents, sodium 2, 2'-bicinchoninate and *p*-hydroxybenzoic acid hydrazide or potassium ferricyanide.

a. 3,5-Dinitrosalicylic acid assay (*82*)

The DNSA assay oxidises reducing sugars with its nitro group, at alkaline conditions and high temperatures (100 ºC), to form 3-amino-5-nitrosalicylic acid, which has a characteristic absorption wavelength at 540 nm **(Figure 4)**. The normal procedure for this assay to test for amylase inhibition is to first pre-incubate the inhibitor with the amylase at 37 ºC for 10 minutes. Starch (1.0 % w/v) is added to initiate the reaction, and an aliquot of the reaction mixture mixed with DNSA reagent and heated to 100 ºC for 5 minutes, to develop its colour, with the absorbance value read at 540 nm.

The DNSA assay was initially introduced as a method to detect reducing substances in urine and blood (*83*). Since its inception, the reagent has been improved by the addition of Rochelle salt (to reduce dissolved oxygen by increasing the ion concentration in the solution), addition of phenol (to increase colour intensity) and sodium bisulfite (to react with oxygen present and stabilize the reaction colour) (*84, 85*). Recently, its application has broadened as a screening tool for α-amylase inhibitors. Although a tedious method, it is also used as a tool to monitor the kinetics of different modes of inhibition (e.g., competitive, non-competitive or uncompetitive inhibition).

As with most colourimetric assays, the DNSA assay is also prone to some interference. For example, substances such as uric acid and polyphenols were reported to reduce DNSA in the presence of glucose (*83*). It was

proposed that the presence of phenols, in addition to the DNSA reagent, increases colour intensity during the colour development stage. Similarly, a reduction in the amino acid cysteine was also reported to interfere with the DNSA assay (*86*). In addition, since this technique requires high temperatures for the DNSA reagent and reducing sugars to develop colour, it is not convenient to conduct the assay directly onto the 96-well microtiter plate. To measure reaction kinetics, multiple samples need to be taken from the reaction mixture to carry out colour development with DNSA subsequently.

Therefore, this method is comparatively quite tedious and requires a relatively long time, especially when it is used for screening a large number of samples. In addition, its sensitivity seems to be easily affected by several factors. For example, the nature of the buffer that is used to dilute the enzyme has been shown to decrease the sensitivity of the DNSA assay; whereas the addition of metals like manganous sulphate, calcium nitrate, and cobalt nitrate increases its sensitivity (*87*). At low substrate concentrations, results obtained from the DNSA assay also reveal inaccuracies (*82, 88*). Several studies found that the DNSA assay consistently produced significantly higher values (about 40-50 % higher) of reducing sugars, than the actual number or compared to the results obtained from the DNSA assay, hence resulting in an overestimation of enzymatic activity (*88-90*). The magnitude of overestimation is dependent on the type of enzymes being tested, and the cause of the overestimation has been attributed to the instability of polysaccharides under the severe conditions of the assay, which involve high temperature and a strong alkaline medium (*89*). The harsh conditions cause the products of the enzyme to be decomposed by DNSA itself, thus releasing more reducing sugar.

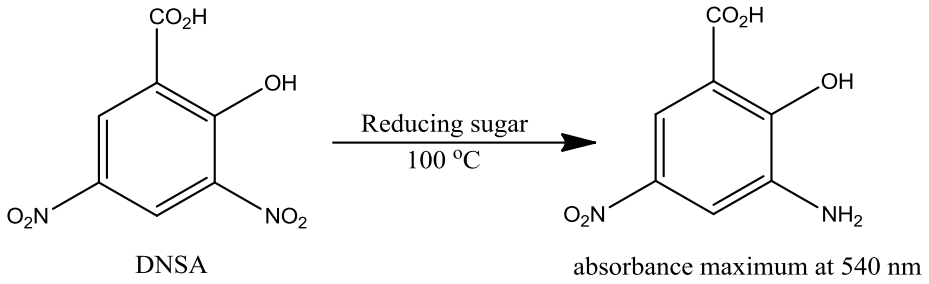

Figure 4. The DNSA assay for determining reducing sugar content (adapted from Wong and Huang, 2013) (*91*).

b. Nelson-Somogyi assay (*92, 93*)

The reducing sugar, when heated with alkaline copper tartrate, reduces the copper from cupric to cuprous oxide, which is treated with arsenomolybdic acid (Folin reagent) to develop intense molybdenum blue that can be monitored at 620 nm. Since this reaction is not stoichiometric, it has to be compared with a set of standard curves. Although the Nelson-Somogyi assay is deemed less convenient as compared to the DNSA assay, it has been reported to be approximately 10 times more sensitive than the DNSA assay (*88*).

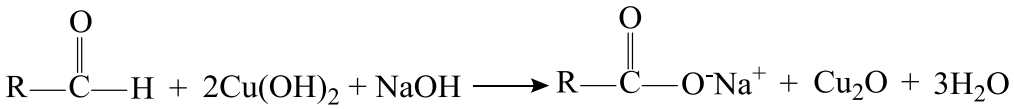

c. 2-Chloro-4-nitrophenyl-4-O-β-D-galactopyranosyl-maltoside (Gal-G2-α-CNP) (*94, 95*)

This method uses the synthetic substrate Gal-G2-α-CNP, which is exclusively cleaved by α-amylase at the aglycone bond, resulting in two products: β-D-galactopyranisylmaltose and 2-chloro-4-nitrophenol (CNP).

The release of CNP can be detected and quantified using absorbance changes at 402 nm.

This method is relatively simple in comparison to the DNSA or chromatographic methods. However, the downside of this technique is that the substrate is synthetic, and the interaction between enzyme and substrate may be very different as compared to natural ones. Further validation of this method is thus needed to remove this possibility.

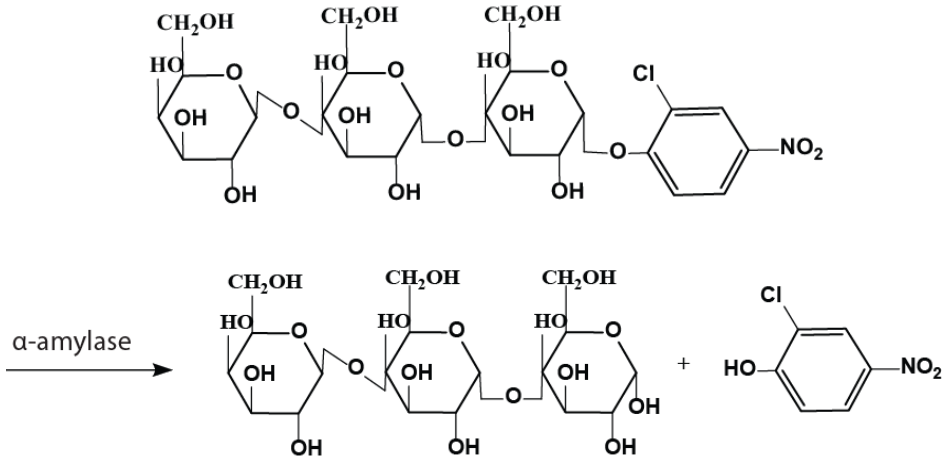

Figure 5. Structure of Gal-G2-α-CNP and its reaction with α-amylase.

d. Capillary electrophoresis (CE) (*96, 97*)

The CE technique has been used to study interactions between drugs and various proteins, including enzymes. There are two major types of methodologies for CE: (1) affinity CE and (2) incubation method (*96*). CE uses evidence of molecular interactions between components via the direct detection of a complex from an equilibrium mixture, where the formation of complexes will result in a peak in the chromatogram. In affinity CE, the ligand is incorporated into the running buffer at increasing concentrations, obtaining the chromatograms for the protein solution. The shift in the migration time of

the peak area is taken as evidence for a potential interaction between the ligand and enzyme. For the incubation method, the enzyme and the ligand are incubated in the solution, which is then subjected to electrophoresis. A strong and stable binding of the emergent ligand-protein complex will form a peak in the chromatogram (*97*).

However, this technique may not yet be widely accepted due to the high cost of the instrument, and in order to increase its sensitivity, laser fluorescence, which is technically demanding to set up, is needed. An additional difficulty of this method is that if the interacting molecules show large differences in their mobility, it would be hard to detect both free and bound species in the same electrophoretic run. This is especially so when the interacting molecules have opposite charges (*98*).

e. Iodine-starch colorimetric method (*99, 100*)

This method is based on the stainability of residual starch and its hydrolytic products after starch digestion. The maltodextrin products of amylolytic activity may not have equal complexing ability with iodine. That is, each sample possesses different maltodextrin compositions, which results in a variety of obtainable iodine stains before reaching its achromic point, which may be a source of misleading results. In addition, methods used within the literature *(89-91)* showed diverse iodine concentrations being applied, which range from 3 μM (*101*) to 0.25 mM (*102*), and the wavelength used to measure colour development varies from 550 nm (*102*) to 700 nm (*99*). Since iodine is a mild oxidant, it might be possible that some antioxidants in the sample may react with iodine and cause interference.

1.7.2 Assays to determine α-glucosidase activity

a. Glucose oxidase/peroxidase (GOP) method

The GOP uses glucose oxidase to catalyse the oxidation of α-D-glucose to gluconic acid, with the formation of hydrogen peroxide. The oxygen that peroxidase liberates from hydrogen peroxide reacts with chromophores (e.g. *o*-dianisidine) to produce products which can be measured using UV-VIS absorbance at specific wavelengths (e.g. 540 nm) **(Figure 6)**. The advantages of this assay are that the methodology is simple and low-cost, which allows it to be applied as a HTS method. Additionally, it also uses natural substrates like maltose and sucrose, and it is highly selective towards glucose. Conversely, the limitations of this assay include its susceptibility towards interference, especially from reducing substances like polyphenols. In particular, flavonoids with structural characteristics of the dihydroxyl groups in the *ortho* position in the B-ring were shown to cause strong interference within this assay (*103*). As such, this seriously hampers its applicability to screen through samples containing reductants (for example botanical extracts).

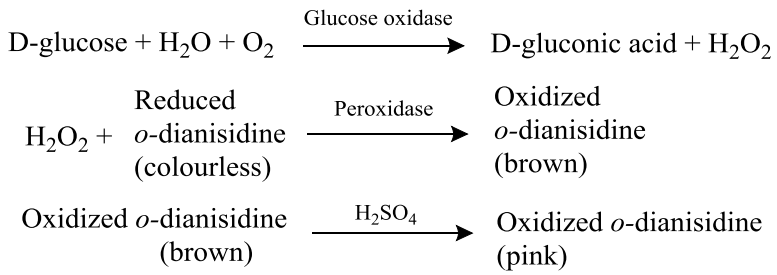

Figure 6. Reaction scheme of the GOP assay to determine α-glucosidase activity.

b. *p*-Nitrophenyl-α-D-glucopyranoside assay

In the human digestion tract, maltose is hydrolyzed by α-glucosidase to produce glucose as its product. However, because glucose cannot be detected by ultraviolet light directly, *p*NPG, a synthetic substrate, is frequently used instead of maltose to measure the activity of α-glucosidase. The substrate *p*NPG is cleaved by α-glucosidase at the α-(1, 4) linkage, which releases *p*-nitrophenol. Also, under basic conditions, *p*-nitrophenol dissociates to *p*-nitrophenolate, and this product can be measured at a UV-absorbance of 405 nm **(Figure 7)**. This method is only suitable for end point readings; it cannot be monitored in real time because the reaction mixture needs to be sampled and treated with a base to form the yellow *p*-nitrophenolate. In order to simplify the method for HTS application, the process was modified by removing the second step of alkalinisation. However, without the alkalisation step, the assay is much less sensitive (*104*). In addition, the short wavelength of this assay makes it prone to background interference from food matrices like black tea infusions that contain natural yellow pigments like flavonoids and carotenoids. In general, this method is useful in screening for enzyme inhibition.

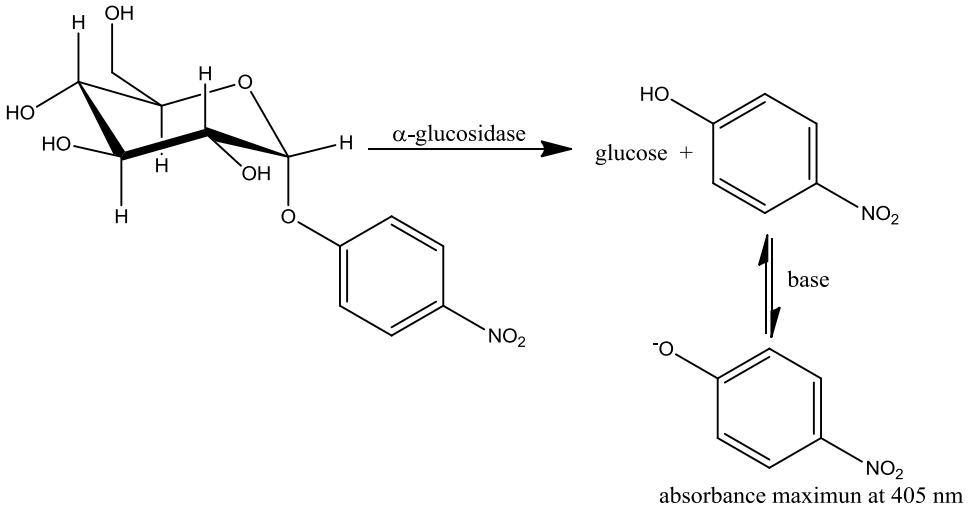

Figure 7. *p*NPG's α-(1,4) linkage cleaved by α-glucosidase to release *p*-nitrophenol and, under basic conditions, dissociates to *p*-nitrophenolate which can be measured at λ = 405 nm (adapted from Wong & Huang, 2013) (*91*).

1.7.3 Physical property-based methods to determine enzyme inhibition

a. Viscosity (*102*, *105*)

The viscometric assay is based on the decrease in the viscosity of starch solution during the enzymatic reaction, by determining the graph of the decrease in viscosity with time. This method is considered to be a sensitive technique which is suitable for monitoring α-amylase activity in a variety of fluids, due to its lack of interference with reducing sugar. A calibration curve is constructed in order to express enzyme activity in absolute terms or the number of catalytic events in unit time (IU). Its drawback is that it is too time-consuming to be used routinely.

b. Turbidity

The turbidity assay is based on the optical density of a sample fluid which arises from the interaction of light and insoluble particles. This physical parameter has been applied to monitor cell growth dynamics in

microbiological and yeast cell studies, by applying the UV-VIS spectrophotometer (*106, 107*). The insoluble particles in the samples will interfere with light transmittance, which relates to thier size, shape, composition of the particles and the wavelength of the incident light (*108*). The relationship between absorbance and transmittance is expressed through **Equation 1**:

$$A = -\mathrm{Log}_{10}{}^{[T]} \text{and } T = {}^{I}/_{I_O} \qquad \textbf{(Equation 1)}$$

where A: absorbance, T: transmission, I: light passing through the sample and I_o: light entering the sample.

This method has recently been adapted to a HTS format for starch hydrolase inhibitors, and can be applied to rapidly quantify food and botanical samples for inhibition (*109-113*). The advantages of applying this assay for enzyme inhibition is that starch, a natural substrate, is used instead of synthetic ones, which is more representative of the reactions taking place in the human body, and different types of enzymes (e.g.α-amylase and α-glucosidase) can be tested using the same assay.

1.8 Plant-based medicinal therapy

It was estimated that about two-thirds of the world's population rely on health care from sources other than conventional biomedicine (*114*). Moreover, the WHO also reported that 80 % of the population in the Asian region depends on traditional medicine as their primary health care (*6*). Complementary and alternative medicine, which includes the use of botanical and natural dietary supplements, have sparked public interest due to their

historicity, effectiveness, fewer side effects and lower cost (*115*). They refer to a broad range of healing philosophies, approaches and therapies outside conventional medicine that stem from different indigenous systems of medicine like ayurveda, kampo, native American medicine, traditional Chinese medicine (TCM), unani, traditional Hawaiian medicine and many others. TCM, for instance, is an ancient Chinese medicinal system which has existed since five thousand years ago. It uses the *Yin-Yang* theory to diagnose human diseases and many herbs were documented for use in disease treatment. In TCM, the etiology of diabetes mellitus is identified as having a lack of *qi*, toxin retention and blood stasis in the body (*115*). The search for drugs and botanical supplements derived from plants has intensified in recent years to search for possible "leads" for the treatment of diabetes. Screening for novel starch hydrolase inhibitors has been carried out in a variety of edible medicinal plants from different regions like China (*116*), India (*117, 118*), the Mediterranean region (*119*), Brazil (*120*), Jordan (*121*), Malaysia (*122, 123*), Nepal (*61, 124*) and South Africa (*125*).

A large proportion of the world's recognized medicinal plants are derived from tropical forests. For example, approximately half (125,000) of the world's flowering plant species live in tropical forests (*126*). Tropical botanicals have evolved sophisticated chemicals to protect themselves from natural enemies, to subdue prey or to survive in a variety of ecosystems; hence they are very biodiverse in their chemical composition, leading to them having a significant role to play in being able to provide new leads in drug discovery. Nonetheless, despite their richness in biochemical resources, the potential of large areas of tropical rainforests remains virtually untapped. This can be seen

in the small percentage of drugs being approved as new compounds. To date, it was estimated that only 1 % of tropical species have been studied for their pharmaceutical potential and about 50 drugs are derived from tropical plants (*126*).

Despite the slow progress of drug discovery in tropical botanicals, there have been several promising discoveries occurring almost exclusively in tropical forests. One example is the anti-AIDS compound produced by the Malaysian tree, a member of the tropical *Garcinia* family (Guttiferae-Clusiaceae). The active compound was found to be (-)-calanolide B and (+)-Calanolide A from *C.lanigerum* whereby (-)-calanolide B was found to be slightly less active than (+)-Calanolide A. (+)-Calanolide A has been synthesized, and is currently in Phase II of clinical trials (*127*). This is just a hint of the massive potential that is hidden within tropical rainforests. Correspondingly, there are continuing issues of conservation of ethnobotanical data and biodiversity, and the urgency to expand exploration of these resources as a source of novel bioactive agents. With an increasing awareness of the value of tropical botanicals, there are concerted efforts from governmental agencies, universities and countries to protect, conserve, study and develop novel drugs that would be of great value to human beings.

1.9 Starch hydrolase inhibitors

1.9.1 Acarbose

Acarbose is currently one of the strongest starch digestion blockers, which broadly inhibit starch hydrolases like glucoamylase, amylase, dextrinase, maltase and sucrose (*128*). It is a pseudomaltotetraose that is a

bacterial secondary metabolite that is produced by strains of *Streptomyces*. Industrially, it is produced by strains of the general *Actinoplanes* sp. SE 50/110 (*129*). Its chemical structure consists of an unsaturated amino cyclitol moiety (ring A), a deoxyhexose (ring B) or acarviosine together with ring A, and a normal maltose moiety (rings C and D) **(Figure 8**). Due to the presence of an inter-cyclic nitrogen atom in the acarviosine unit, the enzyme is unable to cleave the C-N linkage, thus preventing the enzyme from processing other ingested carbohydrates and therefore, glucose cannot be released for absorption. It has been suggested that due to its broad spectrum of inhibitory effects against hydrolases, it can result in serious gastrointestinal side-effects like flatulence and diarrhoea, which is due to undigested oligosaccharides entering the colon and being fermented by bacteria, generating gaseous metabolites as a result (*130*).

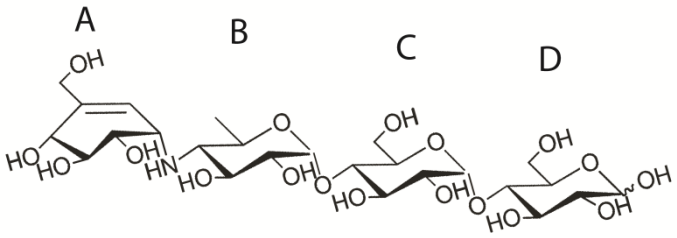

Figure 8. Chemical structure of acarbose.

1.9.2 Proanthocyanidins (PACs)

PACs are the oligomeric and polymeric end products of the flavonoid biosynthetic pathway. PACs belong to the class of phenolic compounds, which are found to be ubiquitous in plants (fruits, bark, leaves and seeds) where they act as protectors against predation. In food, PACs are often linked to the

astringent characteristic associated with foods like wine and teas. As the name suggests, they are characterized by condensed polyphenols or tannins. Their basic building blocks are monomeric flavan-3-ol units and can be linked either through the C4-C8 or C4-C6 (B-type linkages). Another type of linkage, the A-type linkage, links the subunits via the C2-C7 and lacks two hydrogen atoms compared to the B-type PAC (*131*). Within the umbrella of proanthocyanidins, there are still different classes of PAC which depend on the substitution pattern of the monomeric flavan-3-ol units. PACs that exclusively consist of (epi)catechin units are termed procyanidins. Procyanidins can be found in many plants, notably in maritime pine bark, cinnamon, cocoa beans, grape seed and skin (*132*). These are the most abundant type of PACs that exist in plants. In addition, a less common type of PACs are those that contain (epi)afzelechin and (epi)gallocatechin units, called propelargonidin and prodelphinidin respectively. Proanthocyanidins have been linked to quite a number of pharmacological attributes such as antiviral (*133*) and antimicrobial (*134*) activities.

1.9.3 1-Deoxynojirimycin

1-Deoxynojirinycin (1, 5-dideoxy-1, 5-iminoglucitol) (1-DNJ) is a D-glucose analog and a strong inhibitor of glucohydrolases including glucoamylase **(Figure 9)**. For example, 1-DNJ was shown to have a binding constant 10,000 times higher than that of glucose to *Rhizopus* glucoamylase (*135*). It is also known to be a tight-binding competitive inhibitor of sucrase (*136*). During the formation of the enzyme-inhibitor complex, 1-DNJ is assumed to become protonated at its nitrogen atom, leading to a positive

charge, thus mimicking the transition state formed during catalysis of substrate hydrolysis. This allows it to interact tightly with the negative charge in the catalytic centre (*137*).

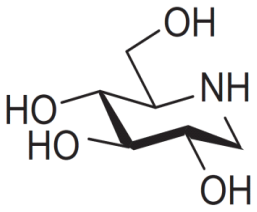

Figure 9. Chemical structure of 1-DNJ.

1.9.4 Thiosugars

The presence of sulphur heteroatoms in thiosugars is responsible for biological activities. For example, a compound like 5-thio-D-glucopyranose is able to inhibit the release of insulin. In addition, thioxyloside has also been shown to be a potential anti-thrombotic agent (*138, 139*). These biological and physicochemical properties are attributed to several factors. Firstly, its sulphur atom possesses different electronic properties (electronegativity) as compared to oxygen atoms. Secondly, the electron density of sulphur atoms is more dispersed. Lastly, the carbon-sulphur bond is longer (ca. 1.8 Ă), and the C-S-C angle (ca. 95-100 º) is also smaller compared to the corresponding structure containing oxygen (*138*). Combined together, it was postulated that perhaps these chemical attributes of sulphur analogs contribute to the biological activity of thio-sugars. For example, thio-sugars are able to easily form sulfoxides due to their ability to remove unsaturated bonds (deoxygenation) and are also oxidized easily to form disulfides (*139*). In contrast, however, there is also evidence to show that the removal of the sulphur group enhances

enzyme inhibitory activity as compared to the original sulphate counterpart (*140*).

a. Salacinol

Salacinol is a thio-sugar compound that has been isolated from an anti-diabetic *ayurvedic* traditional medicine (*Salacia reticulata*). Its structure is comprised of a five member ring, with sulphur as the heteroatom (1, 4-anhydro-4-thio-D-arabinitol), which contains a terminally sulphonylated four-carbon aliphatic branched chain attached to the sulphur heteroatom **(Figure 10)** (*139*). Its special feature is that it possesses a positive charge carried by sulphur, which enables it to bind in a similar fashion as a protonated amine inhibitor to the α-glucosidase active sites (*140*). Experimental studies have shown this class of inhibitors to be very potent, whereby the K_i values were in the micro molar range (i.e., 0.1- 0.19 µM) and its bonds to ntMGAM were stronger compared to acarbose (K_i = 62 µM) (*63*, *141*, *142*). On the other hand, salacinol inhibitors are relatively poor inhibitors of human pancreatic α-amylase (K_i = 75 µM) compared to acarbose, which has a much lower K_i of 15 nM (*143*). Hence, salacinol inhibitors are more selective towards α-glucosidase rather than amylases, and acarbose has a stronger binding preference towards amylases compared to α-glucosidase.

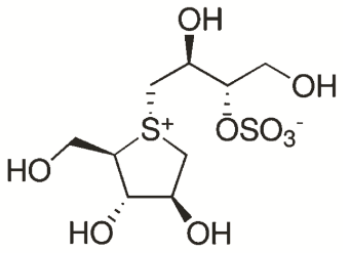

Figure 10. Chemical structure of salacinol.

b. Kotalanol

Kotalanol has a similar core structure to salacinol, which consists of 1, 4-anhydro-4-thio-D-arabinitol. However, instead of its core structure being attached to a four-carbon aliphatic branched chain, it is attached to a seven-carbon polyhydroxylated side chain containing six undefined stereogenic centres including the sulphonium centre **(Figure 11)** (*144*). Interestingly, an experimental study showed that the removal of the sulphate group enhances the inhibitory activity of kotalanol by approximately seven-fold, as compared to the original structure, to give a K_i of 0.03 ± 0.01 µM and 0.19 ± 0.03 µM respectively (*144*). It was suggested that without the bulky sulphate group, the initial positional constraints imposed by the group would be removed, thus allowing the rest of the polyhydroxylated chain to make optimal contact with the ntMGAM active site. Additionally, results also showed that acyclic chains longer than four carbons, such as those found in kotalanol, do not significantly enhance the inhibitory properties of MGAM since the K_i of salacinol (0.19 ± 0.02 µM) and kotalanol (0.19 ± 0.03 µM) are essentially the same (*140*).

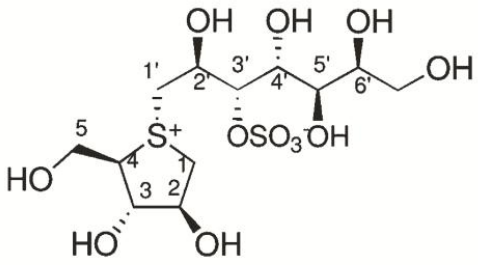

Figure 11. Chemical structure of kotalanol.

1.10 Research aims

In view of the escalating rate of diabetes cases, the search for novel anti-diabetic bioactives from natural sources, particularly from tropical botanicals, has become an urgent matter. *In vitro* studies are usually the starting point in the search for novel bioactive compounds, and they lay the groundwork for future studies. It is not feasible to screen for bioactives via *in vivo* studies as they are too costly and time consuming. However, *in vivo* studies may be used to follow up on important 'leads' generated by *in vitro* studies. As such, it is vital to choose the most suitable *in vitro* assay that mimics bodily reactions as closely as possible, in order for results to have any significant implication. In addition, these assays should be properly validated to generate reliable results and to avoid any false positives. Currently, the two most popular methods to screen for α-glucosidase inhibition are the *p*NPG and the GOP method.

The first two objectives of this project are:

(1) To evaluate the *p*NPG method by assessing the impact of the use of natural versus synthetic substrates on the inhibition constants of acarbose and 1-DNJ on α-glucosidase **(Chapter 2)**.

(2) To assess the impact of polyphenolic compounds commonly found in many botanicals on the GOP assay, in the context of screening for α-glucosidase inhibitors **(Chapter 3)**.

Subsequently, suitable *in vitro* HTS assays were applied to screen through a total of 298 plant samples, which were collected from the Singapore Botanic Gardens, for starch hydrolase inhibition, total phenolic and proanthocyanidin

contents. This screening work was taken a step further in an in-depth study of characterizing inhibitors from the *Etlingera elatior* inflorescence by applying assay-guided fractionation and separation of polyphenolic compounds. Hence, the third and fourth objectives of this project are:

(3) To screen and determine the inhibitory potency of starch hydrolase inhibitors from edible botanicals collected from the Singapore Botanic Gardens **(Chapter 4)**.

(4) To characterize proanthocyanidins from *Etlingera elatior* inflorescence as strong starch hydrolase inhibitors **(Chapter 5)**.

Currently, there are several conventional starch hydrolase inhibitors that are effective but cause undesirable side-effects, like flatulence and diarrhoea. As such, the final part of the project aims to address this issue by exploring the potential of utilizing compounds (e.g. EGCG) that are available in common foods like green tea to potentiate and/or synergize the potency of conventional drugs. The final objective of this study is:

(5) To understand the synergistic mechanisms and potentiating action of epigallocatechin gallate towards acarbose and 1-DNJ on the inhibition of α-amylase activity **(Chapter 6)**.

Chapter 2

Evaluation of the *p*-nitrophenyl α-D-glucopyranoside assay

2.1 Introduction

Synthetic substrates have often been used as a substitute for natural ones due to the convenience of using them to measure enzyme inhibition. One such assay is the *p*-nitrophenyl α-D-glucopyranoside (*p*NPG) colorimetric assay. This assay has been extended to measure inhibition for many years and utilises a synthetic substrate to measure the activity of α-glucosidase. It can be cleaved by α-glucosidase at the α-(1, 4) linkage, which releases *p*-nitrophenol and under basic conditions, and dissociates to *p*-nitrophenolate. This product can be measured at a UV-absorbance of 405 nm.

An important factor that has often been disregarded in selecting assays to test for starch hydrolase inhibition is the choice of substrates. Ideally, the substrates should be physiologically relevant in order for the results to be reliable, and to have accurate implications. In particular, K_i is an important constant which measures the dissociation for the enzyme-inhibitor complex, and K_i' is the inhibition constant for the enzyme-inhibitor-substrate complex. In other words, for a reversible inhibitor, K_i gives an indication of the binding affinity between the enzyme and the inhibitor. The smaller the K_i, the tighter the binding between the enzyme and the inhibitor, thus the stronger the

inhibitory activity. There is a direct relationship between K_i and IC_{50} for competitive inhibitors, as shown by **Equation 2** (*145*):

$$IC_{50} = K_i\left(1 + \frac{[S]}{K_m}\right) \qquad \textbf{(Equation 2)}$$

Currently, there has not been any research which addresses the issue of the validity of the *p*NPG assay. This study aims to compare the use of different substrates (i.e. synthetic vs. native) and how this affects the inhibitor constants. The use of native (maltose) and synthetic (*p*NPG) substrates will be used to test for the inhibitor constants (K_i and $K_i^{'}$) of two well-known α-glucosidase inhibitors (acarbose and 1-deoxynojirimycin).

2.2 Materials and methods

2.2.1 Reagents and instruments

Acarbose (A8980), 1-deoxynojirimycin hydrochloride (D9305), a glucose assay kit (glucose oxidase/peroxidase reagent G3660; *o*-dianisidine reagent D2679), α-glucosidase from intestinal acetone powders from rats (I1630), and 4-nitrophenyl-α-D-glucopyranoside (N1377) were obtained from Sigma-Aldrich Chemical Co. (St. Louis, MO). Absorbance at 540 nm for the GOP method and 405 nm for the *p*NPG method was measured by a microplate reader (Bio-Tek Instruments Inc., Winooski, VT). A sodium phosphate buffer (pH 6.9; 0.1M) was utilized.

2.2.2 Glucose oxidase/ peroxidase method

α-Glucosidase (50 µL) was incubated with 125 µL inhibitor (final concentration of acarbose and 1-DNJ was 0.096, 0.19, 0.38, 0.77 µM and 0.06,

0.12, 0.24, 0.48 µM, respectively) for 5 min before 150 µL of maltose (final concentration of 13.8, 6.9, 3.5, 1.7, 0.87 and 0.4 mM) was added to initiate the reaction. The reaction mixture (40 µL) was sampled at 0, 1, 2, 3, 4 min and inactivated by adding 80 µL of tris-HCl (pH 7.0, 1 M final concentration). The deactivated mixture (40 µL) and glucose reagent (120 µL) were allowed to react for 30 min before the reaction was stopped with H_2SO_4 (120 µL, 6M). Absorbance was read at 540 nm.

2.2.3 *p*-Nitrophenyl α-D-glucopyranoside method

α-Glucosidase solution (120 µL) was incubated with 300 µL of inhibitor (final concentrations of acarbose and 1-DNJ were 0.096, 0.19, 0.38, 0.77, 1.54 mM and 0.06, 0.12, 0.24, 0.48, 0.96 µM, respectively) for 5 min. *p*NPG (360 µL, final concentration was 6.9, 3.45, 1.7, 0.87, 0.43, 0.22 mM) was used to initiate the reaction. The reaction mixture (150 µL) was drawn at 0, 5, 10, 15, 20 min and deactivated with the addition of 50 µL of 0.5 M Na_2CO_3. The absorbance was read at 400 nm.

2.2.4 Graphical methods for determining the mode of enzyme inhibition, K_i and K_i'

The K_m^{app} method was used to estimate both the K_i aand K_i'. Complementary to this, the Dixon method estimates the K_i, whereas the Cornish-Bowden method gives the K_i' and mode of inhibition of the inhibitor. The obtained values from the respective methods were then compared.

2.2.4.1 K_m^{app} method

The K_m^{app} method is based on the Michaelis-Menten **(Equation 3)**. Each experimental data point, with varying substrate concentration and rates, was fitted individually using nonlinear regression to **Equation 3**, to obtain the K_m^{app} value, as well as estimates of V_{max}.

$$v = \frac{V_{max} \cdot [S]}{K_m{}^{app} + [S]} \qquad \textbf{(Equation 3)}$$

Subsequently, estimates of K_i were obtained from a linear regression plot of K_m^{app}/V_{max} (slope) as a function of inhibitor concentration *[I]*, whereby K_i was obtained graphically from the intercept of the x-axis. **Equation 4** describes this relationship (*146*). K_i' can be determined using a plot of $1/V_{max}$ as a function of *[I]* and its value was determined from the x-intercept.

$$\frac{K_m{}^{app}}{V_{max}} = \frac{K_m \cdot [I]}{K_i \cdot V_{max}} + \frac{K_m}{V_{max}} \qquad \textbf{(Equation 4)}$$

2.2.4.2 Dixon method

The initial reaction rates were obtained experimentally with various substrate concentrations. The initial rates were used to estimate the K_m and V_{max} by linear transformation of the original Michaelis-Menten equation of $v = (V_{max}\ S)/(K_m + S)$. A new set of calculated initial rates was obtained from the Michaelis-Menten equation, taking into account the square of the difference between the experimental initial rates and the calculated initial rates. The calculated initial rates were then used to generate the Dixon plot with the reciprocal of the rate of product formation *(1/v)* versus inhibitor concentration,

[I] at various substrate concentrations *[S]*. The plot yields a series of straight lines that intersect at a unique point, where (*i*) coordinate are the $-K_i$. Hence K_i can be read directly off the plot, or it may be obtained by solving two sets of linear regression equations. The Dixon plot is governed by **Equation 5**.

$$\frac{1}{v} = \frac{K_m \cdot [I]}{V_{max} \cdot [S] \cdot K_i} + \frac{1}{V_{max}} \left(1 + \frac{K_m}{[S]}\right) \qquad \textbf{(Equation 5)}$$

2.2.4.3 Cornish-Bowden method

This method is built on the assumption that all common types of inhibition are derived from linear mixed inhibition as a general case, where the rate $\mathscr{v}$ is dependent on the substrate concentration *[S]* and the *i* value of the inhibitor, in accordance with **Equation 6**.

$$\mathscr{v} = \frac{Vs}{K_m\left(1+\frac{i}{K_i}\right)+[S]\left(1+\frac{i}{K_i'}\right)} \qquad \textbf{(Equation 6)}$$

The Cornish-Bowden plot is derived from the rate equation described in **Equation 6**, which takes *s/v* against the inhibitor concentration *i*. From **Equation 6**, *V* is the limiting rate, K_m is the Michaelis constant, K_i is the dissociation constant for the EI complex (or competitive inhibition constant) and K_i' is that of the EIS complex (or the uncompetitive inhibition constant). This plot has a similar appearance to the Dixon plot; however, the *i* coordinate of the intersection point yields the $-K_i'$. This plot is defined through **Equation 7**.

$$\frac{s}{v} = \frac{K_m}{V}\left(1 + \frac{i}{K_i}\right) + \frac{s}{V}\left(1 + \frac{i}{K_i'}\right) \qquad \textbf{(Equation 7)}$$

From this plot, the mode of inhibition may be determined as well. Since K_i' for the competitive inhibitor equals ∞, the lines are parallel and there is no intersection between them. For mixed or non-competitive inhibition, the lines converge and intersect on the *i* axis.

2.2.5 Statistical analysis

Statistical analysis was performed using SPSS software. The K_i and K_i' values are given as means ± standard deviations (SDs). Significant differences between means were analysed using one-way ANOVA (Duncan test) at $p < 0.05$ level.

2.3 Results and discussion

Using the Dixon method as outlined in Section 2.2.4.2, **Figure 12A** shows the reciprocal of the initial rates of product formation (*1/v*) at various maltose concentrations (0.4, 0.9, 1.7, 3.5 and 6.9 mM) which were plotted against various acarbose concentrations (0, 0.096, 0.19, 0.38 µM). Linear regression equations were obtained for each substrate concentration and the negative of the x-axis value at the point of intersection between the straight lines denotes the K_i. Using the Dixon plot, the K_i of acarbose, using maltose as the substrate, was determined to be 0.07 ± 0.01 µM. To confirm this value, a different method ($K_m{}^{app}$) as outlined in Section 2.2.4.1 **(Figure 12D)** was used to calculate the K_i, which was found to be 0.07 ± 0.004 µM. In addition, the $K_m{}^{app}$ method was also applied to calculate the K_i', which was 0.83 ± 0.16 µM **(Figure 12C)**. In addition, the Cornish-Bowden plot shows parallel lines which indicates that acarbose inhibits α-glucosidase competitively **(Figure 12B)**.

Figure 13 shows the inhibition kinetic plots of acarbose with *p*NPG as the substrate. The Dixon plot in **Figure 13A** indicates that the lines intersect at I = 0.13 ± 0.01 mM which is the K_i. Similarly, **Figure 13D** also shows the line intersecting on the x-axis, giving a K_i of 0.13 ± 0.015 mM. K_i' was estimated to be 1.8 ± 0.2 mM by the ${K_m}^{app}$ method **(Figure 13C)**. Finally, **Figure 13B** shows that the curves are parallel to one another, which indicates that acarbose is a competitive inhibitor of α-glucosidase when *p*NPG is used as the substrate, which is the same as when maltose is used as the substrate. Hence, this result demonstrates that for acarbose, the use of a different substrate did not change its mode of inhibition.

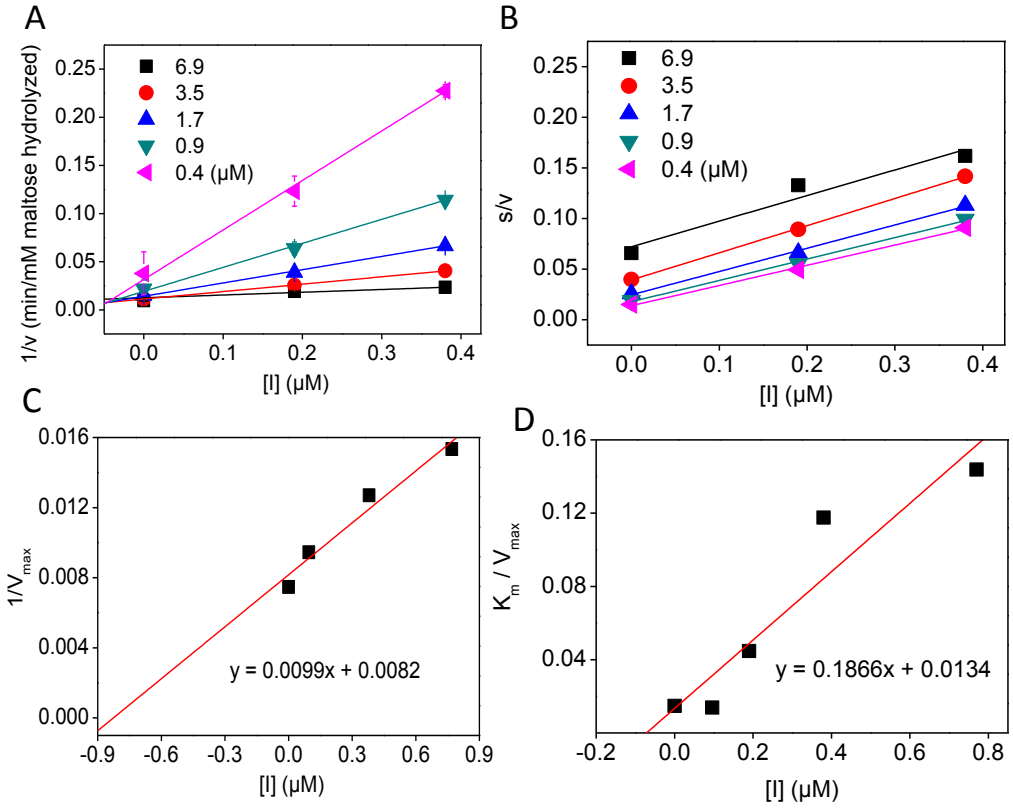

Figure 12. Inhibition kinetic plots of acarbose using maltose as the substrate: (a) Dixon plot of reciprocal rates of the hydrolysis of maltose (*1/v*) versus acarbose concentration [*I*]. The line intersection provides a measure of K_i. (b) Cornish-Bowden plot (*s/v* vs. *I*). (c) Plot of $1/V_{max}$ vs. *[I]* to determine K_i' of α-glucosidase. (d) Plot of K_{mapp}/V_{max} vs. *[I]* to determine K_i of α-glucosidase.

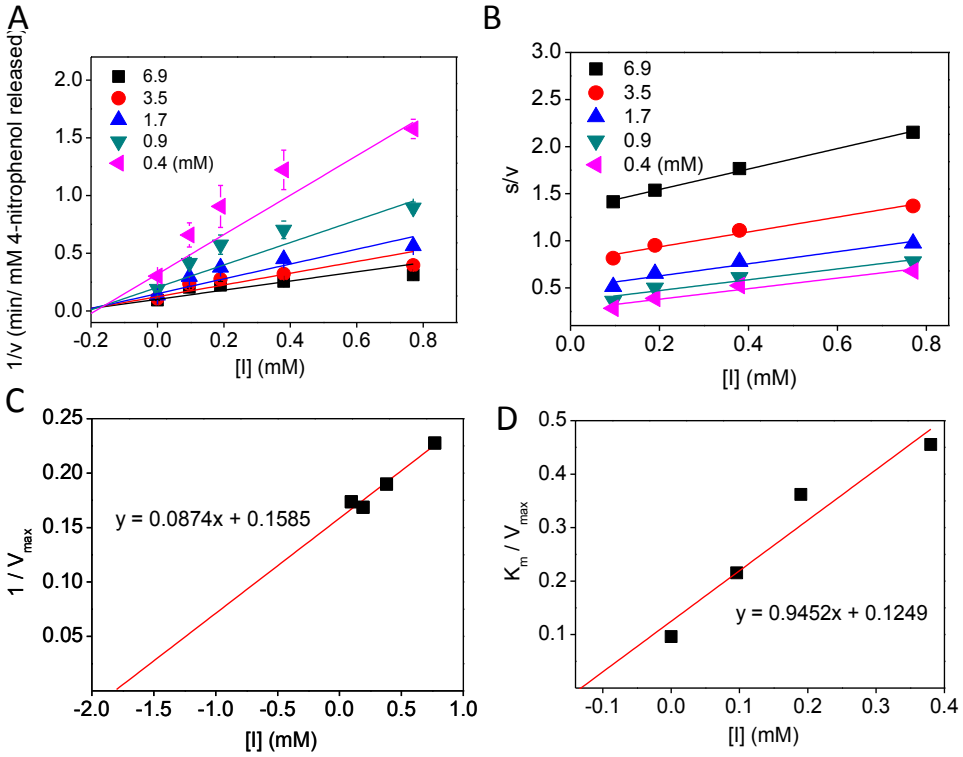

Figure 13. Inhibition kinetic plots of acarbose using *p*NPG as the substrate: (a) Dixon plot of reciprocal rates of 4-nitrophenol release (*1/v*) versus acarbose concentration *[I]*. (b) Cornish-Bowden plot (*[S]/v* vs. *I*). (c) Plot of $1/V_{max}$ vs. *[I]* to determine K_i' of α-glucosidase. (d) A plot of $K_m{}^{app}$) $/V_{max}$ vs. *[I]* to determine K_i of α-glucosidase.

The inhibition kinetic plots of 1-DNJ with maltose as the substrate are shown in **Figure 14**. By using the Dixon plot **(Figure 14A)**, a K_i of 0.01 ± 0.008 µM, where the lines intersect one another, was estimated. The calculated K_i by the $K_m{}^{app}$ method gave a value that was slightly higher (K_i = 0.024 ± 0.0012 µM) **(Figure 14D)**. K_i' values, as determined by the $K_m{}^{app}$ **(Figure 14C)**, and Cornish-Bowden method, were 0.07 ± 0.019 and 0.07 ± 0.005 µM respectively. The mode of inhibition for 1-DNJ was shown to be that of mixed-type inhibition, as seen through the converging lines **(Figure 14B)**.

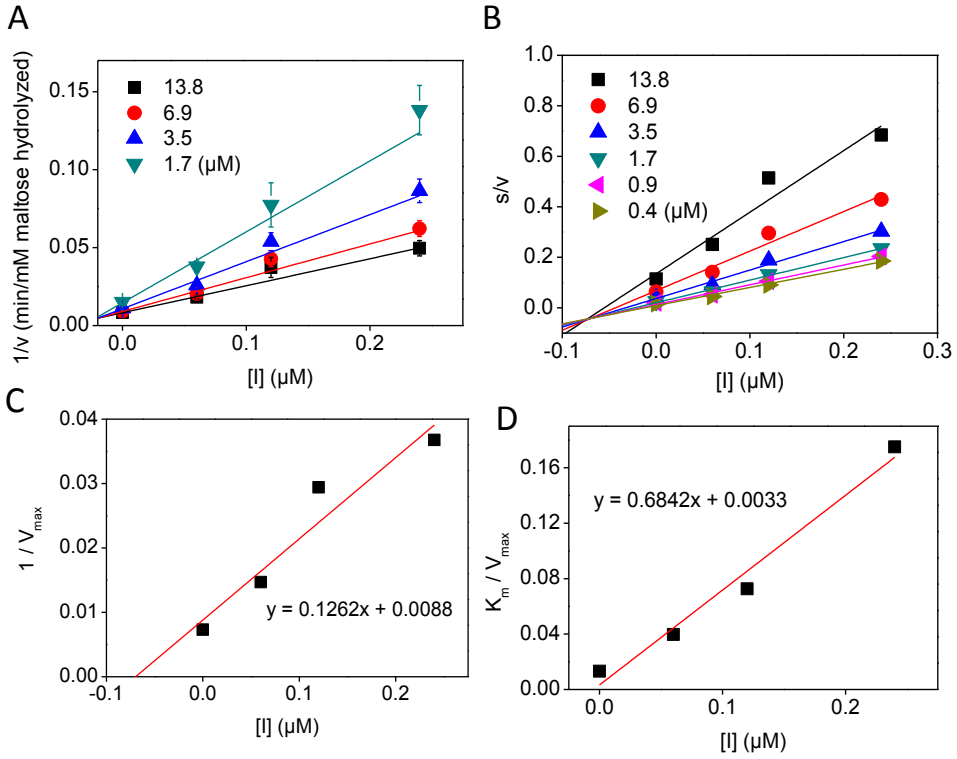

Figure 14. Inhibition kinetic plots of 1-DNJ using maltose as the substrate: (a) Dixon plot of reciprocal rates of the hydrolysis of maltose (*1/v*) versus 1-DNJ concentration *[I]*. (b) Cornish-Bowden plot ([S]*/v vs. I*). (c) Plot of $1/V_{max}$ vs. *[I]* to determine the K_i' of α-glucosidase. (d) Plot of $K_m{}^{app})/V_{max}$ vs. *[I]* to determine the K_i of α-glucosidase.

Figure 15 shows the inhibition kinetic plots of 1-DNJ with *p*NPG as the substrate. K_i, as determined by the $K_m{}^{app}$ **(Figure 15D)** and Dixon plot **(Figure 15A)**, were 0.1 ± 0.06 and 0.18 ± 0.04 µM respectively. On the other hand, K_i' as measured by $K_m{}^{app}$ **(Figure 15C)** and Cornish-Bowden methods were 0.16 ± 0.011 and 0.16 ± 0.006 µM respectively. The Cornish-Bowden plot in **Figure 15B** also shows converging lines, which indicate that 1-DNJ exhibits mixed-type inhibition activity with *p*NPG as the substrate. Hence, this demonstrates that the type of substrate utilised does not influence the mode of inhibition of 1-DNJ.

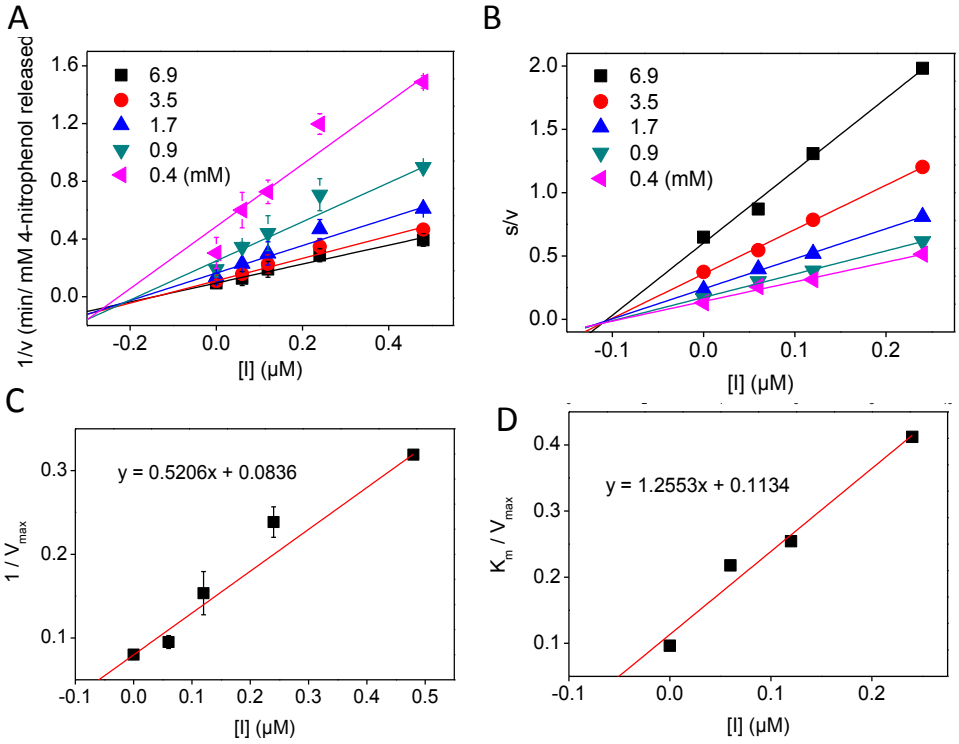

Figure 15. Inhibition kinetic plots of 1-DNJ using *p*NPG as the substrate: (a) Dixon plot of reciprocal rates of 4-nitrophenol release (*1/v*) versus 1-DNJ concentration *[I]*. (b) Cornish-Bowden plot ([S]*/v* vs. *I*). (c) Plot of $1/V_{max}$ vs. *[I]* to determine the K_i' of α-glucosidase. (d) Plot of ${K_m}^{app}/V_{max}$ vs. *[I]* to determine the K_i of α-glucosidase.

Table 1 summarizes the results of inhibition kinetics parameters for 1-DNJ and acarbose; both are known α-glucosidase inhibitors with applications in anti-diabetic medicine. Overall, there were large differences in the K_i and K_i' of both inhibitors, 1-DNJ and acarbose, when different substrates were used. The use of *p*NPG as substrate resulted in a much larger K_i compared to when maltose was used. For example, K_i values, calculated from the Dixon method of 1-DNJ when *p*NPG was used (0.18 ± 0.04 μM), were approximately 20 times larger than the calculated K_i when maltose was used (0.01 ± 0.008 μM). An even more elaborate difference was seen in the K_i of acarbose with different substrates. K_i values of acarbose, estimated using the

Dixon method when maltose was used, were three orders of magnitude smaller (0.07 ± 0.01 µM) than the K_i values when *p*NPG was used (130 ± 15 µM).

Table 1. K_i and K_i' of 1-DNJ and acarbose using K_{mapp}, Dixon and Cornish-Bowden methods with either maltose or *p*NPG as the substrate.

Inhibitor	Substrate	Estimated K_i (µM)				
		K_m^{app}		Dixon	Cornish-Bowden	
		K_i	K_i'	K_i	K_i'	Inhibition mode
1-DNJ [§]	Maltose	0.024 ± 0.0012[a]	0.07 ± 0.019 [a]	0.01 ± 0.008 [a]	0.07 ± 0.005 [a]	Mixed
	*p*NPG	0.1 ± 0.06 [b]	0.16 ± 0.011[b]	0.18 ± 0.04 [b]	0.16 ± 0.006 [b]	Mixed
Acarbose [Ψ]	Maltose	0.07 ± 0.004 [c]	0.83 ± 0.16 [c]	0.07 ± 0.01[c]	N/A	Competitive
	*p*NPG	130 ± 10 [d]	1800 ± 200 [d]	130 ± 15 [d]	N/A	Competitive

[§] Different superscript letters (a and b) indicate significant differences ($p < 0.05$) in K_i or K_i' of 1-DNJ with different substrates.
[Ψ] Different superscript letters (c and d) indicate significant differences ($p < 0.05$) in K_i or K_i' of acarbose with different substrates.

The mode of inhibition was found to be consistent for both acarbose and 1-DNJ, regardless of the type of substrate used. Acarbose consistently displayed competitive inhibition, whereas 1-DNJ displayed mixed inhibition of α-glucosidase. For acarbose, it acted as a competitive inhibitor towards both substrates but surprisingly, the K_i differed greatly. This finding does not correspond to the classical model for competitive inhibition, where the inhibitor binds only to the free enzyme, in contrast to mixed inhibition whereby the inhibitor is able to bind to both the free enzyme as well as the enzyme-substrate complex. Therefore, following this model for competitive inhibition, K_i should be constant regardless of the type of substrate used. We propose that the difference in K_i when different substrates were used was due to acarbose and 1-DNJ competing more easily with maltose as compared to

*p*NPG. This can be seen from the more rapid increase in K_m for maltose as the concentration of inhibitor within the reaction system increases. This finding, however, seem to be in conflict with other literature findings whereby maltose was shown to have a higher affinity towards the active site of the enzyme than the synthetic *p*NPG (*79, 147*). Hence, in theory, inhibitors would be shown to be less potent when maltose is used as the substrate as compared to when *p*NPG is used, due to the strong affinity of maltose towards the enzyme and inhibitors not being able to compete as well. It is possible that there may have been a change in the pH optima of the enzymes when synthetic substrates were used. It was shown previously that the pH optima of α-amylases were higher with synthetic than with natural substrates (*79*). A change in the pH may very well change the enzyme's structure, which may affect the interaction between the enzyme and inhibitor such that the inhibitor may bind more weakly. In addition, the synthetic substrate *p*NPG had very low solubility at room temperature, but improved with warming. Consequently, the activity measured with the synthetic substrate was much lower than with the natural substrate.

Furthermore, from the mathematical relationship outlined in **Equation 2**, we can see that the IC_{50} of an inhibitor is directly related to the K_i. Hence, a larger K_i would result in a larger IC_{50}, and the implications of a significantly different K_i would mean that the IC_{50} calculated when *p*NPG was used as the substrate would reveal *p*NPG as a less potent inhibitor compared to when maltose was applied.

2.4 Conclusion

K_i and K_i' of acarbose and 1-DNJ were determined and compared by applying either natural substrate (maltose) or synthetic substrate (*p*NPG). The K_i measured was consistently higher for both inhibitors when *p*NPG was used, as compared to when maltose was applied as the substrate. A larger K_i translates to larger IC_{50} (i.e. lower potency), which may not be a true depiction of the activity of an inhibitor. These results also show that the mode of inhibition remains the same despite the change in substrate. This study demonstrates the importance of choosing the right substrate; natural substrates should be used instead of synthetic ones in order for results to be representative and applicable.

Chapter 3

Assessment of the degree of interference from polyphenolic compounds on glucose oxidase/peroxidase assay

3.1 Introduction

Due to the increasing global population of type two diabetes, research on finding ways in mitigating this dreadful disease have intensified in recent years (*148*). One way to control hyperglycaemia is through starch hydrolase inhibitors from edible plants, which contain structurally diverse α-glucosidase inhibitors including sugar mimics (*149*) and polyphenolic compounds (*150, 151*). To uncover novel α-glucosidase inhibitors from plants, particularly edible plants, *p*NPG and GOP bi-enzyme assay are widely applied as convenient guides to fractionation and purification of inhibitors. While *p*NPG assay uses a synthetic probe that may not be truly reflective of natural substrates of the enzymes, the GOP assay was developed initially to quantitate the amount of D-glucose in human fluids (*152*). Principally, this assay uses glucose oxidase to oxidize β-D-glucose by molecular oxygen to D-glucono-β-lactone and hydrogen peroxide. In the presence of peroxidase (e.g. horseradish peroxidase), hydrogen peroxide reacts with colourless chromogenic molecules to form colourful dyes that can be quantified conveniently by colorimeters **(Figure 16)**. Many chromogenic compounds have been used as substrates for horseradish peroxidase (*153*). Among them, *o*-dianisidine has been more

widely applied than others. In acidic conditions, the oxidized *o*-dianisidine becomes rose-pink coloured with absorbance maximum at 540 nm **(Figure 17)** (*154*). Due to its convenience, the GOP assay has been applied in many other systems including measurement of α-glucosidase activity and screening for its inhibitors.

Although GOP assay is highly substrate specific and relatively convenient to utilize, it is highly susceptible to various interferences (*155, 156*). The GOP assay utilizes two oxidases and involves complicated redox reaction mechanisms; as such any compounds that can inhibit the two enzymes or react with the reactive intermediates of reaction will cause interferences (*157*). Indeed, there are scattered reports on the interference issue of the GOP assay. Using 4-aminoantipyrine and 3-hydroxybenzoic acid as chromogenic substrates in the GOP assay, it was recently found that green tea polyphenolic compounds cause interferences and lead to false negative results in blood serum glucose concentrations and the interference was suggested to be due to the radical scavenging activity of the polyphenolic compounds (*158*). In another study, polyphenols were also found to interfere because of their reducing activity (*159*). Despite the number of reports addressing the issue of interferences, GOP assay continues to be applied in the quantification of α-glucosidase inhibitory activity of natural products due to its convenience and selectivity of glucose (*160*). Since, natural products often contain polyphenolic compounds, it is important to systematically address the scope and limitations of the GOP assay in quantifying botanical samples on α-glucosidase inhibitory activity. Therefore, we investigated the interference of common polyphenolic compounds found in the plant kingdom on the degree

of interferences on GOP assays by adding sodium dodecyl sulfate (SDS) to stabilize meriquinone intermediates formed during the oxidation of *o*-dianisidine by peroxidase. Our results reported herein will help researchers in using GOP assay in plant extracts to assess the suitability of the assays and provide a guide for avoiding unnecessary false results.

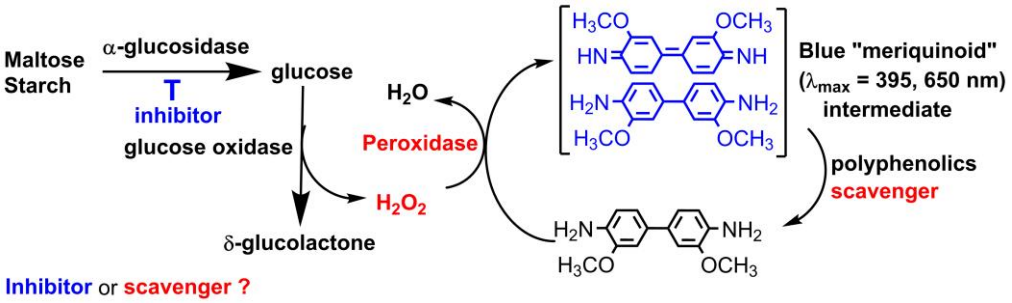

Figure 16. Possible interference principles behind the GOP assay.

3.2 Materials and methods

3.2.1 Reagents and instruments

Chemical reagents were obtained from commercial sources. These compounds include caffeic acid, ferulic acid, rutin, apigenin, chrysin, coumaric acid, gallic acid, hesperedin, hesperetin, kaempferol, luteolin, morin, naringin, quercetin, hydrogen peroxide solution, *o*-dianisidine dihydrochloride, glucose oxidase, and peroxidase from horseradish (Sigma-Aldrich, Singapore); 3, 5-dihydroxyflavone, 3, 7-dihydroxyflavone, 3', 3, 4-trihydroxyflavone, 5, 3', 4'-trihydroxyflavone, 5, 7, 3', 4', 5'-pentahydroxyflavone, 7, 3', 4'-trihydroxyflavone, 7, 8-dihydroxyflavone, fisetin, galangin, gossypetin, and myricetin (Indofine Chem. Co. California, USA); tannic acid (Merck, Germany); ascorbic acid, chlorogenic acid

(Spectrum Chemical Co, Singapore). Microplate reader (Bio-Tek Instruments Inc., Winooski, VT) was used to measure the spectrophotometric readings.

3.2.2 Generation of the meriquinone intermediate and its reactivity with polyphenolic compounds.

o-Dianisidine (0.1 mM), SDS (1.0 mM), H_2O_2 (0.1 mM) and peroxidase (0.25 units) in citrate buffer (pH 4) were reacted for one minute to generate the meriquinone intermediate, which was quantified by UV-absorbance at 395 nm. Polyphenolic compounds with various concentrations were reacted with meriquinone. The decrease in the UV-absorbance over time was monitored for selected compounds including vitamin C, coumaric acid, caffeic acid, gallic acid and EGCG. For the rest of samples, end point readings were carried out at 650 nm. The final concentrations of the polyphenolic compounds were kept at 100 µM. The absorbance readings were taken after 5 min of reaction. The degree of interference was quantified through **Equation 8**:

$$\% \text{ Interference} = 100(A_{blk}-A_s)/A_{blk} \qquad \textbf{(Equation 8)}$$

where A_s is the absorbance of the reaction mixture of the sample with meriquinone at 650 nm, A_{blk} is the absorbance of blank (water).

3.2.3 Determination of the radical scavenging activity using DPPH

Antioxidant radical scavenging activities of the various polyphenolic compounds were determined by using the free radical DPPH microplate assay with methanol (*161*). DPPH reacts with an antioxidant which donates hydrogen and reduces DPPH. A stock solution of 0.1 mM DPPH dissolved in

methanol was prepared and the excess sample was stored in eppendorf tubes covered in aluminium foil and placed in the refrigerator until further use. The polyphenolic compounds were dissolved in DMSO and prepared at various concentrations (0.125, 0.25, 0.5, 1, 2, 4 and 8 mM). Briefly, 15 µL of the polyphenolic compounds at various concentrations were added in triplicate cells. Consequently, 285 µL of DPPH stock (0.1 mM) was added to the 96-well plate using a multichannel pipettor. The microplate was placed into the microplate reader and the change in absorbance was monitored at 517 nm. The results are expressed as IC_{50} which is the concentration which exhibits 50 % radical scavenging activity. The percentage of radical scavenging activity was quantified through **Equation 9**:

$$\%\ \text{Radical scavenging activity} = \left[\left(OD_{control} - OD_{sample}\right)/OD_{control}\right] \text{ x } 100 \quad \textbf{(Equation 9)}$$

Where $OD_{control}$ is the optical density of the blank (DMSO) and OD_{sample} is the optical density of the test sample.

3.2.4 Statistical analysis

All measurements were performed in triplicates and the results are expressed as mean ± standard deviation. Significant differences between means were analysed using one way ANOVA (Duncan test) at $p < 0.05$ level.

3.3 Results and discussion

During the quantification of α-glucosidase activity and measuring the activity of inhibitors, maltose or sucrose were hydrolysed into glucose (and fructose in the case of sucrose). The α-glucosidase activity was measured by the generated glucose by the GOP assay. The commonly used chromophore in

GOP assay is *o*-dianisidine, which is oxidized by peroxidase to give brown azo dye via a blue charge transfer complex meriquinone **(Figure 17)**. The polyphenolic compounds may interfere with the assay by reacting with meriquinone, which will lead to false negatives of the glucose or false positives in α-glucosidase inhibitory activity. To assess the severity of interference by different polyphenolic compounds by reducing meriquinone intermediate, we applied SDS at pH 4 according to literature reports to stabilize the positively charged meriquinone intermediates through electrostatic interaction with the negatively charged surfactant (*162*, *163*).

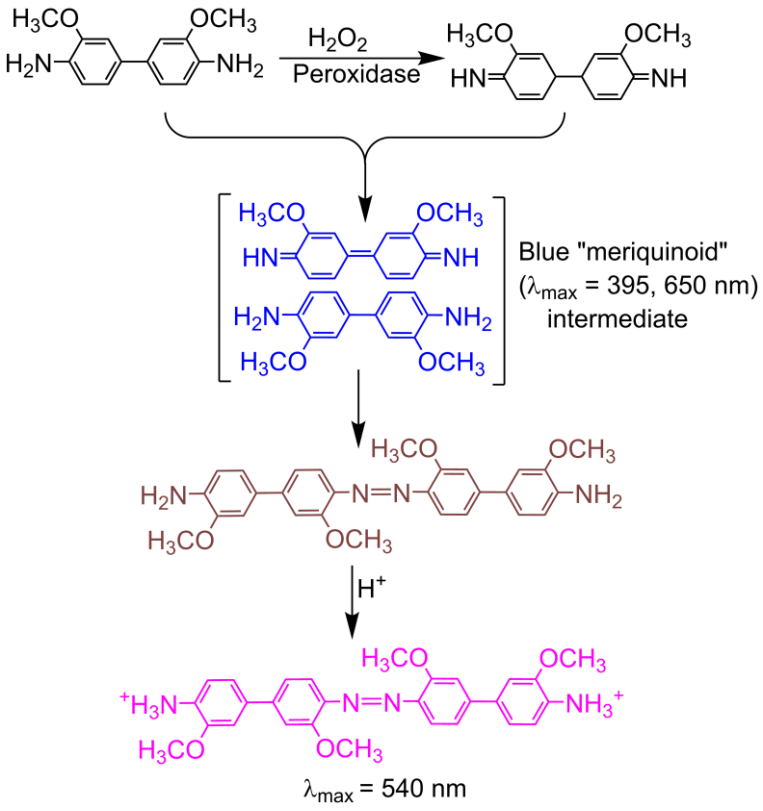

Figure 17. Reaction scheme of *o*-dianisidine oxidation. Hydrogen peroxide reacts with colorless reduced *o*-dianisidine in the presence of peroxidase to form the dianisidine quinonediimine intermediate. Application of SDS suspend the meriquinoid complex intermediate (λ_{max}= 395; 650 nm). Irreversible coupling reaction with two quinonediimines to form the brown bisazobiphenyl product. Bisazobiphenyl product reacts with H_2SO_4 to form a more stable pink colored product (λ_{max}= 540 nm).

3.3.1 Ascorbic acid

When ascorbic acid was added to the meriquinone solution at concentrations of 25 µM and 50 µM (1:4 and 1:2 ratio with reference to H_2O_2), there was an initial marked decrease in absorbance but also a regain of the blue colour from 10 to 250 seconds **(Figure 18A)**. Apparently, the ascorbic acid is consumed quickly by oxidation with meriquinone leading to the fading of blue colour. The increase in absorbance is due to the regeneration of meriquinone intermediates formed by enzymatic catalysed oxidation of *o*-dianisidine as there was a surplus of H_2O_2. When ascorbic acid was added at a ratio of 1:1 with H_2O_2 (100 µM), there was a dramatic reduction in the meriquinone solution to a colourless solution without any regain of colour. This finding suggests that vitamin C only reacts with meriquinone but does not inhibit peroxidase.

We further monitored the reduction kinetics of the meriquinone intermediate reaction with coumaric acid, caffeic acid, gallic acid, and epigallocatechin gallate with concentration equal to that of H_2O_2 **(Figure 18B)**. Coumaric acid with only one hydroxyl group (OH) did not show much reactivity, while caffeic acid can lead to 50% interference at steady state throughout the remaining time. A further addition of an OH group in gallic acid was shown to reduce 75% of the absorbance values, from 0.8 to 0.2. The dependency on the number of OH groups in the phenolic acid is consistent with the increasing reducing activity from mono to tri-OH moieties. These preliminary results prompted us to systematically evaluate the interference of common polyphenolic compounds.

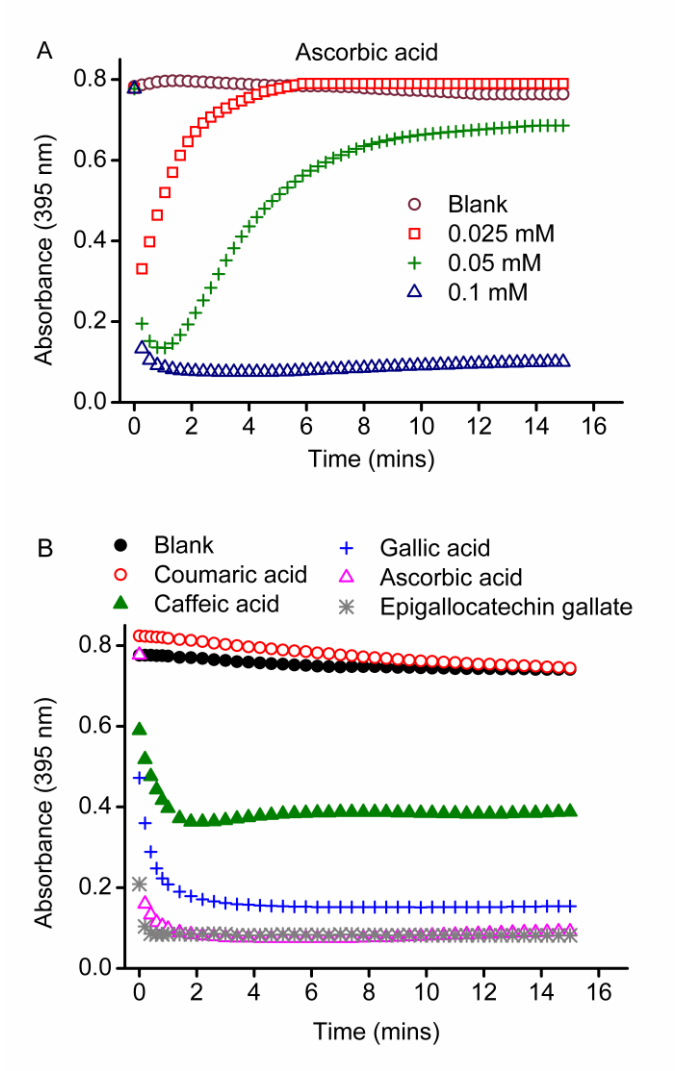

Figure 18. (A) Reduction kinetics of the meriquinone structure monitored at 395 nm for 15 minutes at various stoichiometries of H_2O_2 concentration to ascorbic acid (ratio of 4:1, 2:1 and 1:1). (B) Reduction kinetics (monitored at 395 nm for 15 minutes) of the meriquinone structure of coumaric acid, caffeic acid, gallic acid, ascorbic acid and EGCG at stoichiometric ratio of 1:1 H_2O_2: sample concentration.

3.3.2 Reduction of meriquinone intermediate by polyphenolic compounds

To delineate the structure and activity relationship, we measured 31 commonly found polyphenolic compounds and the results are shown in **Figure 19** arranged by their structural groups. Each class of compounds will be discussed respectively. The degree of interferences was divided in three

groups whereby polyphenolic compounds with a % interference of less than 20 would be classed as having "no interference" (grey colour). Degree of interference between 20-70 % are classed as the "intermediate interference" group (blue colour) and polyphenolic compounds with interference above 70 % are considered to have "high interference" (red colour).

Flavones. As shown in **Figure 19A**, chrysin and apigenin have no interference ($p < 0.05$) indicating that the A ring OH group at 5 and 7 positions do not enable them in reduction of meriquinone. In contrast, apigenin isomer, 7 (or 5), 3′, 4′-trihydroxyflavone exhibit significant activity. This plus the fact that luteolin having a similar activity suggests that the catecholic unit is sufficient for the reduction of meriquinone. In agreement with this, 7, 8-dihydroxyflavone also has a comparable activity albeit it has only two OH groups. In this series, pentahydroxyflavone possesses the strongest activity because it has three *ortho*-OH groups at the B ring.

Flavanones. The common flavanones naringin, hesperetin and its glycoside counterpart hesperedin all showed intermediate interference activity as shown in **Figure 19B**. The reason was that the B rings of the tested flavones do not contain catecholic units. Apparently, methoxylation of catechol unit will lead to a reduced activity. In addition, there was no difference between hesperidin and hesperetin suggesting that the OH group in C-7 position of the A ring does not contribute to the activity of reducing meriquinones. These flavanones do possess some antioxidant activity, although the activity is much weaker compared with many other flavonoids (*164, 165*). Similar to the case of rutin, the glycosylation of hesperedin did not influence the interference percentage ($p > 0.05$).

Phenolic Acids. Coumaric acid shows a partial interference even though it only has one OH group, this is very different from that of isoflavones, which have multiple OH groups but only has very weak interferences **(Figure 19C)**. In addition, ferulic acid and caffeic acid show stronger interferences that is comparable to that of chlorogenic acid. Gallic acid also exhibits strong interference. Therefore, it is reasonable to conclude that hydrolysable tannins, which are the major group of polyphenolic compounds in the plant kingdom, will also have strong interference because gallates are the main moiety in hydrolysable tannins. Indeed, tannic acid shows a strong interference. Similarly, caffeic acid has two OH groups arranged in the *ortho* position and was shown to have percent interference of 88.91 ± 2.35 which was comparatively high. The percent interference of caffeic acid was not significantly different ($p > 0.05$) to that of gallic acid (due to the additional OH group) and ferulic acid (due to the CH_3O group). In the case of ferulic acid, one methoxy substitution at the *ortho* position relative to the hydroxyl group slightly decreased the interference (84.89 ± 2.8), but the decrease was not significant ($p > 0.05$). *Ortho* substitution with an electron donor of a methoxy group stabilizes the aryloxyl radical and thus its antioxidative action. However, the impact of a methoxy group is far from being equivalent to the addition of a hydroxyl group. The removal of either the methoxyl or hydroxyl group results in the phenolic ring resulted in a sharp decrease in the % interference as seen by the coumaric acid structure. Monophenols are known to be less efficient in antioxidant activity (*166, 167*).

Flavan-3-ols. Similar to previous reports, we found that all flavan-3-ols (catechins) exhibit strong interferences **(Figure 19D)**. At the tested

concentration, there was no difference among the catechins. The catecholic units in the B ring and/or the *ortho*-trihydroxy groups in the B ring and galloyl units are certainly potent in reducing meriquinones (*168*).

Flavonols. With eleven compounds, this group is the largest category and all of them exhibit a certain degree of interference **(Figure 19E)**. The degree of interference is roughly correlated to the number of OH groups except rutin, which has four OH groups but the interference activity is much weaker than that of its aglycone quercetin. Therefore, 3-OH group contributes significantly to the activity. In this series, the *ortho*-OH group at B ring increase the activity as it is apparent by comparing the values of kaempferol and quercetin. 3, 5-dihydroxyflavone, 3, 7-dihydroxyflavone and galangin showed intermediate interference. These three compounds have a similar feature in that it lacks any hydroxy group in the B-ring of its structure but differ in the OH group present in the A and C-ring. The hydroxy position of 3, 7-dihydroxyflavone showed a significantly stronger interference compared to 3, 5- dihydroxyflavone. Galangin, which has OH groups on the 3, 5, 7-position did not significantly increase interference compared to 3, 7-dihydroxyflavone. The addition of a hydroxyl group (monohydroxyl substitution) in the B-ring as seen in kaempferol increased the percent interference significantly ($p < 0.05$). It has been proposed that the single 4'-hydroxyl group in the B-ring has the potential to conjugate with the 3-hydroxyl group through conjugation of the C-ring.

The phenoxyl radical formed could abstract an electron from the radical cation to generate a dication and the phenolate (*166*). The addition of another hydroxyl group in the 5' position of the B-ring as seen in myricetin did

not significantly ($p > 0.05$) alter the interference as compared to quercetin. This is on par with other studies, which have shown that the presence of a third hydroxyl group in the B-ring at C-5 position did not enhance the effectiveness of myricetin compared to quercetin (*167*). The stabilizing effect of the extra radical is provided by only one of the two hydroxyls *ortho* to the hydrogen-donating hydroxyl group (*168*). Studies have also suggested that a hydrogen atom is most likely donated from the 3-OH, which leads to a more stable radical tautomer (*169, 170*). The radical scavenging property of flavonoids has been attributed to the number of OH's that are present in the ring structure (*171, 172*).

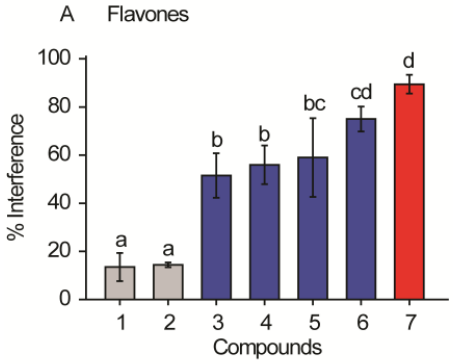

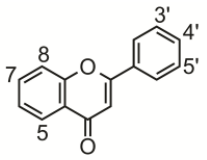

No.	Name	5	7	8	3'	4'	5'
1	Chrysin	OH	OH				
2	Apigenin	OH	OH			OH	
3	7,3',4'- trihydroxyflavone		OH		OH	OH	
4	5,3',4'- trihydroxyflavone	OH			OH	OH	
5	Luteolin	OH	OH		OH	OH	
6	7,8- dihydroxyflavone		OH	OH			
7	5,7,3',4',5'- pentahydroxyflavone	OH	OH		OH	OH	OH

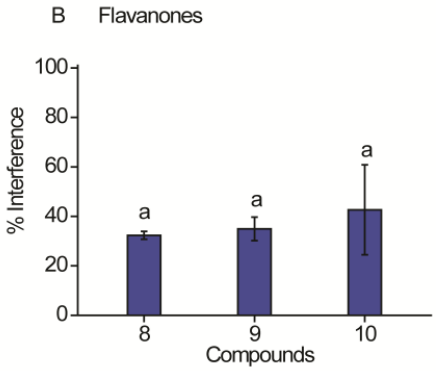

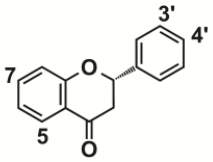

No.	Name	5	7	3'	4'
8	Hesperedin	OH	$C_{12}H_{22}O_{10}$ (rutinose)	OH	OCH_3
9	Naringin	OH	$C_{12}H_{22}O_{10}$ (rutinose)		OH
10	Hesperetin		OH	OH	OCH_3

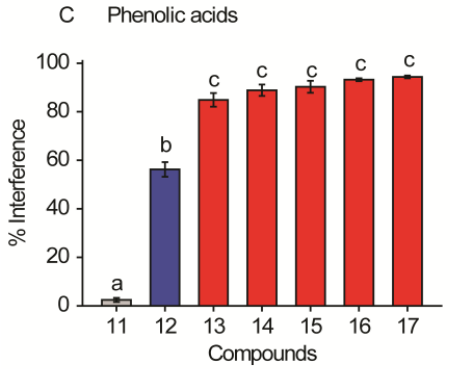

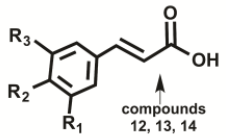

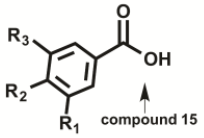

No.	Common name	R1	R2	R3
11	Quinic acid			
12	Coumaric acid		OH	
13	Ferulic acid	OCH_3	OH	
14	Caffeic acid	OH	OH	
15	Gallic acid	OH	OH	OH
16	Chlorogenic acid			
17	Tannic acid			

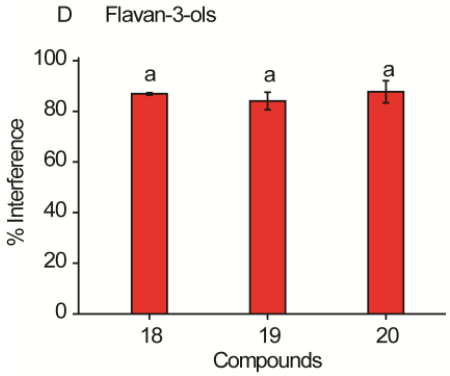

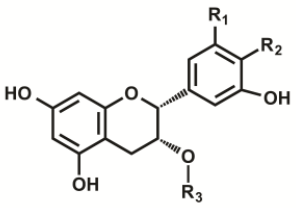

No.	Common name	R1	R2	R3
18	(-)-epicatechin		OH	
19	(-)-epigallocatechin	OH	OH	
20	(-)-epigallocatechin gallate	OH	OH	galloyl

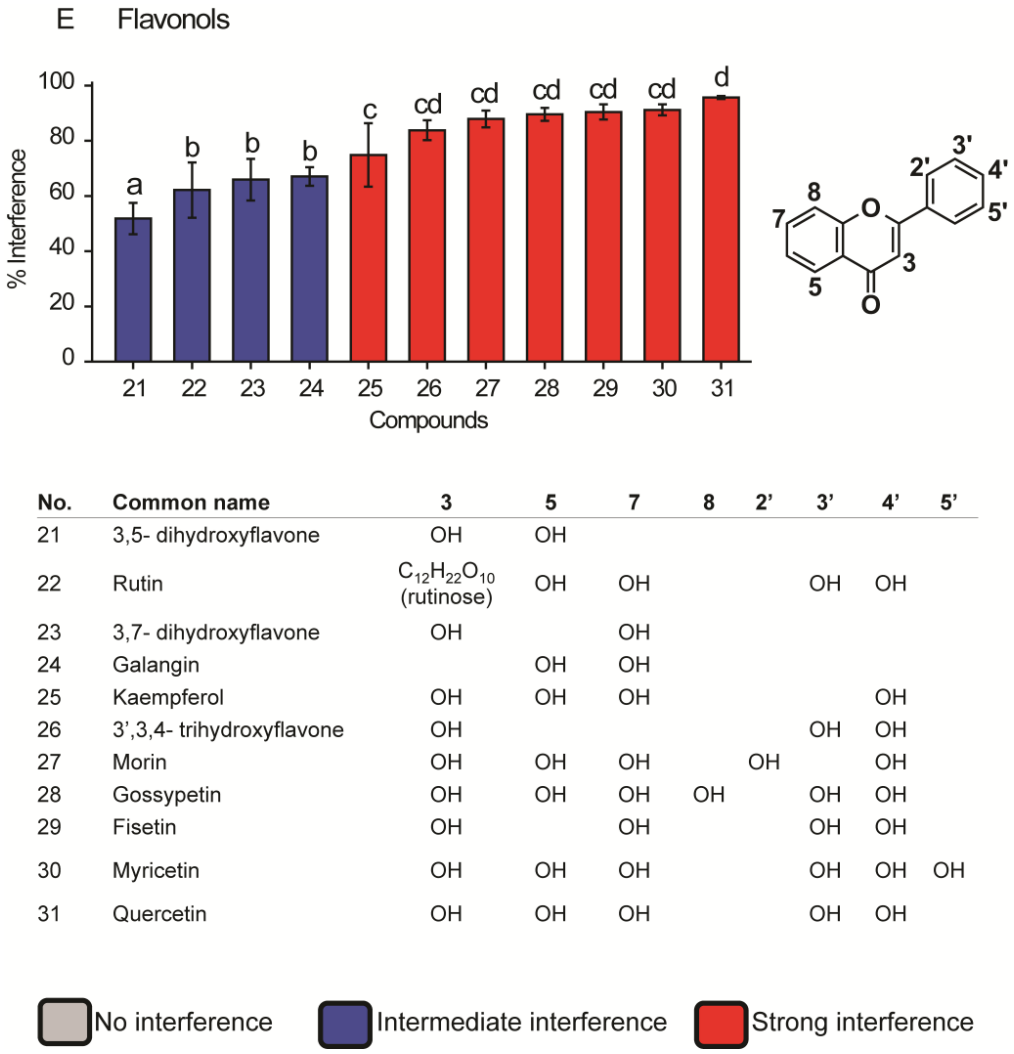

No.	Common name	3	5	7	8	2'	3'	4'	5'
21	3,5- dihydroxyflavone	OH	OH						
22	Rutin	$C_{12}H_{22}O_{10}$ (rutinose)	OH	OH			OH	OH	
23	3,7- dihydroxyflavone	OH		OH					
24	Galangin		OH	OH					
25	Kaempferol	OH	OH	OH				OH	
26	3',3,4- trihydroxyflavone	OH					OH	OH	
27	Morin	OH	OH	OH		OH		OH	
28	Gossypetin	OH	OH	OH	OH		OH	OH	
29	Fisetin	OH		OH			OH	OH	
30	Myricetin	OH	OH	OH			OH	OH	OH
31	Quercetin	OH	OH	OH			OH	OH	

Figure 19. Interference of various compounds (represented in numerics) and subdivided according to their respective classes. (A) Flavones (B) Flavanones (C) Phenolic acids (D) Flavan-3-ols (E) Flavonols. Significant difference between means were analysed using one way ANOVA (Duncan test) where different alphabets represent significant differences at the $p < 0.05$ level.

In addition, the configuration of the H-donating hydroxyl groups is also one of the main structural features, which influence the antioxidant capacity of phenolics (*173*). Furthermore, compounds in the "high interference" group possess many OH groups that are in the *ortho* position. The *ortho* arrangement of OH groups causes the development of Intramolecular Hydrogen Bond which is able to stabilize the radical, leading to

a lower O-H Bond Dissociation Enthalpy (BDE). The BDE governs the ability of a particular flavonoid to donate hydrogen atoms and the lower the BDE value, the higher the ability of a flavonoid to donate hydrogen (*174*).

3.3.3 Correlation of degree of interference and antioxidant activity measured by 2, 2-Diphenyl-1-picrylhydrazyl (DPPH) radical scavenging activity

Since meriquinone is an oxidant and its reaction with polyphenolic compounds has some similarity to the reaction used in measuring the antioxidant activity as the DPPH assays. If there is a good correlation of interference and the DPPH assay, one might be able to apply the DPPH assay to conveniently distinguish the likelihood of interference of any given plant extracts. Therefore we attempted to correlate the degree of the interference and the IC_{50} of the polyphenolic compounds for DPPH assay and the results are shown in **Figure 20**. In general, those compounds with a high interference also had a high antioxidant activity (i.e. low IC_{50} of DPPH assay) but there was no linear correlation. Therefore, DPPH may be qualitatively applied to judge the potential interference of the GOP assay. Measuring the turbidity decrease during enzymatic starch hydrolysis is a faithful way to test enzyme activity and it is not subjective to interference due to reducing activity of the phenolic compounds. We applied this method to evaluate inhibitory activity of α-glucosidase, and found that these compounds have no measurable activity. These results highlighted the limitation of the GOP assay in natural products.

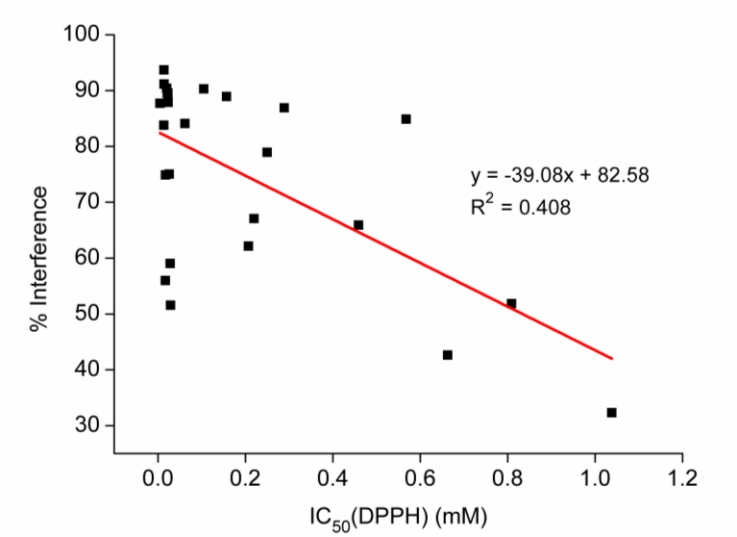

Figure 20. Correlation between % Interference of compounds and the IC_{50} of DPPH (mM).

3.4 Conclusion

In conclusion, I have illustrated that the majority of polyphenolic compounds found in the plant kingdom have a significant interference on the GOP assay. Since the reaction with the free radical intermediate is likely to be a reduction reaction it is reasonable to assume that, radical scavengers will have a false positive interaction. This effectively makes the GOP assay not useful in measuring the α-glucosidase inhibition activity of botanical extracts. It is essential to test the interference first before applying the GOP assay for quantification of α-glucosidase activity. Recently, our group developed a high throughput method for screening α-glucosidase and α-amylase inhibition activity of natural products using turbidity changes (*175*). In this assay, natural starch was applied as the substrate and acarbose was used as a reference standard. Since turbidity is a physical parameter of the starch solution, one would expect that it would be more resistant to the interference of chemical reactions.

Chapter 4

Screening of edible plants from the Singapore Botanic Gardens for starch hydrolase inhibitors

4.1 Introduction

Plant-based medicinal therapy like that of TCM, Indian Ayurveda and Arabic unani has been applied since ancient times to treat or prevent different kinds of metabolic diseases. Moreover, herbal remedies seem to offer a gentler yet effective means of managing diseases like diabetes, but the actual mechanism or active compositions are not known. Although it is commonly believed that they hardly have any adverse effects on the body, verification through rigorous scientific research is required (*176*). Many of these medicinal plants originate from rainforests. Southeast Asian rainforests are known to be home to some hundreds of medicinal plants which are biochemically diverse, in addition to providing an important resource for natural medicine, as well as for discovering new cures. In fact, many of the currently available drugs are directly or indirectly derived from plants; for instance, the commercially available hypoglycaemic drug, metformin, is derived from *Galega officinalis* (*177*). There are about 800 plant species that have been reported to possess anti-diabetic properties (*178*). Yet it was estimated that less than 10% of these plant species have been investigated chemically (with less than 1% assessed in greater detail) (*179*).

A 1991 report on diabetes by the World Health Organisation (WHO recommended that intensive research on the beneficial effects of medicinal plants be performed in order to capitalise on the medicinal benefits derived from their bioactive components. In line with this recommendation, our study focuses on the screening of medicinal plants from the Southeast Asian region. The Healing Garden, launched in 2010, is located within the Singapore Botanic Gardens (SBG) and is considered to be one of the largest medicinal gardens in the Southeast Asia region, spanning 1.5 hectares. The Healing Garden showcases an extensive collection of over 500 species of medicinal plants that have been traditionally used in Southeast Asia and other tropical regions of the world. Our research will specifically be selecting for starch hydrolase inhibitors by applying high-throughput screening methods. One of the aims of this paper is to discover more specific and effective enzyme inhibitors (already an important area of investigation), particularly found in edible botanicals. This area of research is vital because conventional drugs like acarbose, which is a known AGH inhibitor when ingested, produces undesirable gastrointestinal side effects like diarrhoea, flatulence and abdominal pain, making it unpopular as an anti-diabetic drug (*47*). It was hypothesized that the reason behind the side effects caused by these drugs was because of their non-specificity in targeting different glycosidases, resulting in abnormal bacterial fermentation of undigested carbohydrates in the colon (*48*). Additionally, this study also screens for the total phenolic contents (TPC) of the various plant sample extracts. Polyphenolic compounds have been linked to an overall increase in glucose homeostasis and insulin resistance through various mechanisms like increasing insulin-dependent glucose uptake via GLUT4, protecting pancreatic β-cells against oxidative damage, inhibiting intestinal sodium-dependent glucose

transporters (SGLT1 and SGLT2) and several others (*180*). In order for the team to obtain a wide selection of medicinal plants, permission was obtained to launch a sampling exercise on plants grown in the Healing Gardens.

4.2 Materials and methods

4.2.1 Reagents and instruments

Porcine pancreatic α-amylase (A3176, type VI-B), rat intestinal α-glucosidase (I1630), corn starch (S4126), acarbose (A8980), Folin-Ciocalteu's phenol reagent, anhydrous sodium carbonate, gallic acid, 4-dimethylaminocinnamaldehyde (D4506), and hydrochloric acid (37%) were purchased from Sigma-Aldrich (St. Louis, MO, USA). Procyanidin A2 (min. 99%) was purchased from Cfm Oska Tropitzsch (Marktredwitz, Germany).

4.2.2 Collection, preparation and extraction of botanical materials

The plant materials were collected between the periods of December 2012 to July 2013 from the Healing Gardens located within SBG. The plants were authenticated by SBG and current plant names have been verified with The Plant List (www.theplantlist.org), which is a collaborative online database created and updated by the Royal Botanic Gardens, Kew and Missouri Botanical Garden. Samplings were done under the supervision of at least one SBG officer who also verified the identification of the plants. Immediately after the sample collection, parts of the plant (leaf, stem and flower) were separated, washed thoroughly and blotted dry to remove any possible trace of impurities or potential contamination. Subsequently, samples were frozen in a -20 ºC freezer, frozen dried and ground to powder with an electric grinder.

Each of the resulting powdered samples (0.5 g) were accurately weighed into a 50 mL centrifuge tube and extracted with 10 mL of solvent mixture acetone, methanol and water at a ratio of 2:2:1 (AMW; 2:2:1, v/v). Different groups of compounds, with varying polarities, respond to different mixtures of extraction-solvent systems, which will collectively influence the potency for enzyme inhibition. This particular solvent mixture was selected according to a previous study (*109*) that compared different extraction methods, such as 100 % water and 70 % ethanol. It was discovered that this solvent ratio of AMW; 2:2:1, v/v gave the highest enzyme inhibition activity; hence, this solvent mixture will be utilised in this study. The centrifuge tube was stirred vigorously with a vortex until all the powder was suspended within the solvent and this was followed by continuous extraction using a rotary shaker for 24 hours at room temperature. After the extraction, the samples were centrifuged at 4000 rpm/min for 15 minutes at 15 ºC, and the supernatant collected and filtered using filter paper. Volatiles were evaporated by a rotary evaporator and the dried residue weighed and further dissolved in AMW solvent mixture for further tests.

4.2.3 Determination of total phenolic content (TPC)

The TPC was estimated using the Folin-Ciocalteu reagent according to previous protocols (*181, 182*). Firstly, 20 µL of sample extract supernatants were diluted to appropriate levels and mixed with 100 µL of 10 % (v/v) F-C reagent, vortexed thoroughly and allowed to react for 15 minutes at room temperature. Sodium carbonate (80 µL, 700 mM) was added to the mixture and allowed to stand for 30 minutes at room temperature for colour development. Gallic acid was used as a standard (50 µM- 2.5 mM gallic acid

in 95 % v/v methanol) and the results are expressed in terms of gallic acid equivalents (GAE). Absorbance was read at 765 nm using a multi-detection microplate reader (Synergy HT, Bio-Tek).

4.2.4 Determination of Proanthocyanidins content

A validated and improved 4-dimethylaminocinnamaldehyde (DMAC) colourimetric method (*183*) was applied to estimate the concentration of proanthocyanidin in sample extracts. Acidified ethanol was prepared by adding concentrated (36 %) hydrochloric acid (12.5 mL) to distilled water (12.5 mL) and ethanol (75 mL, 91 %) in a glass bottle, and mixed. The DMAC reagent (0.1 %) was prepared by weighing 0.05 g of DMAC to 50 mL of acidified ethanol. For the analysis, the incubation chamber was pre-heated to 25 ºC. Seventy microliters of control, standard, blanks and samples were dispensed into the well of a 96-well plat where the control is definted as the working solution without the test extract, the standard is procyanidin A2 solution, the sample is the working solution with the test extract and the blank is the dissolving solvent for the standard. The DMAC reagent (210 µL) was added to the wells, bringing the final volume to 280 µL/well. Aliquots of stock solution (1.5 mL) of procyanidin A2 containing 1 mg was dissolved in 10 mL of ethanol (91 %) to give a final concentration of 100 µg/mL and stored in - 30 ºC. During analysis, 250 µL of ethanol (91 %) was added to 1 mL of stock solution in a 1.5 mL conical tube, and vortexed to give a working solution of 80 µg/mL procyanidin A2 solution. The working solution was diluted twice to generate a calibration standard curve (80, 40, 20, 10, 5, 2.5, 1.25 and 0.625 µg/mL). Maximum absorbance readings were taken at 640 nm for 25 min

using a Synergy HT microplate reader. The results are expressed in terms of procyanidin A2 equivalents (PAE).

4.2.5 High-throughput turbidity assay of α-amylase and α-glucosidase inhibition activity

The inhibition activity was determined using a method that was previously established (*175*). Aliquots of PPA powder were dissolved in phosphate buffer (0.1 M, pH 6.9, spiked with 50 ppm of $CaCl_2$) to give a stock concentration of 4 mg/mL and stored in small vials at -30 ºC. The α-glucosidases were extracted from rat intestinal acetone powder by dissolving 0.5 g of the powder in 20 mL of phosphate buffer and stirred in an ice-bath for 30 minutes before it was centrifuged at 2000 g at 4 ºC for 10 minutes. The supernatant was collected and stored at -30 ºC at aliquots of 250 µL as a stock solution until further use. During analysis, 200 µL of α-amylase / α-glucosidase stock solution was diluted in 3.8 mL of phosphate buffer to give a working stock solution. Corn starch (0.5 g) was dispersed in 25 mL of phosphate buffer in a beaker and stirred through with a magnetic stirrer until it became a milky mixture. The starch suspension was then placed on a hotplate, for 2 min at 400 ºC with continued stirring at 300 rpm, until the solution reached boiling point to produce a gelatinized semi-translucent solution. In each well, 20 µL of PPA (0.2 mg/mL) was mixed with a series of concentration of plant extracts (20 µL) or acarbose as a positive control (final concentration of 40, 27, 18, 12, 8, 5, 3.5 and 2.3 µg/mL) and pre-incubated in the microplate reader for 15 minutes at 37 ºC.

The reaction was initiated by adding 60 µL of the 2 % gelatinized corn starch to each well containing the pre-incubated enzyme-inhibitor mixture.

The 96-well plate was immediately placed onto the microplate reader, and the UV absorbance monitored at 660 nm for 2 hours, with one reading per 30 seconds, and shaking to ensure sufficient mixing and to avoid starch sedimentation. The percentage inhibition is calculated by **Equation 10** where $AUC_{inhibitor}$ is the area under the curve (AUC) of the inhibitor and $AUC_{control}$ is the area under the curve without inhibitors. The IC_{50} is the inhibitor concentration required to produce 50 % inhibition. The concept of acarbose equivalence (AE) was applied and is defined by **Equation 11.**

$$\text{Inhibition (\%)} = 100 \text{ x } \frac{AUC_{inhibitor} - AUC_{control}}{AUC_{inhibitor}} \quad \textbf{(Equation 10)}$$

$$\text{Acarbose equivalence (AE)} = \frac{IC_{50} \text{ of acarbose}}{IC_{50} \text{ of sample}} \quad \textbf{(Equation 11)}$$

4.3 Results and discussion

The turbidity assay was shown to be an effective HTS that could assist in identifying bioactive compounds in botanicals. A total of 298 plant samples were initially collected from the Singapore Botanic Gardens and tested for α-amylase and α-glucosidase inhibition. Preliminary screenings indicated that 170 plants did not show any inhibitory activity. Based on literature reports, another 57 plants were deemed either inedible or toxic, leaving a total of 71 plant samples that are "edible" and "medicinal". "Edible" refers to the category of plants that can be eaten as everyday vegetables, whereas "medicinal" refers to plants that have been used as therapeutic agents (not limited to diabetes) by indigenous people. The IC_{50}, acarbose equivalents (AE) of α-amylase and α-glucosidase inhibitory activity, TPC and PAC of the 71

edible plant extracts are summarized in **Table 2**. Out of the 71 edible plants that were screened, 14 showed promise in terms of their usage in traditional medicinal (which may or may not have been used traditionally to treat diabetes) and they all have varying strength of inhibitory activity against α-amylase and α-glucosidase. These 14 plants are *Antidesma ghaesembilla, Antidesma bunius, Mesua ferrea, Lepisanthes alata, Synsepalum dulcificum, Tamarindus indica, Azadirachta indica, Syzygium cumini, Chrysophyllum cainito, Garcinia mangostana, Laurus nobilis, Drobalanops aromatica, Atuna racemosa and Madhuca longifolia.* Their traditional medicinal uses, enzyme inhibitory activity, PAC and TPC contents are described in greater detail in the following sections.

In order to illustrate the potencies of each plant extract against both α-amylase and α-glucosidase, **Figure 21** shows a scatter plot between the AE of plant samples against α-glucosidase (y-axis) and α-amylase (x-axis). This plot gives a visual assessment of the different inhibitory strengths of each plant sample against the two enzymes, α-amylase (x-axis) and α-glucosidase (y-axis), with three categories of inhibition strength: weak, medium and strong. Thus, each group represents a different combination of inhibition strength against α-glucosidase and α-amylase, and is divided into 9 groups (A, B, C, D, E, F, G, H, and I). Groups A, B and C represent categories of plant extracts that have strong inhibitory activity against α-glucosidase and weak, medium and strong inhibitory activity for α-amylase, respectively. Groups D, E and F are plants that showed medium inhibitory activity against α-glucosidase and weak to strong inhibitory activity against α-amylase respectively. Finally, groups G, H and I are plant extracts that exhibit low inhibitory activity against

α-glucosidase and weak to strong inhibitory activity against α-amylase respectively. A representative sample from each group will be selected and systematically discussed in greater depth in the following sections.

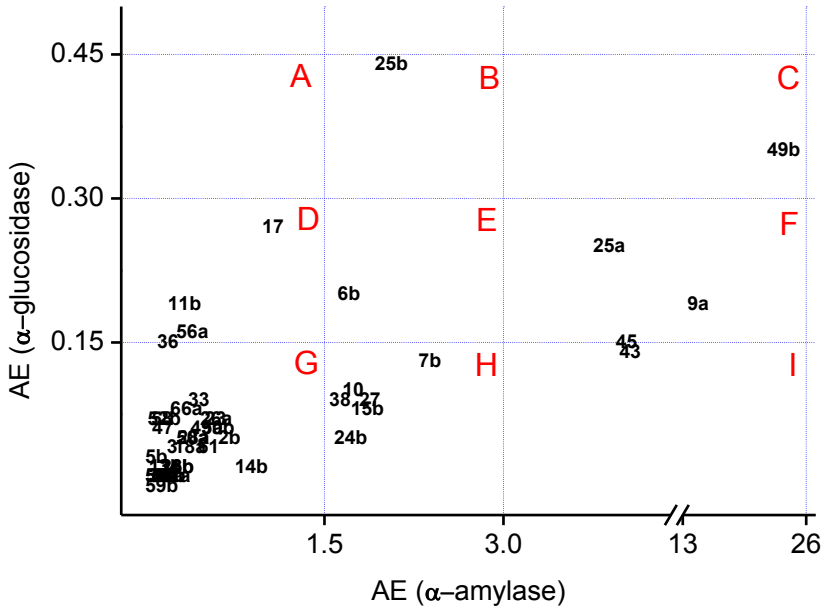

	Level of inhibition activity		Plants within the category
	α-glucosidase	**α-amylase**	
A	Strong	Weak	Nil
B	Strong	Medium	**25b**: Dryobalanops aromatica
C	Strong	Strong	**49b**: Mesua ferrea
D	Medium	Weak	**36**: Garcinia mangostana; **56a**: Parkia speciosa; **68a**: Syzygium cumini; **11b**: Baccaurea parviflora; **17**: Chrysophyllum cainito
E	Medium	Medium	**6b**: Antidesma bunius
F	Medium	Strong	**45**: Madhuca longifolia; **25a**: Dryobalanops aromatica; **9a**: Atuna racemosa
G	Weak	Weak	**59b**: Phyllanthus pulcher; **5a**: Annona muricata; **52a**: Muntingia calabura; **35**: Garcinia atroviridis; **16a**: Cananga odorata; **44**: Lepisanthes rubiginosa; **54b**: Orthosiphon aristatus; **41**: Laurus nobilis; **31a**: Flacourtia inermis; **13b**: Bixia orellana; **70a**: Terminalia catappa; **34**: Galphimia glauca; **26b**: Etlingera elatior; **28b**: Eurycoma longifolia; **71b**: Ziziphus mauritiana; **14b**: Butea monosperma; **5b**: Annona muricata; **3**: Alstonia angustifolia; **18a**: Cinnamomum camphora; **61**: Punica granatum; **50a**: Misocarpus sundaicus; **28a**: Eurycoma longifolia; **2b**: Aleurites moluccana; **47**: Melaleuca cajuputi; **49a**: Mesua ferrea; **50b**: Misocarpus sundaicus; **52b**: Muntingia calabura; **58**: Phyllanthus acidus; **26c**: Etlingera elatior; **23**: Cynometra ramiflora; **69b**: Tamarindus indica; **66a**: Synsepalum dulcificum; **33**: Flemingia strobilifera
H	Weak	Medium	**24b**: Dillenia indica; **15b**: Calophyllum inophyllum; **38**: Hamelia patens; **27**: Eugenia uniflora; **10**: Azadirachta indica; **7b**: Antidesma ghaesembilla
I	Weak	Strong	**43**: Lepisanthes alata

Figure 21. Correlation plot of AE (α-amylase) and AE (α-glucosidase).

i. Group A (Strong α-glucosidase, weak α-amylase inhibitory activity)

Regression analysis showed that the AE of α-glucosidase and AE of α-amylase had only a weak positive correlation (R^2 = 0.32). As such, there are rarely strong α-glucosidase inhibitors with little to no inhibitory activity against α-amylase. In this study, there were no such plants that fit within this category.

ii. Group B (Strong α-glucosidase, medium α-amylase inhibitory activity)

***49: Dryobalanops aromatica* (Dipterocarpaceae)**

Dryobalanops aromatica is also commonly known as the Borneo camphor. This genus is apparently unique, with only a total of seven species that exist worldwide, most of which are confined to the tropical forests of Malaysia (*184*). Previous studies showed that this genus is a good source of resveratrol oligomers such as cis- and trans-diptoindonesin B (*185*), malaysianol A, laevifonol, ampelopsin, α-viniferin, ε-viniferin, diptoindonesin A and bergenin (*184*) Furthermore, dammarane triterpenes can also be found in the resin of the plant (*186*).

Results in this study indicated the TPC of the stem to be about 10 times higher (4501 ± 908 mg GAE/g plant extract) than that of the leaves (411 ± 58 mg GAE/g plant extract). Similarly, the PAC of the stems was also significantly higher than that of the leaves, which were 2696 ± 285 and 66 ± 15 mg PAE/gram plant extract respectively. The strength of inhibitory activity for α-glucosidase and α-amylase is quite unique in that it has relatively high inhibitory activity against α-glucosidase (AE = 0.44) and medium inhibitory activity against α-amylase (AE = 1.92).

iii. Group C (Strong α-glucosidase, strong α-amylase inhibitory activity)

51: Mesua ferrea (Calophyllaceae)

Mesua ferrea, commonly known as Ceylon ironwood, is a tree from the family Calophyllaceae that is indigenous to tropical Asia. In folk medicine, its flowers, leaves, seeds and roots have medicinal properties, and it is used to treat fever, dyspepsis and renal diseases (*187*). In addition, the lipophilic extract of the woody trunk of the tree seems to show significant anti-bacterial activity, which has sparked research interest to seek out the active compounds. Phytochemical investigations show the occurrence of xanthones, coumarins, biflavones, cyclohexanedione derivatives and essential oils (*187*). So far, there have been quite a number of xanthones isolated from the heartwood bark, such as a series of 4-alkyl and 4-phenyl 5, 7-dihydroxycoumarins (*188*), ferruol A (*189*), mesuaxanthones (*190*), 1, 5-dihydroxyxanthone (II), euxanthone 7-methyl ether (IV) and β-sitosterol (*191*), and ferxanthones (*192*). Coumarin derivatives have been isolated from the seeds; canophylial, canophyliol and canophyllic acid from the leaves.

Results in this study show that it has one of the strongest activity amongst the 71 plant samples with an IC_{50} of 0.5 ± 0.01 µg/mL for α-amylase. Interestingly, the activity for α-glucosidase was a lot weaker in comparison (IC_{50} = 22.7 ± 1.8 µg/mL). Besides that, it was also shown to have the highest TPC (6025 ± 1120 mg GAE/g crude extract) which may be related to its high activity against α-amylase. The high PAC content of 220 ± 6 mg PAE/gram of crude extract is likely responsible for its high activity.

iv. Group D (Medium α-glucosidase, weak α-amylase inhibitory activity)

***41: Garcinia mangostana* (Clusiaceae)**

Garcinia mangostana, commonly known as mangosteen, is a tropical tree from India, Myanmar, Malaysia, Philippines, Sri Lanka and Thailand (*193*). The pericarp of the mangosteen fruit has been used medicinally in Southeast Asian countries and in ayurvedic medicine to treat diarrhoea, skin infections, wounds, amoebic dysentery and cholera (*194-196*). The pericarps were found to be rich in xanthones, which are thought to have remarkable biological activity. There are about fifty xanthones that have been isolated from the pericarp (*193*). For α-amylase inhibition activity, however, Loo and Huang (2007) found that the lipophilic xanthone, containing a fraction of the pericarp, did not show any activity of α-amylase, although the inhibitory activity of α-glucosidase was not tested. The fraction which was able to inhibit α-amylase significantly (IC_{50} = 5.2 µg/mL) was attributed to the presence of oligomeric PACs (*197*). On the other hand, another study, which focused on the inhibition of α-glucosidase (*p*NPG assay), showed that xanthones were potent α-glucosidase inhibitors (IC_{50} = 3.2 µg/mL) (*198*). In addition, the study also showed that the ethanolic extract was able to elicit reduction of postprandial blood glucose levels in STZ-induced rats.

Results in this study indicate that extracts from *G.mangostana* leaves are able to inhibit α-amylase and α-glucosidase with IC_{50} of 20 ± 1 µg/mL and 57 ± 1 µg/mL respectively. TPC and PAC tests reveal high phenolic and proanthocyanidin contents of 783 ± 158 mg GAE/g plant extract and 237 ± 18 mg PAE/gram sample respectively.

44: Syzygium cumini (Myrtaceae)

Syzygium cumini, commonly known as jambolan, is thought to have originated from India or the East Indies, but has since found its way into many other countries like Thailand and the Philippines. In Unani and TCM, the leaves and bark are used to control blood pressure and gingivitis. However, the specialty of this plant lies in its seeds, where a decoction of the seeds, taken orally, is reputed to treat diabetes (*199*). An *in vivo* study isolated a compound called mycaminose and showed that it was able to reduce the blood glucose level in STZ-induced diabetic rats (*200*). In addition, *in vitro* studies have shown the seeds to exhibit α-glucosidase inhibition activity (8 ± 0.17 mg/mL), and the active compound inhibiting α-glucosidase isolated and identified as apigenin 7-*O*-glucoside (*201*). Several compounds like myricetin and betulinic acid were isolated from the seeds, and shown to be able to inhibit α-amylase *in vitro (202).* Much attention was focused on the seeds of this plant, as compared to the leaves. However, the seeds were not tested in this study, as no seed samples were available.

The results from this study indicated that leaf extracts were also able to inhibit α-amylase (IC_{50} = 30.9 ± 5.7 µg/mL) and α-glucosidase (IC_{50} = 100 ± 7 µg/mL). TPC tests estimated phenolic contents of about 109 ± 20 mg GAE/g in pure plant extract. The estimated proanthocyanidin content for the leaves was quite low (10 ± 2 mg PAE/gram extract), suggesting that enzyme inhibition may not be due to the proanthocyanidins.

***48: Chrysophyllum cainito* (Sapotaceae)**

Chrysophyllum cainito is native to the Greater Antilles in the Caribbean and has since been cultivated throughout the tropics in Taiwan, India, Thailand, Philippines, Vietnam, Malaysia, Indonesia and Northern Australia. This plant is best known for its fruit, also known as the star apple fruit, which is nutritious and high in antioxidants. Traditionally, the ripe fruits are eaten to treat for inflammation caused by laryngitis, pneumonia and haemorrhages, or are cooked as anti-pyretics. The bark, latex and seeds also have medicinal uses, and are taken to stop diarrhoea, dysentery and haemorrhages. The plant is also taken as a remedy for diabetes, and the decoction of its leaf is taken orally for hyperglycaemia (*203*).

Results in this study showed, for the first time, that *C. cainito* was able to inhibit α-amylase (IC_{50} = 29 ± 1 µg/mL) and α-glucosidase (IC_{50} = 26 ± 7 µg/mL). TPC and PAC tests revealed high amounts of phenolic and proanthocyanidin content, which were 599 ± 74 mg GAE/g pure plant extract and 159 ± 28 mg PAE/gram sample respectively. It is thus reasonable to believe that PACs are responsible for this inhibition.

v. Group E (Medium α-glucosidase, medium α-amylase inhibitory activity)

***46: Antidesma bunius* (Phyllanthaceae)**

Antidesma bunius is a fruit tree that is native to Southeast Asia and Northern Australia. Its fruits have been used to make jam and wine (*204*), possessing a sour taste similar to that of immature cranberries. In the Philippines, it was reported that a concoction of its leaves is used ethnobotanically to manage blood sugar levels (*205*). The general

phytochemical profile of its fruit indicates that it contains flavonoids, phenolics and organic acids (*206*), and its leaves and bark contain dammara-20, 24-dien-3β-ol, friedelin, epitaraxerol and other triterpenoids (*207*). Previous reports have shown that the leaf extracts are active against α-glucosidase (*208*).

Experimental results from this study also show that the leaves are active against α-amylase, with an IC_{50} of 2.4 ± 0.01 µg/mL, and its TPC and PAC were calculated to be 315 ± 35 mg GAE/g plant extract and 86 ± 9 mg PAE/gram sample respectively.

vi. Group F (Medium α-glucosidase, high α-amylase inhibitory activity)

***50: Atuna racemosa* (Chrysobalanaceae)**

Atuna racemosa, commonly known as merbatu, is widely available throughout Malesia and Oceania, spanning the Malay Peninsula to the Pacific Islands of Fiji, Tonga, and Samoa (*209*). The plant extract is reported to be used as an anti-inflammatory massage oil. The plant also has medicinal properties, and its inner, living bark may be soaked in water to make a concoction that is used to treat abdominal pains. Its leaves are also reported to have anti-inflammatory properties and are used to reduce swelling on the leg (*209*). Indeed, the kernel of the nut is shown to possess antibacterial properties, where its potency is dependent on the maturity of the kernel (*210*).

The TPC and PAC contents of the leaves are 305 ± 63 mg GAE/g plant extract and 230 ± 36 mg PAE/g sample respectively. The plant extract displays higher inhibitory activity against amylase (AE = 13.49) compared to

that of glucosidase, which we categorised in the medium range of inhibitory activity (AE = 0.19).

42: Madhuca longifolia (Sapotaceae)

Madhuca longifolia, also widely known as the 'butternut tree' or 'mahua', is considered to be a multi-purpose forest tree, whereby it can be used for food, fodder or fuel. The tree can be found in tropical regions, and is largely located in the central and north Indian plains and forests. Its flowers and fruits are used as food, and is widely consumed by the tribes of western Odisha (*211*). The bark of the plant has been reported to possess anti-diabetic activity (*212*).

TPC and PAC contents were shown to be 326 ± 69 mg GAE/g plant extract and 99 ± 16 mg PAE/gram sample respectively. Our results also indicate that the extracts are active against α-amylase with an IC_{50} and AE of 0.9 ± 1.0 µg/mL and 3.94 respectively. For α-glucosidase, the IC_{50} and AE values were 17.1 ± 0.8 µg/mL and 0.15 respectively.

vii. Group G (Weak α-glucosidase, weak α-amylase inhibitory activity)

33: Synsepalum dulcificum (Sapotaceae)

Synsepalum dulcificum is an evergreen shrub that is native to the western tropics and west central Africa. It has been introduced into many Southeast Asian countries, Australia, and in the United States. Its red berries contain an interesting glycoprotein called miraculin, which is tasteless on its own, but remarkably able to modify a sour taste into a sweet taste. Studies have also reported that miraculin can reduce insulin resistance in rats (*213*). In the stems, there were a number of compounds isolated, namely: dihydro-

feruloyl-5-methoxytyramine, (+)-syringaresinol, (+)-epi-syringaresinol, 4-acetonyl-3, 5-dimethoxy-*p*-quinol, *cis*-*p*-coumaric acid, *trans*-*p*-coumaric acid, *p*–hydroxybenzoic acid, syringic acid, vanillic acid, veratric acid, N-*cis*-feruloyltyramine, N-*trans*-feruloyltyramine and N-*cis*-caffeoyl tyramine (*214*). For the leaves, eight compounds were reported to be isolated, namely: sitosterol and stigmasterol, pheophytin-a, pheophytin-b, lupeol, lupenone, lupeol acetate, and tocopheryl quinone (*215*).

This work is the first of its kind to study the inhibitory activity of this species against α-amylase and α-glucosidase. The IC_{50} values of the leaf extract for α-amylase and α-glucosidase are 22.0 ± 18.0 and 37.9 ± 3.6 µg/mL respectively.

32: Tamarindus indica (Leguminosae)

Tamarindus indica, popularly known as tamarind, is an important multi-purpose tropical fruit tree originating from the Indian subcontinent. It is widely used as traditional medicine in India, Africa, Pakistan, Nigeria and most tropical countries. Although a lot of research focuses on the fruit pulp of this tree, every part of the plant, from the root to the leaf, may be beneficial for human needs. Traditionally, it has been used to treat many ailments including abdominal pain, diarrhoea, wounds, malaria, fever, constipation and eye diseases. It is also rich in phytochemicals and is reported to possess anti-microbial, anti-malarial, hepatoprotective, anti-asthmatic, laxative, anti-hyperlipidemic and anti-diabetic effects (*199, 216*). For anti-diabetic properties, several *in vivo* experiments have indicated that the aqueous extract of the leaves and seed of *T.indica*, when fed to diabetic wistar rats, lowered blood glucose levels to normal in a glucose tolerance test (*217-219*). *In vitro*

studies also showed that the extract of the leaves led to an α-amylase inhibition of 90 % (*220*).

Similarly, results in this study indicated that the stems of the plant inhibited α-amylase with an IC_{50} of 4.4 ± 1.0 µg/mL and α-glucosidase with an IC_{50} of 30.2 ± 12.7 µg/mL. TPC and PAC tests revealed relatively high amounts of phenolic and proanthocyanidin content of 413 ± 70 mg GAE/g plant extract and 201 ± 17 mg PAE/g respectively.

***8: Laurus nobilis* (Lauraceae)**

Laurus nobilis originated from tropical southern Asia, and is now distributed in the West Indies, South and Central America, the Mediterranean region and in Africa. Traditionally, it has a variety of medicinal uses. It can be taken orally as a carminative, tranquilizer, to improve circulation, antispasmodic for abdominal colic, to induce menstruation and as an emmenagogue. Externally, it may be applied as an anti-rheumatic, and to soften tumours and ulcers. Some of its reported pharmacological activities are its anti-bacterial, anti-hypertensive, anti-inflammatory, anti-fungal and hypoglycaemic effects, among several others (*199*). A study found that the consumption of 1-3 g/day of *L.nobilis* for 30 days was able to decrease the risk factors for diabetes and cardiovascular diseases (*221*). Several *in vitro* studies have shown the essential oil obtained from *L.nobilis* to be potent inhibitors of α-amylase and α-glucosidase (*222*, *223*).

viii. Group H (Weak α-glucosidase, medium α-amylase inhibitory activity)

***38: Azadirachta indica* (Meliaceae)**

Azadirachta indica, famously known as the 'neem tree', is used in ayurvedic medicine for treating diabetes mellitus and peptic ulcers. Due to its medicinal properties, this plant has been extensively studied over the past, which has led to the isolation and characterization of more than 135 compounds (*224*). *In vivo* studies showed that the seed oil and leaf extracts are able to lower blood glucose in diabetic animals (*225, 226*). The active compounds that are thought to be responsible for its hypoglycaemic effect comes from tetranortriterpenoids called meliacinolin (*227*).

Results in this study show that *A. indica* inhibited α-amylase (IC_{50} = 17 ± 1 µg/mL) and α-glucosidase (IC_{50} = 73 ± 7 µg/mL). TPC and PAC tests revealed relatively high amounts of phenolic and proanthocyanidin content of 189 ± 27 mg GAE/g crude extract and 35 ± 5 mg PAE/gram sample respectively.

***39: Antidesma ghaesembilla* (Phyllanthaceae)**

Antidesma ghaesembilla is a wild, edible, dioecious plant and its leaves have been used by the tribal people of the Western Ghats as medicine for headaches. Its stem is used to stimulate menstrual flow, and the fruit used as a purgative (*228*).

Experimental results from this study show that the leaves and stem both have strong inhibitory activity against α-amylase, with IC_{50} values of 1.4 ± 0.01 and 2 ± 0.01 µg/mL respectively. Their activity against α-glucosidase, however, was much lower compared to α-amylase (IC_{50} = 17.6 ± 7.9 µg/mL).

The TPC for the stem and leaves were estimated to be about 186 ± 23 and 360 ± 65 mg GAE/g plant extract respectively. For the proanthocyanidin content, the leaves have much lower levels of proanthocyanidins (48 ± 7 mg PAE/gram plant extract) as compared to the stems (171 ± 27 mg PAE/gram plant extract).

ix. Group I (Weak α-glucosidase, strong α-amylase inhibitory activity)

***40: Lepisanthes alata* (Sapindaceae)**

Lepisanthes alata is a small tree of about 4-5 m tall originating from the Sapindaceae family. The aril of the fruits can be eaten when it has ripened, and the young leaves are usually cooked and eaten as vegetables in southern Thailand (*229*). Results in this study indicate that the leaves possess relatively strong inhibitory activity against α-amylase (IC_{50} = 7 ± 0.01 μg/mL) and α-glucosidase (50 ± 4 μg/mL). The active compound of this plant warrants further research.

Table 2. The total phenolic content, proanthocyanidins content, IC_{50} & acarbose equivalent of α-amylase & α-glucosidase of plant extracts collected from the Singapore Botanic Gardens.

No.	Latin Name	Common names	Plant part	Edibility [e]	TPC ± SD (mg GAE/g plant extract)[a]	PAC ± SD (mg PAE/ gram sample) [b]	IC_{50} (amylase) µg/mL ± SD [c]	AE [d] (amylase)	IC_{50} (AGH) µg/mL ± SD [c]	AE [d] (AGH)
1	*Alangium ridleyi*	Lajik kuning, medong	leaf	Medicinal	2689 ± 1433	2 ± 0.5	-	-	337.4 ± 0.0	0.02
2	*Aleurites moluccana*	tutui, candlenut; nuez, nuez de India (Puerto Rico);lumbang (Guam); Sakan (Palau); lama (Am. Samoa), Candlenut Tree, Belgaum Walnut, Kekui Oil Plant, Bancouloilplant, Lumbangoilpant, Otaheite walnut, Candle Nut, Stonechestnut, Indian Walnut, Candlenutree, Candlenu Tree	stem	Medicinal	91 ± 7	39 ± 4	5.0 ± 2.0	0.61	73 ± 11	0.05
			leaf	Medicinal	240 ± 48	106 ± 20	-	-	42	0.29
3	*Alstonia angustifolia*	Pulai Penipu Paya; Red-leaved Pulai	leaf and stem	Medicinal	369 ± 74	274 ± 46	13 ± 4	0.18	83 ± 9	0.04
4	*Anacardium occidentale*	Cashew Nut; Gajus; Cashew; Janggus; Jambu Gajus; Jambu Golok; Keterek; Terek; Jambu Bongkok; Jagus	leaf	Medicinal	299 ± 74	162 ± 30	-	-	32 ± 4	0.11
			stem	Medicinal	428 ± 49	139 ± 81	-	-	-	-
5	*Annona muricata*	Brazilian pawpaw, soursop, prickly custard apple, Soursapi	leaf	Edible	195 ± 19	75 ± 9	401 ± 267	0.00	181 ± 112	0.01
			stem	Edible	313 ± 49	-	620 ± 183	0	332 ± 59	0.03

No.	Latin Name	Common names	Plant part	Edibility [e]	TPC ± SD (mg GAE/g plant extract)[a]	PAC ± SD (mg PAE/ gram sample) [b]	IC_{50} (amylase) µg/mL ± SD [c]	AE [d] (amylase)	IC_{50} (AGH) µg/mL ± SD [c]	AE [d] (AGH)
6	*Antidesma bunius*	Its common Philippine name and other names include bignay, bugnay or bignai, Chinese-laurel,Herbert	leaf	Edible	315 ± 35	86 ± 9	2.4 ± 0.0	1.33	-	-
		River-cherry,Queensland-cherry,salamander-tree,wild cherry,and currant tree.	stem	Edible	296 ± 55	105 ± 13	22 ± 3	1.61	60 ± 28	0.20
7	*Antidesma ghaesembilla*	Sekinchak, Black Currant Tree; Gunchak; Gunchek; Guchek; Gunchian; Gunchin	leaf	Edible	186 ± 23	48 ± 7	2.0	1.60	-	-
			stem	Edible	360 ± 65	171 ± 27	1.4 ± 0.0	2.29	18 ± 8	0.13
8	*Ardisia elliptica*	Seashore Ardisia; Mata Pelanduk; Penah; Periah; Buah Letus; Cempenai; Daun Bisa Hati; Mata Ayam; Mata Itek; Mata Pelandok; Mempenai; Rempenai	leaf	Medicinal	271 ± 11	88 ± 7	-	-	14 ± 2	0.21
9	*Atuna racemosa*	Merbatu	leaf	Medicinal	305 ± 63	230 ± 36	1.4 ± 0.4	13.49	0.9 ± 4.0	0.19
			stem	Medicinal	378 ± 37	213 ± 24	-	-	11 ± 1	0.25

No.	Latin Name	Common names	Plant part	Edibility [e]	TPC ± SD (mg GAE/g plant extract)[a]	PAC ± SD (mg PAE/ gram sample) [b]	IC_{50} (amylase) µg/mL ± SD [c]	AE [d] (amylase)	IC_{50} (AGH) µg/mL ± SD [c]	AE [d] (AGH)
10	*Azadirachta indica*	The English name neem is borrowed from Hindi. The Urdu, Arabic, and Nepali names are the same. Other vernacular names include Nimm in Sindhi and Punjabi, Nim in Bengali, Vembu (Tamil), Arya Veppu (Malayalam), Azad Dirakht (Persian), Nimba, Arishta, Picumarda (Sanskrit, Oriya), Limdo (Gujarati language) Kadu-Limba (Marathi), Dogonyaro (in some Nigerian languages -- Hausa), Margosa, Nimtree, Vepu, Vempu, Vepa (Telugu), Bevu (Kannada), Kodu nimb (Konkani),(Kohomba, Sinhala), Tamar (Burmese), sầu đâu, xoan Ấn Độ (Vietnamese), (Sdao, Khmer), สะเดา (Sadao, Thai), אזדרכת (Hebrew), "Maliyirinin" (Bambara language) and Paraiso (Spanish). In East Africa it is also known as Muarubaini (Swahili), sisibi (in some Ghanaian	leaf and stem	Medicinal	189 ± 27	35 ± 5	17 ± 1	1.65	73 ± 7	0.10

No.	Latin Name	Common names	Plant part	Edibility [e]	TPC ± SD (mg GAE/g plant extract)[a]	PAC ± SD (mg PAE/ gram sample) [b]	IC_{50} (amylase) µg/mL ± SD [c]	AE [d] (amylase)	IC_{50} (AGH) µg/mL ± SD [c]	AE [d] (AGH)
		languages such as kusaal).								
11	*Baccaurea parviflora*	Setambun; Setamban; Wild Rambai; Rambai Hutan	stem	Medicinal	235 ± 36	115 ± 10	48.8 ± 49.8	0.19	-	0.19
12	*Barringtonia racemosa*	Hippo apple	stem	Edible	248 ± 15	2 ± 0.3	374	0.01	-	-
			leaf	Edible	289 ± 56	6 ± 1	65	0.04	-	-
13	*Bixia orellana*	Lipstick Plant; Achiote; Anatto; Kesumba; Jarak Belanda; Annato Dye Plant; Kunyit Jawa; Kesumba Keling	stem	Medicinal	177 ± 31	116 ± 11	69 ± 20	0.03	200 ± 42	0.02
			leaf	Medicinal	333 ± 48	37 ± 7	43 ± 13	0.06	-	-
14	*Butea monosperma*	Flame of the Forest; Bastard Teak; Palasa	leaf	Non-edible	139 ± 27	46 ± 8	-	-	-	-
			stem	Non-edible	96 ± 7	12 ± 3	13.1 ± 0.6	0.75	321 ± 6	0.02
15	*Calophyllum inophyllum*	Alexandrian laurel,balltree,beach calophyllum,beach touriga,beautyleaf, Borneo-mahogany,[1] Indian doomba oiltree,Indian-laurel, laurelwood,satin touriga,and tacamahac-tree	stem	Medicinal	337 ± 81	67 ± 9	2.0 ± 0.5	1.72	32 ± 6	0.08
16	*Cananga odorata*	Kenanga; Ilang Ilang; Ylang Ylang; Kenanga Hutan; Perfume Tree; Cananga; Kenanga Utan; Chenanga; Nyai ; Nerian	leaf	Medicinal	71 ± 7	6 ± 0.8	117 ± 83	0.05	899 ± 378	0.01
			stem	Medicinal	85 ± 8	16 ± 3	174 ± 88	0.03	-	-

No.	Latin Name	Common names	Plant part	Edibility [e]	TPC ± SD (mg GAE/g plant extract)[a]	PAC ± SD (mg PAE/ gram sample) [b]	IC_{50} (amylase) µg/mL ± SD [c]	AE [d] (amylase)	IC_{50} (AGH) µg/mL ± SD [c]	AE [d] (AGH)
17	*Chrysophyllum cainito*	Cainito, caimito, star apple, golden leaf tree, abiaba, pomme du lait, estrella, milk fruit and aguay. It is also known by the synonym Achras cainito. In Vietnam, it is called vú sữa	leaf and stem	Edible	599 ± 74	159 ± 28	29 ± 1	0.98	26 ± 7	0.27
18	*Cinnamomum camphora*	Camphor Tree; Japanese Camphor Tree	leaf	Medicinal	310 ± 68	68 ± 12	32 ± 7	0.24	257 ± 200	0.04
19	*Cinnamomum javanicum*	Lawang	leaf and stem	Medicinal	42 ± 4	3 ± 0.3	-	0.05	-	-
20	*Combretom quandrangulare*	Takeo bushwillow	stem	Medicinal	286 ± 45	16 ± 2	-	-	-	-
21	*Combretom quandrangulare*	-	leaf	-	297 ± 40	4 ± 0.8	-	-	-	-
22	*Costus curvibracteatus*	-	leaf	-	320 ± 44	1 ± 0.4	-	-	-	-
23	*Cynometra ramiflora*	Cynometra	leaf and stem	Medicinal	395 ± 135	217 ± 19	16 ± 4	0.50	103 ± 68	0.07
24	*Dillenia indica*	Elephant apple, Chulta/Chalta or Ouu	stem	Medicinal	123 ± 21	88 ± 9	12.1 ± 0.2	1.58	37 ± 35	0.05
25	*Dryobalanops aromatica*	Borneo Camphor, Camphor Tree, Malay Camphor, or Sumatran Camphor,	leaf	Medicinal	411 ± 58	66 ± 15	2.8	3.75	32 ± 5	0.25
			stem	Medicinal	4501 ± 908	2696 ± 285	1.2 ± 1.2	1.92	8.0 ± 0.1	0.44
26	*Etlingera elatior*	Torch Ginger, Ginger Flower, Red Ginger Lily, Torch Lily, Wild Ginger,	flower	Edible	170 ± 9	102 ± 10	70 ± 10	0.46	129 ± 12	0.07

No.	Latin Name	Common names	Plant part	Edibility [e]	TPC ± SD (mg GAE/g plant extract)[a]	PAC ± SD (mg PAE/ gram sample) [b]	IC_{50} (amylase) µg/mL ± SD [c]	AE [d] (amylase)	IC_{50} (AGH) µg/mL ± SD [c]	AE [d] (AGH)
		Combrang, Bunga Kantan, Philippine Wax Flower, Xiang Bao Jiaing, Indonesian Tall Ginger, Boca de Dragón, Rose de Porcelaine, Porcelain Rose	stem	Edible	82 ± 7	29 ± 2	26 ± 6	0.13	127 ± 20	0.02
27	*Eugenia uniflora*	Pitanga, Surinam Cherry, Brazilian Cherry, or Cayenne Cherry	leaf and stem	Medicinal	552 ± 149	19 ± 3	5.6 ± 2.0	1.79	121.5	0.09
28	*Eurycoma longifolia*	Tongkat ali	stem	Medicinal	194 ± 32	130 ± 18	149 ± 162	0.13	117 ± 96	0.02
			leaf	Medicinal	241 ± 23	129 ± 8.2	24 ± 19	0.27	54.8 ± 0.4	0.05
29	*Ficus benjamina*	Weeping fig, Benjamin's fig, or ficus tree	leaf and stem	Non-edible	108 ± 15	35 ± 5	-	-	-	-
30	*Ficus deltoidea*	Mistletoe fig, mas cotek	flower	Medicinal	8944 ± 863	216 ± 30	-	-	-	-
			leaf	Medicinal	242 ± 29	403 ± 16	-	-	-	-
			stem	Medicinal	52 ± 9	50 ± 6	-	-	-	-
31	*Flacourtia inermis*	Lovi-lovi, or batoko plum	stem	-	97 ± 9	23 ± 1.5	-	-	35.0 ± 5.5	0.08
			leaf	Medicinal	175 ± 38	6 ± 1	177 ± 66	0.11	290 ± 206	0.01
32	*Flacourtia jangomas*	Indian plum, coffee plum	leaf	Edible	237 ± 19	2 ± 0.6	48.0	0.07	-	-
33	*Flemingia strobilifera*	Bracteate Flemingia; Serengan	leaf and stem	Medicinal	205 ± 17	152 ± 21	11 ± 2	0.36	57 ± 8	0.09

No.	Latin Name	Common names	Plant part	Edibility [e]	TPC ± SD (mg GAE/g plant extract)[a]	PAC ± SD (mg PAE/ gram sample) [b]	IC_{50} (amylase) µg/mL ± SD [c]	AE [d] (amylase)	IC_{50} (AGH) µg/mL ± SD [c]	AE [d] (AGH)
34	*Galphimia glauca*	Shower of Gold	leaf and stem	Medicinal	356 ± 63	38 ± 3	21 ± 20	0.11	170 ± 14	0.02
35	*Garcinia atroviridis*	Asam Gelugor; Gelugor	leaf and stem	Medicinal	297 ± 61	4 ± 1	87 ± 39	0.03	394 ± 38	0.01
36	*Garcinia mangostana*	Mangosteen	leaf and stem	Edible (fruit)	783 ± 158	237 ± 18	20.0	0.10	57.0	0.15
37	*Gustavia gracillima*	Heaven lotus	leaf	Non-edible	3320 ± 663	78 ± 16	-	-	7.4 ± 1.6	0.34
38	*Hamelia patens*	Firebush, Hummingbird Bush, Scarlet Bush and Redhead.	leaf and stem	Medicinal	392 ± 54	173 ± 14	6.8 ± 1.4	1.54	89.5 ± 6.4	0.09
39	*Hibiscus mutabilis*	Confederate rose or the cotton rosemallow	leaf	Edible	17 ± 2	3 ± 0.4	61.0	0.05	-	-
40	*Hibiscus rosa-sinensis*	Rose mallow, Chinese hibiscus, China rose and shoe flower,	stem	Edible	95 ± 21	-	-	-	-	-
41	*Laurus nobilis (bay leaves)*	True Laurel; Bay Laurel; Sweet Bay; Bay Tree	leaf and stem	Edible	136 ± 34	42 ± 7	35 ± 0.0	0.09	356 ± 158	0.01
42	*Leea indica*	Bandicoot Berry	leaf	Medicinal	8011 ± 540	223 ± 17	-	-	6.0 ± 1.1	0.35
43	*Lepisanthes alata*	Chinese Averrhoe, Johore Fruit, Malaysian,Lepisanthes, Trengganu Cherry.	leaf and stem	Edible	380 ± 71	129 ± 14	7.0 ± 0.0	3.97	50.0 ± 4.0	0.14
44	*Lepisanthes rubiginosa*	赤才 chi cai	leaf and stem	Edible	156 ± 40	52 ± 9.6	32.0 ± 4.2	0.06	127.5 ± 6.4	0.01

No.	Latin Name	Common names	Plant part	Edibility [e]	TPC ± SD (mg GAE/g plant extract)[a]	PAC ± SD (mg PAE/ gram sample) [b]	IC_{50} (amylase) µg/mL ± SD [c]	AE [d] (amylase)	IC_{50} (AGH) µg/mL ± SD [c]	AE [d] (AGH)
45	*Madhuca longifolia*	Mowra Butter Tree; Indian Butter Tree	leaf and stem	Medicinal	326 ± 69	99 ± 16	0.9 ± 1.0	3.94	17.1 ± 0.8	0.15
46	*Manihot esculenta*	Manioc, yuca, balinghoy, mogo, mandioca, kamoteng kahoy, and manioc root,	leaf	Medicinal	105 ± 10	26 ± 4	-	-	-	-
47	*Melaleuca cajuputi*	Cambodia : smach chanlos; Danish : punk tree; (Filipino) : swamp tea-tree; (Indonesian) : galam (Sundanese); Malay) : gelam; (Thai) : samet-khao; Vietnamese) : c[aa]y tr[af]m; paper-bark tree; kayu puteh	leaf and stem	Medicinal	-	-	35 ± 7	0.06	124 ± 16	0.06
48	*Melastoma malabhricus*	Senduduk	leaf	Medicinal	627 ± 66	14 ± 2.3	-	-	132 ± 13	0.06
49	*Mesua ferrea*	Ceylon ironwood, Indian rose chestnut, or Cobra's saffron),	leaf	Medicinal	310 ± 58	193 ± 35	6.0 ± 2.0	0.38	56 ± 13	0.06
			stem	Medicinal	6025 ± 1118	220 ± 6	0.5 ± 0.0	21.88	23 ± 2	0.35
50	*Misocarpus sundaicus*	Sugi	leaf	Medicinal	352 ± 78	110 ± 30	13 ± 3	0.26	57 ± 8	0.05
			stem	Medicinal	427 ± 88	217 ± 19	6.7 ± 0.7	0.47	44.0 ± 1.4	0.06
51	*Moringa concanensis*	Konkan Moringa	leaf and stem	Medicinal	50 ± 10	1 ± 0.2	2760 ± 1315	0.01	-	-

No.	Latin Name	Common names	Plant part	Edibility [e]	TPC ± SD (mg GAE/g plant extract)[a]	PAC ± SD (mg PAE/ gram sample) [b]	IC_{50} (amylase) µg/mL ± SD [c]	AE [d] (amylase)	IC_{50} (AGH) µg/mL ± SD [c]	AE [d] (AGH)
52	*Muntingia calabura*	Amaican cherry, Panama berry,Singapore cherry, Bajelly tree, Strawberry tree; (Spanish) bolaina, yaman aza,cacaniqua, capulín blanco, nigua, niguito, me mizo or memiso; (Indonesia) kersen,talok; (Vietnamese) Trứng cá (thực vật); and (Filipino) alatris, aratilis, manzanitas andsarisa.	stem	Edible	358 ± 42	115 ± 13	408 ± 313	0.02	931 ± 26	0.07
			leaf	Edible	376 ± 41	37 ± 6	109.5 ± 0.7	0.00	115 ± 7	0.01
53	*Myristica fragrans*	Nutmeg, Mace	leaf	Edible	593 ± 107	181 ± 21	-	-	23.0 ± 0.0	-
54	*Orthosiphon aristatus*	umis kucing (Indonesia) misai kucing (Malaysia). US- it may be commonly known as Cat's Whiskers or Java tea.	leaf	Edible	234 ± 48	13 ± 2	121 ± 12	0.03	-	-
			stem	Edible	291 ± 45	70 ± 10	505 ± 35	0.06	695 ± 106	0.01
55	*Pachira aquatica*	Malabar chestnut, Guiana chestnut, provision tree, saba nut, monguba (Brazil), pumpo (Guatemala) and is commercially sold under the names money tree and money plant.	stem	Edible	39 ± 6	1 ± 0.2	-	-	-	-
			leaf	Edible	160 ± 34	48 ± 5	3.6 ± 0.0	0.93	-	-
56	*Parkia speciosa*	Petai; Nyiring; Nitta Tree	leaf	Medicinal	27 ± 3	13 ± 2	15.9 ± 0.8	0.26	129 ± 159	0.16

No.	Latin Name	Common names	Plant part	Edibility [e]	TPC ± SD (mg GAE/g plant extract)[a]	PAC ± SD (mg PAE/ gram sample) [b]	IC_{50} (amylase) µg/mL ± SD [c]	AE [d] (amylase)	IC_{50} (AGH) µg/mL ± SD [c]	AE [d] (AGH)
57	*Pentadesma butyracea*	Shea butter, butter tree	leaf and stem	Medicinal	382 ± 82	109 ± 11	-	-	16.7 ± 1.2	0.15
58	*Phyllanthus acidus*	Otaheite gooseberry, Malay gooseberry, Tahitian gooseberry, country gooseberry, star gooseberry, West India gooseberry, damsel, grosella (in Puerto Rico), karamay (in the PHilippines), or simply gooseberry tree	leaf and stem	Edible	30 ± 4	6 ± 1.1	88 ± 4	0.05	323 ± 25	0.07
59	*Phyllanthus pulcher*	Kelurut tanjong, naga buana, semelit patong (Malaysia)	leaf	Medicinal	30 ± 4	7 ± 1.4	-	-	-	-
			stem	Medicinal	249 ± 83	99 ± 13	428 ± 403	0.00	1980 ± 60	0.00
60	*Premna serratifolia*		leaf	-	95 ± 9	3 ± 0.4	-	-	-	-
61	*Punica granatum (pomegranate)*	Pomegranade	leaf and stem	Medicinal	546 ± 82	2 ± 0.5	24.0	0.44	183 ± 36	0.04
62	*Quassia amara*	Amargo, Bitter-ash, Bitter-wood	leaf and stem	Medicinal	563 ± 188	2 ± 0.7	-	-	412 ± 309	0.02
63	*Rhodamnia cinerea*	Bangka, merampuyan, andong (indonesia); mempoyan bukit, menkoyan pinang (malaysia); taung-kamyaing (myanmar); Khee tai, phae, ya waeng (Thailand); Silverback;	leaf	Medicinal	490 ± 89	138 ± 21	-	-	20.5 ± 2.1	0.41

No.	Latin Name	Common names	Plant part	Edibility [e]	TPC ± SD (mg GAE/g plant extract)[a]	PAC ± SD (mg PAE/ gram sample) [b]	IC_{50} (amylase) µg/mL ± SD [c]	AE [d] (amylase)	IC_{50} (AGH) µg/mL ± SD [c]	AE [d] (AGH)
		poyan, Borneo: Siri-siri, Talinga basing								
64	*Rhodomyrtus tomentosa*	Downy rose myrtle, downy myrtle, hill gooseberry, hill guava	leaf and stem	Medicinal	6809 ± 416	146 ± 9	-	-	-	-
65	*Senna alata*	Candle bush	leaf	Medicinal	157 ± 34	22 ± 3	29.0	0.36	-	-
66	*Synsepalum dulcificum*	Miracle fruit	leaf	Edible	183 ± 39	76 ± 5	22 ± 18	0.21	38 ± 4	0.08
67	*Syzygium antisepticum*	Borneo: Aeba, Jambu hutan, Obah	stem	Medicinal	369 ± 36	68 ± 6	11.2 ± 0.9	0.22	-	-
68	*Syzygium cumini*	syzygium cumini is also known as jambul/jambhul/jambu/jambula/jamboola, Java plum, jamun, jaam/kalojaam, jamblang, jambolan, black plum, Damson plum, Duhat plum, Jambolan plum or Portuguese plum. Malabar plum may also refer to other species of Syzygium. This fruit is called Neredu Pandu in Telugu, Naaval Pazham in Tamil, Njaval Pazham in	leaf	Edible	109 ± 20	10 ± 2	31 ± 6	1.18	100 ± 7	0.16

No.	Latin Name	Common names	Plant part	Edibility [e]	TPC ± SD (mg GAE/g plant extract)[a]	PAC ± SD (mg PAE/ gram sample) [b]	IC_{50} (amylase) µg/mL ± SD [c]	AE [d] (amylase)	IC_{50} (AGH) µg/mL ± SD [c]	AE [d] (AGH)
		Malayalam, Nerale Hannu in Kannada, Jam in Bengali, Jamukoli in Oriya and Jambu in Gujarat. In the Philippines, common names include duhat in the Tagalog-speaking regions, lomboy in the Cebuano-speaking areas and inobog in Maguindanao. It is called Dhanbu in Maldives and Dhuwet/Juwet in Javanese. Among its names in Portuguese are jamelão, jambolão, jalão, joão-bolão, manjelão, azeitona-preta, baga-de-freira, brinco-de-viúva and guapê, always with lower case, the early four derived from the Konkani name jambulan.They are called rotra in the Malagasy language (Madagascar)	stem	Medicinal	438 ± 76	73 ± 7	-	-	-	-

No.	Latin Name	Common names	Plant part	Edibility [e]	TPC ± SD (mg GAE/g plant extract)[a]	PAC ± SD (mg PAE/ gram sample) [b]	IC_{50} (amylase) µg/mL ± SD [c]	AE [d] (amylase)	IC_{50} (AGH) µg/mL ± SD [c]	AE [d] (AGH)
69	*Tamarindus indica*	Tamarind in Indonesia and Malaysia, tamarind is known as the asam (or asem) Jawa (means Javanese asam), In the Philippines, tamarind is referred to as sampaloc, which is occasionally rendered as sambalog in Tagalog and sambag in Cebuano. The Vietnamese term is me. In Taiwan, it is called loan-tz. In Myanmar, it is called magee-bin (tree) and magee-thee (fruit). The tamarind is the provincial tree of the Phetchabun province of Thailand, where it is called má kăam (มะขาม). In Laos, it is called ໝາກຂາມ (maak-kham). In Malagasy, it is called voamadilo and kily.	leaf	Edible	237 ± 77	99 ± 17	-	-	71 ± 9	0.02
			stem	Edible	413 ± 70	201 ± 17	4.4 ± 1.0	0.73	30 ± 13	0.07
70	*Terminalia catappa*	榄仁树, Sea Almond; Ketapang; Indian Almond; Tropical	stem	Medicinal	86 ± 7	2 ± 0.3	-	-	-	-

No.	Latin Name	Common names	Plant part	Edibility [e]	TPC ± SD (mg GAE/g plant extract)[a]	PAC ± SD (mg PAE/ gram sample) [b]	IC_{50} (amylase) µg/mL ± SD [c]	AE [d] (amylase)	IC_{50} (AGH) µg/mL ± SD [c]	AE [d] (AGH)
		Almond Tree; Lingtak; Bastard Almond; Singapore Almond; Telisai; Jelawai Ketapang; Pacific Almond	leaf	Medicinal	464 ± 57	3 ± 0.3	141 ± 94	0.04	323 ± 116	0.02
71	*Ziziphus mauritiana*	Ber, Chinee Apple, Jujube, Indian plum and Masau	leaf	Edible	281 ± 57	118 ± 22	20.3	-	87 ± 28	0.02
			stem	Edible	259 ± 39	119 ± 19	22 ± 4	0.16	112 ± 66	0.02

[a] TPC ± SD is the mean total phenolic content and its standard deviation measured from three readings of the plant extract.
Data is expressed as milligrams of gallic acid equivalent per gram of plant extract (mg GAE/ g plant extract).
[b] PAC ± SD is the mean proanthocyanidin content and the standard deviation taken from three readings of the plant extract.
Data is expressed as milligrams of procyanidin A2 equivalent per gram of plant extract (mg PAC/ g plant extract).
[c] IC_{50} is the concentration of plant extract which inhibits 50 % of α-amylase / α-glucosidase. Data is expressed as micrograms per millilitres ± standard deviation (µg/mL ± SD).
[d] AE is the acarbose equivalent of α-amylase / α-glucosidase.
[e] Botanicals labelled as "edible" are eaten as everyday foods (e.g. vegetables) whereas plants labelled under "medicinal" are taken occasionally to treat certain ailments.
Hyphens signify tests not carried out and that the data is not available.

4.3.1 Correlation studies

In order to assess if a particular group of compounds (i.e. proanthocyanidins and polyphenols) contributed significantly to the inhibitory activities of starch hydrolases, two correlation studies were carried out. The first set of correlation studies was between the proanthocyanidin contents, estimated using the DMAC assay, with the AE of α-amylase and α-glucosidase. **Figure 22 A** and **B** show the PAC-AE correlation of both amylase and α-glucosidase to be weak, with R^2 values of 0.1 and 0.32 respectively. The second set of correlation studies was between the TPC and AE of α-amylase and α-glucosidase. Our results show that TPC had a weak to no correlation with the AE of α-amylase (R^2 = 0.0214) and α-glucosidase (R^2 = 0.1889) **(Figure 22 B** and **C)**.

Overall, PAC contents had higher correlation with the inhibition of starch hydrolases. As such, our results suggest that proanthocyanidins contribute more towards the inhibition of starch hydrolases as compared to phenolic contents. The reasons contributing to the lack of correlation observed between PAC and TPC contents, with the inhibitory strength of starch hydrolases, suggests that starch inhibitory activity is not caused exclusively by a specific group of compounds, but possibly through interactions occurring between different groups of compounds, which could give a cumulative inhibitory effect. Additionally, the presence of specific compounds, with potent inhibitory activity, may be present. Contrary to the lack of correlation observed with TPC-enzyme inhibition and PAC-enzyme inhibition, the mean TPC and PAC was shown to possess relatively strong positive correlation **(Figure 23)** with each other (R^2 = 0.65), which is expected, since procyanidins

are phenolic oligomers that are mainly composed of (+)-catechin and (-)-epicatechin.

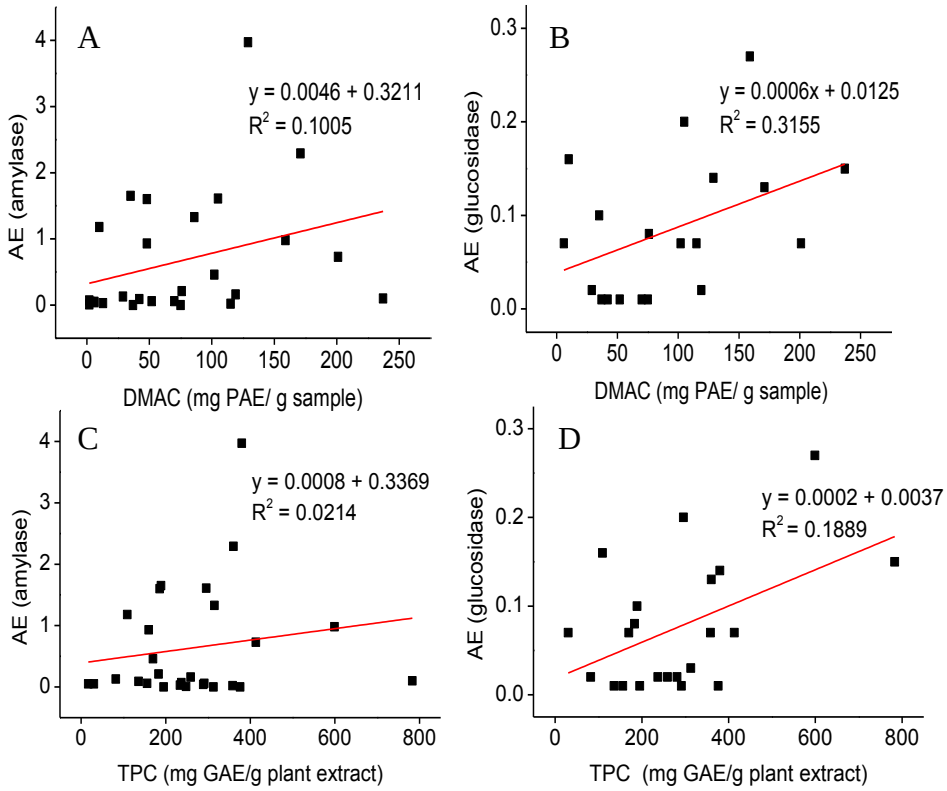

Figure 22. Correlation of (A) PACs and AE (α-amylase), (B) PACs and AE (α-glucosidase), (C) TPC and AE (α-amylase) and (D), TPC and AE (α-glucosidase).

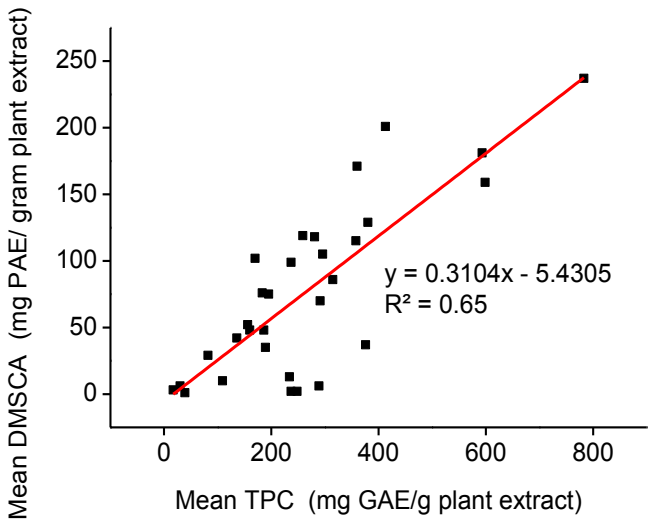

Figure 23. Correlation between the mean TPC and PACs values.

4.4 Conclusion

In summary, we have shown that the turbidity assay is an effective high-throughput methodology for the evaluation of starch hydrolase inhibition, in screening botanical materials. Furthermore, some of the selected botanicals show great potential as a source of novel inhibitors, and lay the groundwork for future in-depth studies of isolation and characterization of pure inhibitors from botanicals. It should also be noted that this study is based on *in vitro* methodologies. Since *in vitro* methods are over-simplistic, further *in vivo* studies, which are more complicated but more representative of the human body, are warranted.

Chapter 5

Characterization of proanthocyanidins from torch ginger flower (*Etlingera elatior)* as strong starch hydrolase inhibitors

5.1 Introduction

Etlingera elatior is a flower which is also known by many different common names as torch ginger, ginger flower, red ginger lily, torch lily, wild ginger, combrang, bunga kantan, philippine wax flower, xiang bao jiang, indonesian tall ginger, boca de dragón, rose de porcelain and porcelain rose (*230*). The flower is used as an ingredient in many Southeast Asian cuisines. For example, the flower buds are used as important ingredients in the nonya laksa dish as well as in 'rojak' (*231*). In North Sumatra, the buds are used for a dish called 'arsik ikan mas' and in Thailand, it is ingredient of Thai salad. In East Malaysia, the young shoots are consumed by indigenous communities as a condiment, eaten raw or cooked as a vegetable (*232*). Some of the traditional uses/effects of this flower include its use in reducing the odour of fish and in the inhibition of pathogenic bacteria and moulds on food (*233*). In Malaysia, the fruits of *E. elatior* may be applied as a remedy for earache and its leaves for cleaning wounds (*234*).

Based on the available literature, the main flavonoids that have been identified in the leaves of *E. elatior* are kaempferol-3-glucuronide, quercetin-3-glucuronide, quercetin-3-glucoside, and quercetin-3-rhamnoside (*235*).

Quantitatively, the dry weight of the flower has been estimated to be about 286 mg/ kg (*236*). The quantitative amount of quercetin in the extracts of *E. elatior* as determined by HPLC analysis was 1.18 ± 0.06 mg/ 100 mg (*233*).

3-*O*-caffeoylquinic acid, 5-*O*-caffeoylquinic acid (chlorogenic acid), and 5-*O*-caffeoylquinic acid methyl ester were isolated from the leaves of *E.elatior (237).* The leaves were also shown to be non-toxic to normal liver and kidney cells. *In vivo* brine shrimp lethality tests also showed that the methanolic extract of the flower exhibited a very high LC_{50} value, which signifies that this plant is not toxic to humans (*238*). Two new compounds and six known compounds of diarylheptanoids, labdane diterpenoids and steroids were isolated, namely 1, 7-bis(4-hydroxyphenyl)-2,4,6-heptatrienone (1), demethoxycurcumin (2), 1, 7-bis(4-hydroxyphenyl)-1,4,6-heptatrien-3-one (3), 16-hydroxylabda-8 (17), 11,13-trien-16,15-olide (4), stigmast-4-en-3-one (5), stigmast-4-ene-3, 6-dione (6), stigmast-4-en-6b-ol-3-one (7), 5α, 8α-epidioxyergosta-6,22-dien-3β-ol (8). Compounds 5 and 7 were shown to have high anti-tumour activity (*239*).

The *E. elatior* extract was shown to be able to protect bone marrow from the damaging effects of lead toxicity and it is suggested that it can be used as a therapeutic agent against chronic lead intoxication in combination with lead chelating agents (*240, 241*). Leaves of the *E.elatior* displayed high tyrosinase inhibition activity, which has implications in application in foods and cosmetics, as neither hyperpigmentation in human skin nor enzymatic browning in fruits are desirable (*242*). The ethanolic extracts of *E. elatior* have antimicrobial activity and are cytotoxic to HeLa cells (*243*).

As such, current literature strongly suggests that extracts from *E. elatior* are of medicinal value. However, this is the first time the anti-diabetic effect of its α-amylase inhibition activity has been carried out in depth. Reported herein are the results of my attempts to elucidate the active compounds in the inflorescence of *E. elatior*. More specifically, by applying a high throughput assay, I successfully identified PACs in the flower extract as potent α-amylase inhibitors. In addition, polyphenolic profiles of several active fractions that may have contributed to its inhibition activity were studied. This work shows that *E. elatior* possesses potent inhibitors which may serve as functional ingredients in reducing PPHG.

5.2 Materials and methods

5.2.1 Reagents and instruments

The reagents were purchased from commercial sources: Folin & Ciocalteu's phenol reagent (Merck, Darmstadt, Germany), sodium carbonate (Sigma, cat. no. S7795), and gallic acid (Sigma, cat. no. 48630).

5.2.2. Extraction and purification of proanthocyanidins from *Etlingera elatior* inflorescence

E.elatior (5 kilograms) was sampled from the Singapore Botanic Gardens or purchased from the Pasir Panjang wholesale market in Singapore. The flowers were washed thoroughly and blot dried to remove any traces of possible impurity or potential pesticide contamination. The inflorescences were then frozen in a - 20 ºC freezer, freeze dried and subsequently grounded to powder. The resulting powder was extracted with methanol at a ratio of 1:10 (w/v) powder to solvent with shaking for 24 hours at room temperature.

The initial methanolic crude extract, after washing with a variety of immiscible solvents with different polarities, was concentrated. The concentrated methanolic extract was diluted to obtain a 95 % aqueous methanolic solution. The extract was "defatted" with an equal volume of *n*-hexane three times. Two distinct layers were collected using a separation funnel and the methanolic layer was evaporated to dryness and re-dissolved in water. The solution then underwent successive partitioning of chloroform ($CHCl_3$), ethylacetate (EtOAc) and *n*-butanol (*n*-BuOH) as shown in **Figure 24**.

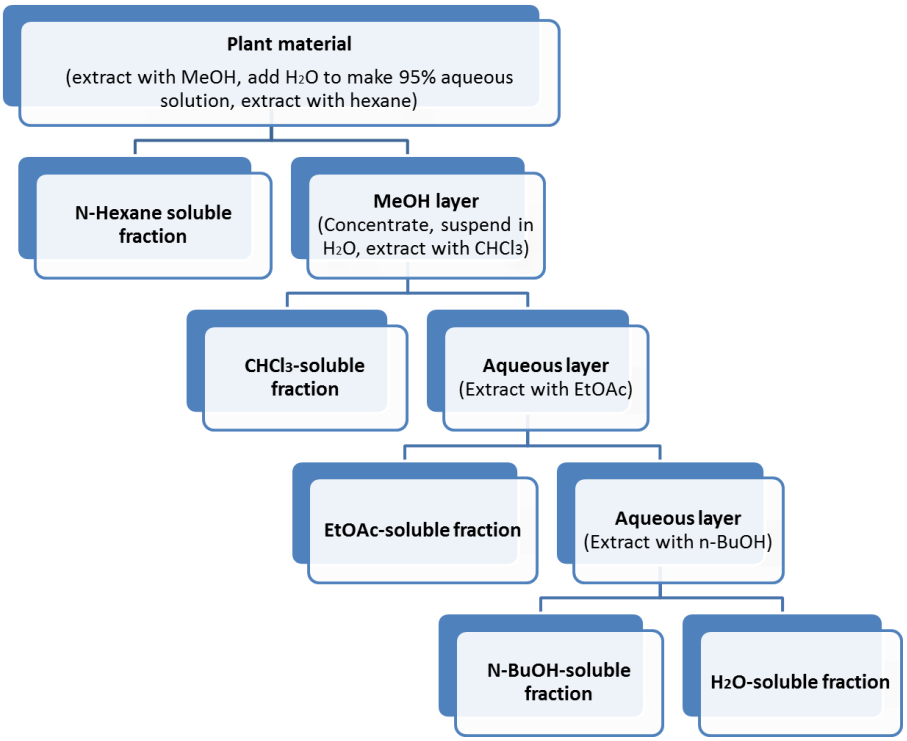

Figure 24. Purification of *E.elatior* extract by liquid-liquid partitioning

5.2.3 Sephadex LH-20 fractionation of butanol and aqueous extract

Butanol extract (0.5 g dissolved in methanol) was loaded on to the Sephadex LH-20. The column was eluted using a linear elution gradient of increasing percentage of methanol-water (0, 20, 40, 60, 80, 100 % v/v), and 100 mL of eluent was collected for each gradient.

5.2.4 Characterization of proanthocyanidins in *E. elatior*

Ten milligrams per millilitre of aqueous (in water), butanol (in water) and ethyl acetate (in methanol) fractions were filtered through an RC 0.45 µm membrane filter before 20 µL was injected for HPLC analysis (250 x 4.6 mm i.d., 5 µm, Develosil diol with a 4 x 4 mm i.d. guard column of the same materials. The materials came from Seto, Japan). The elution conditions were as follows: flow rate of 1.0 mL/min; column temperature of 35 °C; mobile phase A of 2 % acetic acid in acetonitrile; mobile phase B of acidic aqueous methanol (CH_3OH: H_2O: HOAc, 95:3:2 v/v/v). The first mobile phase condition was 7 % of B held isocratic for 3 minutes, before ramping solvent B to 37.6 % over 57 minutes, and then to 100 % of B for 3 minutes thereafter. B was held at 100 % for 7 minutes prior to returning to the starting condition (7 % of B) in 6 minutes. The column was equilibrated with 7 % of B for 5 minutes prior to the next run. The electrospray ionization mass spectra were recorded from a Finnigan/MAT LCQ ion trap mass spectrometer (San Jose, CA) equipped with a TSP 4000 high-performance liquid chromatography (HPLC) system, which included an UV6000LP photodiode array detector (set at 280 nm), P4000 quaternary pump and AS3000 autosampler, at a set column temperature of 35 ºC. The heated capillary and voltage were maintained at 250 °C and 4.5 KV respectively. Nitrogen was operated at 80 psi for the sheath gas

flow rate and 20 psi for the auxiliary gas flow rate. The full scan mass spectra from *m/z* from 50-500 were acquired in both positive and negative ion modes with a scan speed of 1 s/scan.

5.2.5 Determination of α-amylase inhibition activity of *E. elatior* fractions

The inhibition activity was determined using a method that was established previously (*175*). The method was described in detail in section 4.2.5.

5.2.6 Determination of Total phenolic contents

The TPC method was described in detail in section 4.2.3.

5.2.7 Determination of Proanthocyanidin content

The DMAC method was described in section 4.2.4.

5.3 Results and discussion

5.3.1 Determination of TPC and PAC of *E. elatior* extract

The TPC of the butanol extract of *E. elatior* was determined using the Folin-Ciocalteu method. The result was a 371.1 ± 48.0 mg GAE/g extract. The proanthocyanidin content of a crude extract of the *E. elatior* flower was a 754.7 ± 113.1 µg PAE/g extract.

5.3.2 α-Amylase inhibition activity of *E. elatior* fractions

Figure 25 shows the kinetics of change in the optical density of inhibitors present in the various fractions against α-amylase and the AUC, which translates to the dose response curves as shown in the insets. **Figure 25 A, B, C** and **D** show the inhibitory activity for aqueous, ethyl acetate, butanol

and acarbose respectively and the IC_{50} of the various fractions are shown in **Table 3.** The aqueous extract was the most potent fraction as compared to the other crude fractions, with an IC_{50} of 13 ± 3 µg/mL. The potency of the aqueous extract was still less active as compared to acarbose (IC_{50} = 8 ± 2 µg/mL). Following this, the butanol fraction was the next most active fraction (IC_{50} = 89 ± 14 µg/mL). Further purification of the butanol fraction (fraction G) via Sephadex LH-20, which was washed with 100 % methanol, resulted in an increase in the potency of the butanol fraction (IC_{50} = 37 ± 5 µg/mL). Finally, the ethyl acetate fraction had little activity (IC_{50} = 321 ± 12 µg/mL) while the hexane and chloroform fractions exhibited no inhibitory activity.

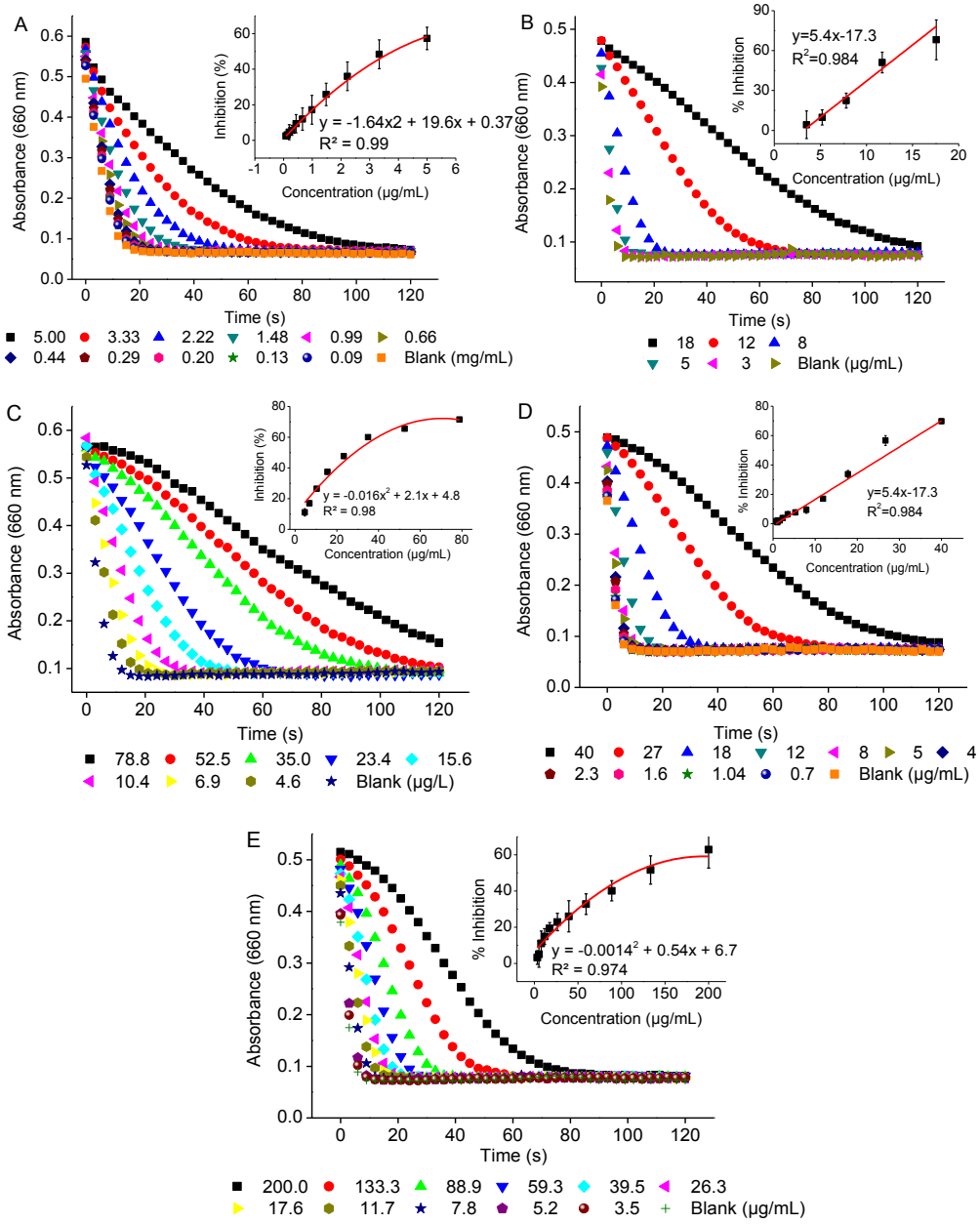

Figure 25. Change in optical density measured at 660 nm at various concentrations of *E. elatior* fractions (A) acarbose, (B) aqueous, (C) butanol, (D) LH-20 fraction G from butanol and (E) Ethyl acetate. Insets show the dose-response curve.

Table 3. The IC_{50} of α-amylase inhibition activity of various fractions.

Fractions	**IC_{50} (µg/mL)**
Acarbose	8 ± 2
Aqueous	13 ± 3
Butanol	88.6 ± 14
LH-20 Fraction G from BuOH 100% MeOH	37 ± 5
Ethyl acetate	321 ± 12
Hexane	No inhibition
Chloroform	No inhibition

5.3.3 Proanthocyanidin identification of active crude extracts from *E. elatior* inflorescence

The *E. elatior* PACs were separated and analysed by a Develosil diol HPLC column that gave chromatographic separations based on the degree of polymerisation (or molecular weight), which was determined by the ESI-MS^n negative mode to obtain the distribution of different oligomers. **Figures 26 A, B** and **C** show the HPLC chromatograms of PACs from different fractions (i.e. aqueous, butanol and ethyl acetate). Identification of OPCs was based on their mass spectra as well as a comparison of their retention times to previously published reports. Their molecular weights and fragment ions are summarised in **Table 4**. Peak 3 gave the *m/z* value of 866 [290 x 3 - (3-1) x 2]. Its cationic MS^2 gave daughter ion peaks at *m/z* 695, 577, 406 and 286, indicating a procyanidin skeleton composed of three (epi)catechin moieties. Peak 4 has a *m/z* of 1154 [290 x 4 – (4-1) x 2]. Its main cationic MS^2 fragments gave peaks at *m/z* 867 and 579. Hence, its main fragment ions are at *m/z* 287 and 575, which are common fragments from interflavanoid bond cleavage. A mass of *m/z* 287 was a quinone methide (epi)catechin, which indicated that (epi)catechin was the extension unit that makes up the tetrameric PAC.

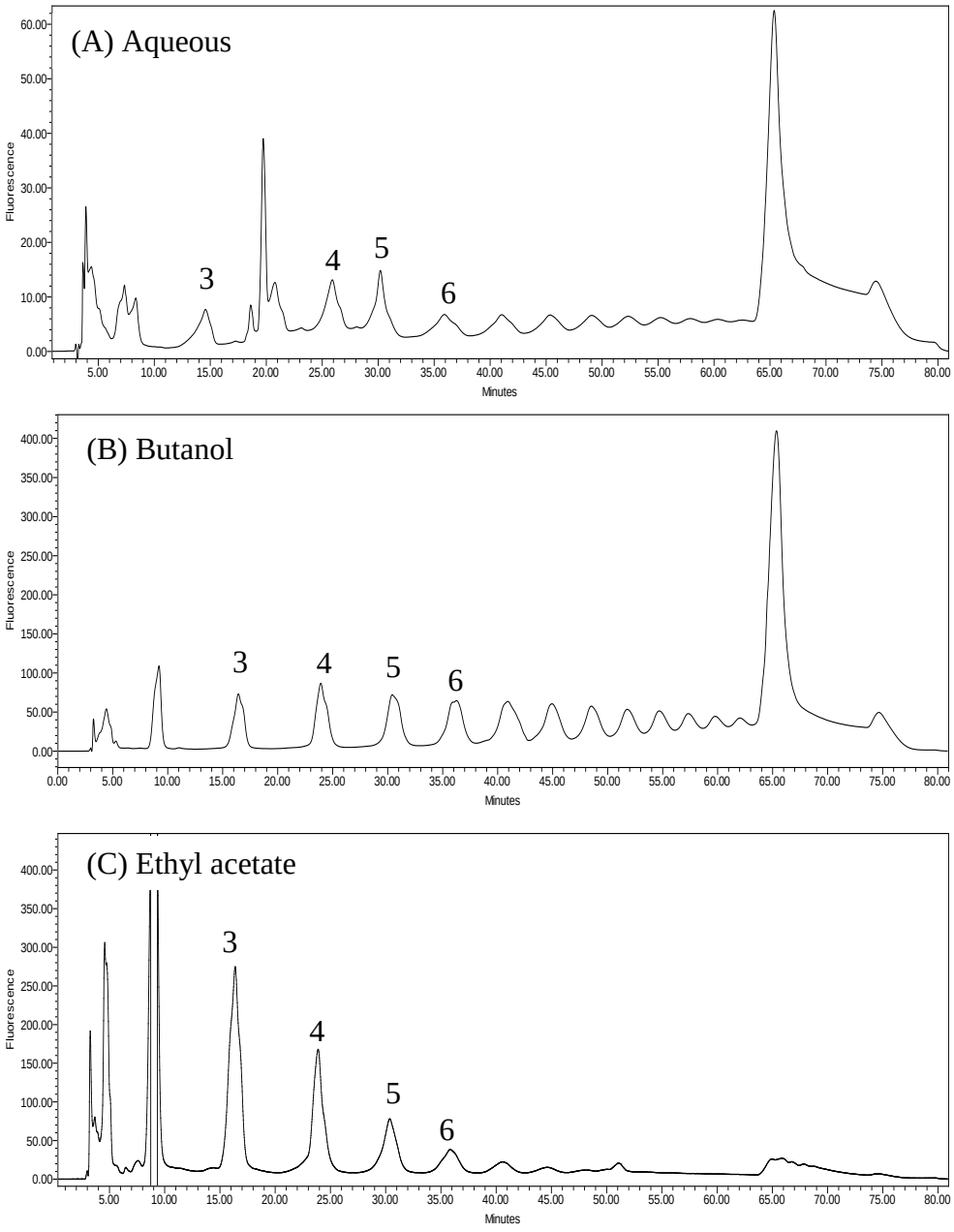

Figure 26. HPLC chromatograms of proanthocyanidin profiles from (A) aqueous, (B) butanol and (C) ethyl acetate fractions.

Table 4. Identification of proanthocyanidins in crude extracts of *E. elatior*.

Peak no.	t_R (mins)	MW	MS (m/z)	MS^2 ions (m/z)	Tentative compound assignments
3	16	866	867 $[M]^+$, 865 $[M-H]^-$	579 $[M]^+$, 695, 577, 406, 286 $[M-H]^-$	Trimer (B type)
4	23	1154	1155 $[M]^+$, 1153 $[M-H]^-$	867, 579 $[M]^+$, 1135, 983, 865, 739, 575 $[M-H]^-$	Tetramer
5	30	1442	1443 $[M]^+$, 1441 $[M-H]^-$	478, 419 $[M]^+$, 1236, 961, 720 $[M-H]^-$	Flavan-3-ols pentamers
6	35	1730	1731 $[M]^+$, 1732 $[M-H]^-$	478, 419 $[M]^+$, 1153, 864 $[M-H]^-$	Flavan-3-ols Hexamer

Peak 5 has a *m/z* of 1442 [290 x 5 – (5-1) x 2] and peak 6 has a *m/z* of 1730 [290 x 6 – (6-1) x 2], which can be identified as pentamers and hexamers with (epi)catechin B type linkage, respectively.

In order to quantify the different oligomeric procyanidins, of different degrees of polymerisation from the various fractions, pure standards are required. Nevertheless, an estimation of the quantity of procyanidins can be carried out by an integration of the area under the curve of the peaks. **Figures 26 A** and **B** show that the aqueous and butanol fractions contain more procyanidins that are of a higher degree of polymerization (DP > 7) as compared to the ethyl acetate fraction **(Figure 26 C)**. Previous studies showed that higher procyanidin oligomers exhibit stronger inhibitory activity as compared to polyphenolic monomers (*244*). Similarly, our results also indicate that ethyl acetate, with low amounts of higher procyanidin oligomers, has lower inhibitory activity (IC_{50} = 321 ± 12 µg/mL) compared to the butanol (IC_{50} = 88.6 ± 14 µg/mL) and aqueous (IC_{50} = 13 ± 3 µg/mL) fractions, which contain higher amounts of polymeric oligomers.

5.3.4 Determination of α-amylase inhibition activity of fractions of butanol extract with Sephadex LH-20

Purification and fractionation of the butanol extract with Sephadex LH-20, with increasing percentage of methanol/water, generated 0, 20, 40, 60, 80 and 100 % methanolic fractions, which are named as fraction 1, 2, 3, 4, 5 and 6 respectively. Fraction 1 did not show any inhibitory activity, and direct injection on the mass spectrometer suggests that high amounts of chlorogenic acid are present in the 100 % water fraction. Fraction 2 (20 % methanol) gave slight inhibitory activity (IC_{50} = 2.85 mg/mL), whereas fraction 3 (40 % methanol) and 4 (60 % methanol) had no activity at all. The last two fractions, 5 (80 % methanol) and 6 (100 % methanol), had relatively high α-amylase inhibition, with IC_{50} of 0.861 and 0.037 mg/mL respectively. Direct injection of fraction 5 revealed a predominant mass ion with a *m/z* value of 464, which could potentially be identified as isoquercitrin, since *E. elatior* has been reported to be rich in quercetin derivatives (*235*). Direct mass injection of fraction 6 reveals predominant *m/z* values of 1153, 865, 576 and 354, which indicates that this fraction could be enriched with proanthocyanidins.

5.3.5 Fractionation of aqueous extract with Sephadex LH-20

Fractionation via the Sephadex LH-20 was also carried out with the aqueous extract, since it had the highest inhibitory activity with the same gradient run of methanol/water (0, 20, 40, 60, 80 and 100 %) as was done with the butanol extract. The LH-20 fractions will be designated as fractions 7, 8, 9, 10, 11 and 12 respectively, from the lowest methanol percentage to the highest. Fractions 7, 8 and 9 showed little or no activity, and direct mass injection of fraction 7 showed high contents of chlorogenic acids. α-amylase

inhibitory activity was progressively stronger from fractions 10 to 12, with fraction 12 being the most active. Direct mass injection of fractions 11 and 12 indicated similar mass profiles, whereas fraction 10 was different. As such, further analyses of fractions 10 and 12, using a LC-MS^n with a C18 column, were done to separate and identify potential inhibitors.

5.3.6 Identification of compounds in fraction 10 by LC-MS^n

The HPLC chromatogram of fraction 10 is shown in **Figure 27**. Identification of the peaks obtained by LC-MS is summarised in **Table 5.** Peak 1 had $[M+H]^-$ at *m/z* 449, with a fragment at *m/z* 287 (loss 162 due to potential amu: hexose moiety), and was identified as kaempferol-3-*O*-glucoside (*245*). Peak 2 had a $[M+H]^+$ ion at *m/z* 579, with fragment ions at *m/z* 427, 409 and 291, which indicated that it was a dimer of procyanidin B1 (*246*). Peak 3 had a $[M+H]^+$ ion at *m/z* 290 with a fragment ion at 273 (loss of 18 due to potential amu; water), which is likely to be an epi (catechin) moiety. Peak 4 had a $[M+H]^+$ ion at *m/z* 627, daughter ions at *m/z* 465, 303 at ESI-MS^2, and a sequential loss of 303 by ESI-MS^3 respectively, which indicates a quercetin–hexose–hexose structure of $C_{27}H_{30}O_{17}$. Hence, this peak was assigned to be quercetin-3,4'-O-di-β-glucopyranoside (*247*). Peak 5 was assigned as chlorogenic acid with [M+H] at *m/z* 355, with a MS^2 of *m/z* 162 (caffeic acid) and *m/z* 174 (for the fragment of trihydroxycyclohexanecarboxylic acid). MS^3 also gave a fragment *m/z* of 144 (loss of water molecule) (*248*). Peak 6 showed a mass [M-H] at *m/z* 521 with a fragment mass of *m/z* 270 (from the glucoside moiety) which may tentatively be identified as diconiferyl alcohol glucoside. Peak 7 had a mass [M+H] at *m/z* 368, with a fragment mass of *m/z* 350 (loss of water molecule). Since *E.*

elatior is rich in chlorogenic acid, it is possible that this peak may be from chlorogenic acid derivatives; hence, it was assigned as feruloyl quinate (*249*). Peak 8 showed a mass [M-H] of *m/z* 505 and secondary ions of *m/z* 269. Tertiary ions at *m/z* 268, 226 and 182 were observed. Based on its mass, a tentative assignment of peak 8 was given as feruloyl malate (4-O-8 coupled) coniferyl alcohol. The mass spectral data is shown in **Appendix 2**.

5.3.7 Identification of compounds in fraction 12 by LC-MS^n

HPLC chromatograms (in 2-D and 3-D) of fraction 10 are shown in **Figure 28**. Identification of the peaks obtained by LC-MS is summarized in **Table 6**. Peak 9 showed a [M+H] ion at *m/z* 280, and MS^2 ions at *m/z* 244 and 216 (loss of 2 water molecules) which could tentatively be identified as coumaroyl aspartate (*250*). Peaks 10 and 12 were identified as 1, 7 bis(4-hydroxyphenyl)-2, 4, 6 hetatrienone [M+H] ion at *m/z* 294 and MS^2 fragment at 276. This compound has been previously isolated and characterized from *E. elatior* (*239*). Peak 11 showed a mass [M+H] at *m/z* 268 and a MS^2 fragment at *m/z* 135, with a loss of *m/z* 133, which is characteristic of the compound genistein (*251*). Stigmast-4-en-6β-ol-3-one and 5α, 8α–epidioxyergosta-6, 22-dien-3β-ol both possess a molecular weight of 428 g/mol, have previously been isolated in the ginger flower, and can possibly be identified in peak 13 (*239*). Peak 14 can be identified as dicaffeoylquinic acid, which, according to the diagnostic fragmentation pattern, involves cleavage of the caffeoyl and quinic (*m/z* 190) moieties (*252*). Our spectral data showed a mass of $[M–H]^-$ ion at *m/z* 707 and secondary and tertiary peaks at *m/z* 353 and 190 respectively (*253*). Peak 15 was identified as β-stigmasterol with a [M+H] ion

at *m/z* 415 and MS^2 fragment at 406 which was previously identified in *E. elatior* (*239*). The mass spectral data is shown in **Appendix 3**.

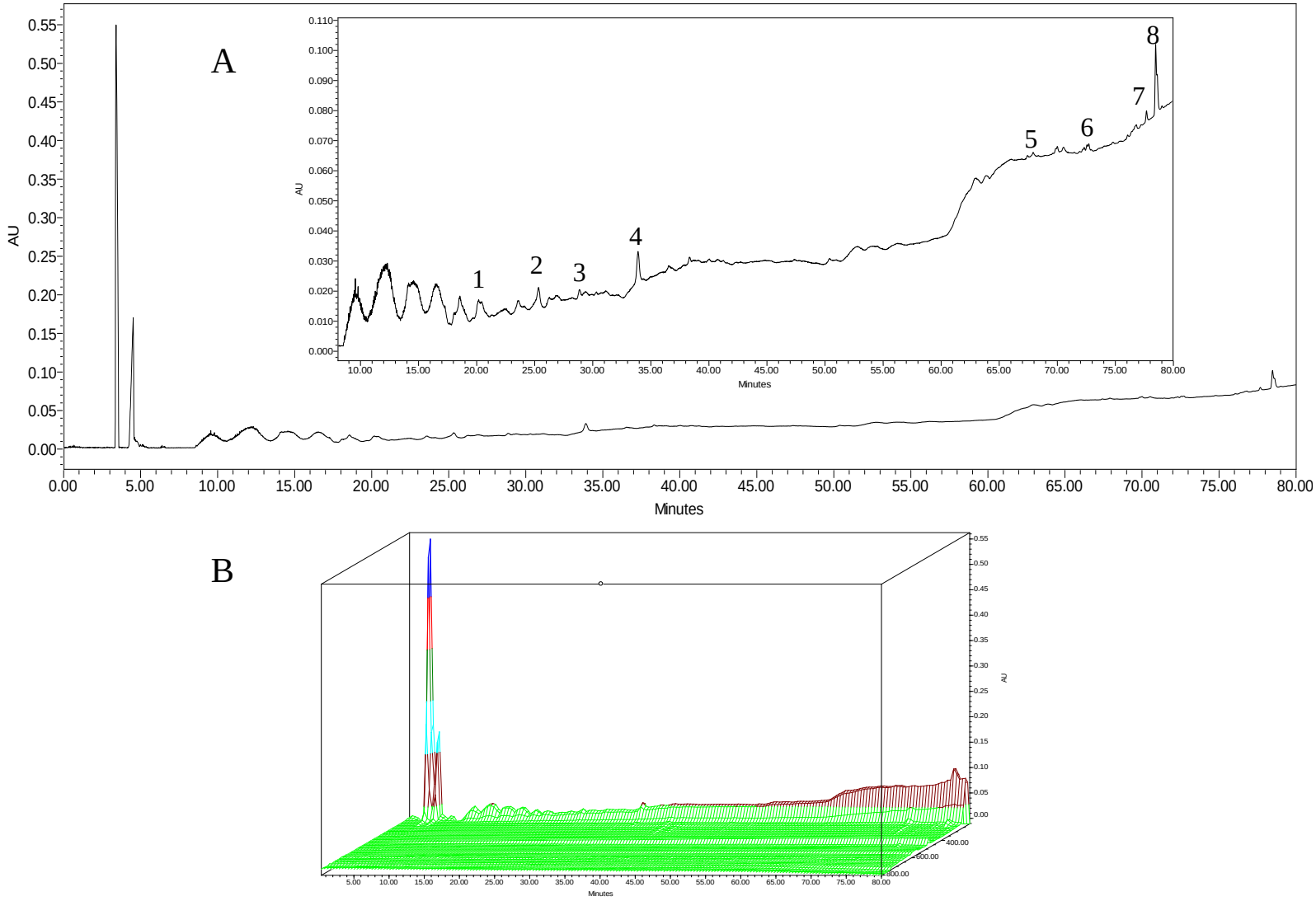

Figure 27. HPLC chromatograms of aqueous extract (fraction 10) in (A) 2-D and (B) 3-D.

Table 5. Identification of polyphenolic compounds from the aqueous extract (fraction 10) by HPLC-MS^n

Peak no.	t_R (mins)	UV_{max} (nm)	MW	MS (m/z)	MS^2 ions (m/z)	MS^3 ions (m/z)	Tentative compound assignments	References
1	22.5	211	448	**449** $[M]^+$	287	-	Kaempferol-3-o-glucoside (Astragalin)	Kajdžanoska, 2010
2	25.3	279	578	**579** $[M]^+$	427, **291**	270	Procyanidin B1	Venter, 2013
3	30.3	-	290	**291** $[M]^+$	273, **122**	-	Epi(catechin)	-
4	34.8	-	626	**465** $[M]^+$	465, 303	303	Quercetin-3,4'-O-di-β-glucopyranoside	Shui and Leong, 2004
5	71	-	354	**355** $[M]^+$	162, 174	144	Monocaffeoylquinic acid	Wong, 2007
6	74.4	-	520	**519** $[M-H]^-$	269, 181	**268,** 226, 164	Diconiferyl alcohol glucoside/ alaschanioside C	Saracoglu 2003
7	75.1	-	367	**368** $[M]^+$	350	332	Feruloyl quinate	Simirgiotis, 2013
8	78.8	-	506	**505** $[M-H]^-$	269	268, 226, 182	Feruloyl malate (4-O-8 coupled) coniferyl alcohol	-

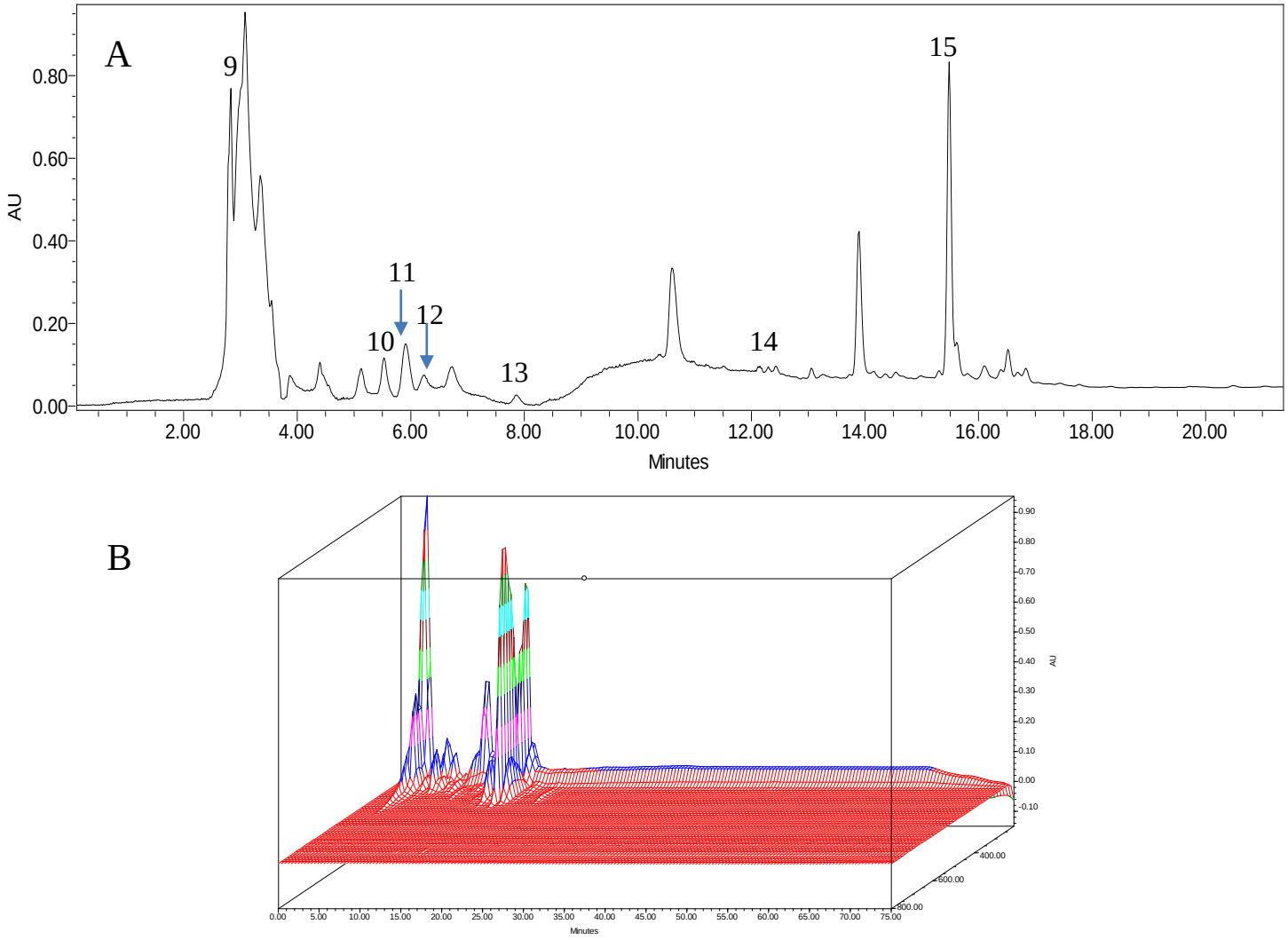

Figure 28. HPLC chromatograms of aqueous extract (fraction 12) in (A) 2-D and (B) 3-D.

Table 6. Identification of polyphenolic compounds from the aqueous extract (fraction 12) by HPLC-MS^n.

Peak no.	t_R (mins)	UV_{max} (nm)	MW	MS (m/z)	MS^2 ions (m/z)	MS^3 ions (m/z)	Tentative compound assignments	Reference
9	3.3	-	279	**280** $[M]^+$	262	244, 216	Coumaroyl aspartate	Pereira-Caro *et. al.*, 2013
10	5.5	261	293	294 $[M]^+$	276	**258,** 230, 132	1,7 bis(4-hydroxyphenyl)-2,4,6 hetatrienone	Habsah, 2005
11	5.9	223, 274	268	268 $[M]^+$	135	-	Genistein	Ye *et. al.*, 2012; Kang *et. al.*, 2007
12	6.2	211, 258	293	294 $[M]^+$	276	258, 230. 132	1,7 bis(4-hydroxyphenyl)-2,4,6 hetatrienone	Habsah, 2005
13	7.8	250	428	429 $[M]^+$	411	-	Stigmast-4-en-6β-ol-3-one 5^{α}, 8^{α} – epidioxyergosta-6,22-dien-3β-ol	Habsah, 2005
14	12.2	-	706	**707,** 353$[M-H]^-$	353	190	Dicaffeoylquinic acid	Jaiswal and Kuhnert, 2010
15	15.4	219, 242, 329	414	**415** $[M]^+$	406	-	β-stigmasterol	

5.4 Conclusion

This study indicates that the potent α-amylase inhibition of *E. elatior* extract was largely attributed to the presence of PACs. However, it is likely that there may be other inhibitors present that may have added to the inhibitory activity of α-amylase, especially in the aqueous fraction. However, there are more compounds within the fractions that have not been adequately separated on the column, and hence could not be characterised. It is possible that these unseparated compounds may have contributed to the observed inhibition of α-amylase. Hence, the present data warrants further in-depth study to elucidate, isolate and characterise potential active inhibitors.

Chapter 6

Synergism of epigallocatechin gallate towards dracoflavan B and acarbose on the inhibition of α-amylase

6.1 Introduction

There is much research currently done that screens for anti-diabetic drugs in plants that contain polyphenolic secondary metabolites (*254*). Nonetheless, many of these polyphenolic compounds have poor serum bioavailability (*255*) and are unable to enter the circulatory system to influence cellular interactions; consequently, a viable and promising strategy of controlling this disease is via the gastrointestinal tract, since a large portion of ingested polyphenolic compounds remains there and proceeds to the large intestine for microbiota biotransformation (*256*). Hence, this suggests that part of the health benefits derived from polyphenol-rich diets stem from its bioactivity within the gastrointestinal tract. Current conventional drugs, like acarbose, work through the gastrointestinal tract by inhibiting starch hydrolases like α-amylase and α-glucosidase. Starch digestion is retarded by inhibiting these enzymes, thus slowing down glucose absorption, which leads to a decrease in PPHG (*5*). These strong inhibitors are effective, but cause undesirable side-effects like flatulence and diarrhoea (*257*). In view of this, we propose drug combination as a plausible means of reducing these undesirable side-effects, by decreasing the dosage of the active inhibitors while maintaining its efficacy for glycaemic control. In addition, much work has

been done on individual inhibitors, but not on exploring the potential of synergism between drug combinations. TCM has utilised combination therapies for more than 2500 years to treat diseases, and TCM practitioners believe that synergistic interactions between the components of a single plant or a mixture of medicinal plants play a vital role for their therapeutic efficacy (*258, 259*).

In line with this, there have been several studies which look into the action of synergism, by combining commonly found flavonoids in foods with acarbose. For example, a combination of cyanidin-3-glucoside, cyanidin-3-galactoside and cyanidin-3,5-diglucoside with low concentrations of acarbose were shown to produce synergistic inhibition of maltase and sucrose (*260*). In addition, green tea extracts, green tea polyphenols or EGCG, when combined with acarbose, produced synergistic effects to inhibit α-amylase and α-glucosidase at low concentrations (*261*). Polyphenol-rich extracts from blackcurrant and rowanberries were also shown to potentiate the inhibition caused by acarbose. Their results showed that blackcurrant and rowanberry extracts inhibited α-glucosidase with an IC_{50} of 20 and 30 µg GAE/mL respectively, which is lower than the IC_{50} of acarbose (~ 40 µg/mL). The combination of acarbose at its IC_{50} value, and berry extracts at their IC_{50} values, caused increased inhibition (*262*). The additive effect between acarbose and cinnamon extract was also noted (*263*). Dried plant extracts of *Hibiscus sabdariffa* (Roselle), *Chrysanthemum indicum* (Chrysanthemum), *Morus alba* (Mulberry), *Aegle marmelos* (bael), and *Clitoria ternatea* (Butterfly pea) were combined with mulberry extract, and the results showed an additive interaction with intestinal maltase inhibition. In addition,

chrysanthemum, mulberry and bael extracts, together with roselle extract, produced synergistic inhibition against α-amylase. It was noted, however, that the author applied the glucose-oxidase/peroxidase method to quantify AGH inhibition, which is prone to interference by many phenolic compounds. Interference could lead to false positives, hence, it is unclear as to whether the synergistic/additive effects produced are due to false positives or actual inhibition (*264*).

Many epidemiological studies have investigated the roles of green tea consumption and its benefits to human health, such as prevention of cancers and cardiovascular diseases, improvement of the immune system, fighting obesity and diabetes (*265*). Epigallocatechin gallate (EGCG) is one of the main polyphenolic components in green tea, and it has also been linked to disease prevention. In addition, another component includes dracoflavan B (DFB), a compound isolated from 'dragon's blood', a common name used for the resins and saps of four types of plant genera: *Croton* (Euphorbiaceae), *Dracaena* (Dracaenaceae), *Daemonorops* (Palmaceae) and *Pterocarpus* (Fabaceae) (*266*). The resin from 'dragon's blood' is collected from *Daemonorops draco* in Southeast Asian countries. DFB, a highly selective inhibitor of α-amylase, does not show activity against α-glucosidase (unpublished data). This work hypothesizes that the application of a more highly selective inhibitor against α-amylase would result in fewer side effects. Two different inhibitory compounds were applied: DFB and acarbose, in combination with EGCG, to assess the synergistic effects on enzyme inhibition using the turbidity assay **(Figure 29)**.

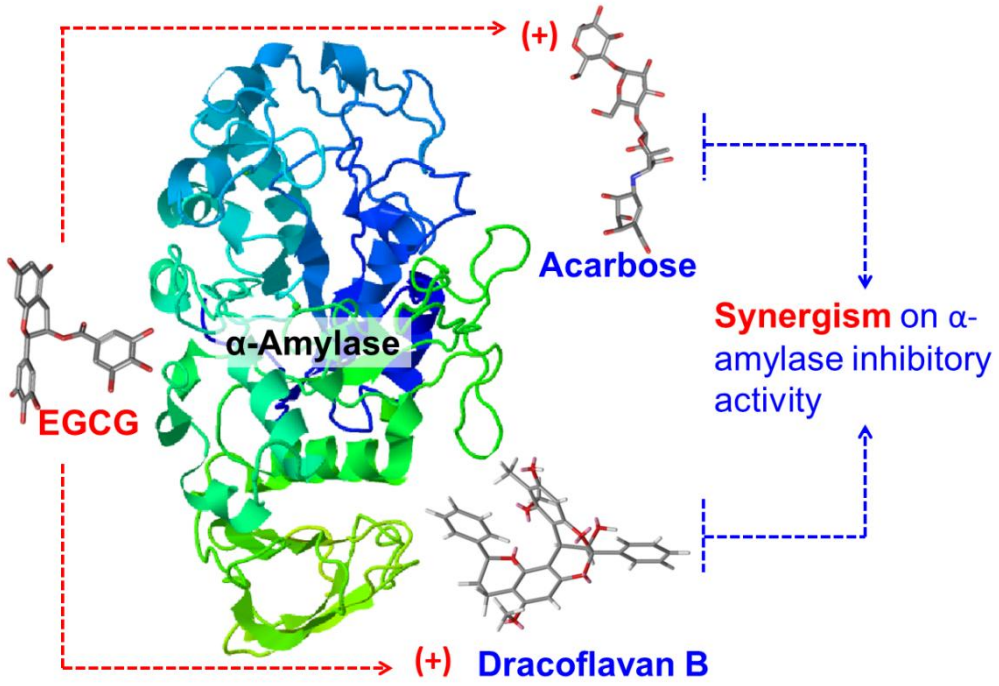

Figure 29. The combination of EGCG with DFB and acarbose for synergism in α-amylase inhibition activity.

Docking studies were applied in order to better understand the mechanism of synergy. Quantification of synergistic effects was done using the combination index (CI), which compares the doses of inhibitors, independently and in combinations, that produce the same level of inhibition experimentally (*267*).

6.2 Materials and methods

6.2.1 Reagents and instruments

α-amylase (A3176, type VI-B, from porcine pancreas), corn starch (S4126), acarbose (A8980) and epigallocatechin gallate (E4143) were obtained from Sigma-Aldrich Chemical Co. (St. Louis, MO, USA). Dracoflavan B was isolated from the resin from *Daemonorops draco*.

6.2.2 Determination of inhibition using turbidity method

The turbidity method was described in detail in section 5.2.5.

6.2.3 Experimental design of inhibitor combinations

DFB/EGCG: A fixed concentration of DFB (74 µM) was combined with various concentrations of EGCG (22, 44, 87, 349 µM). *Acarbose/EGCG:* A fixed concentration of acarbose (7.7 µM) was combined with various concentrations of EGCG (34, 136, 273, 545 µM). Each combination series was serially diluted by 1.5 times to give a dose-response curve.

6.2.4 Combination index and median effect equation (*268, 269*)

The combination index (CI) was calculated using **Equation 12**, where $(D)_1$ and $(D)_2$ are doses of DFB and EGCG in the combination system respectively. $(D_x)_1$ and $(D_x)_2$ are doses of DFB and EGCG alone. $(D_x)_1$ and $(D_x)_2$ values were calculated using the median effect outlined in **Equation 13**, whereby the fundamental rule governing this equation is the mass-action law.

$$\text{Combination Index (CI)} = \frac{(D)_1}{(Dx)_1} + \frac{(D)_2}{(Dx)2} \qquad \textbf{(Equation 12)}$$

$$\log\left(\frac{f_a}{f_u}\right) = m \log D - m \log D_m \qquad \textbf{(Equation 13)}$$

where $(f)_a$ = Fraction affected by D, $(f)_u$= Fraction unaffected (i.e. $(f)_u$ = 1-$(f)_a$), D = Dose or concentration of drug, D_m = Median effect dose (i.e. IC_{50}), m = Coefficient signifying the shape of the dose-effect relationship. CI < 1, CI = 1, and CI > 1 represents synergism, additive and antagonistic effect.

6.2.5 Statistical analysis

Statistical analysis was performed using SPSS software. The IC_{50} and CI values are given as means ± standard deviations (SDs). Significant differences between means were analysed using one-way ANOVA at the $p < 0.05$ level.

6.2.6 Molecular docking studies

The *holo* (Protein data bank identification: 1OSE) structure of α-amylase containing the inhibitor acarbose was obtained from the Protein Data Bank. The structures were first prepared via the Protein Preparation Wizard in Maestro, where 1) proper bond orders were added, 2) hydrogen atoms that were not present in the crystal structure were added, and 3) residues that had missing side chains were filled in using Prime. All water molecules that were 5 Å away from the inhibitor were removed. The protonation states of the residues were assigned using PROPKA at the physiological pH of 7.4. The dracoflavan B and epicatechin gallate were also prepared in Maestro. The docking was run from the graphical user interface accessible within Maestro. The top 5 poses for each ligand were retained and scored with the Extra Precision scoring function. The respective poses for the primary active site, secondary site 1 (SS1) and 2 (SS2), that had the lowest score, were exported for molecular dynamics (MD) simulations.

TIP3-P water molecules were added in an octahedron box with a distance of 20 Å. Counterions were added to maintain a neutral environment in the system. Minimisation was conducted via a two-step approach. With the proteins restrained, the solvent was first minimised for 5,000 steps via the steepest descent method, and an additional 5,000 steps via the conjugate

gradient method. The protein-solvent system was then minimised till the change in RMS converged to 0.01 kcal mol^{-1} $Å^{-1}$. The system was then heated from 0 to 300 K for 100 ps. Equilibration was done at a constant temperature of 300 K, with a time step of 2.0 fs for 5 ns. Snapshots were taken every 1 ps during the simulation to generate the coordinate trajectory file. Temperature regulation was done using Langevin dynamics, with the collision frequency set to 4 ps^{-1}. The heat bath coupling of the system was set to 2 ps and the simulations were done with isotropic position scaling. Equilibration was done at a constant pressure of 1 bar with a pressure relaxation time of 2 ps. All the bonds involving hydrogen were constrained using SHAKE. The distance cutoff for non-bonded interactions was set to 12 Å.

Three trajectories with different seed numbers were run for each protein-ligand complex. The binding free energies were then calculated with Sietraj and averaged between the three trajectories. Visualization of the protein-ligand complexes was done with the Visual Molecular Dynamics software.

6.3 Results and discussion

6.3.1 Inhibition of the various combinations of DFB and EGCG

Figure 30 (upper left) shows the dose-response curves of the maximum fixed concentration of DFB at 74 µM, spiked with EGCG at concentrations 22, 44, 87 and 349 µM, and each DFB and/or EGCG combination was serially diluted step-wise by a factor of 1.5. Our results show that as the concentration of EGCG increases, the slope of the dose-response curve becomes steeper, thus resulting in a smaller IC_{50} value. The same trend

was seen with acarbose and EGCG **(Figure 30**, **upper right)**. Acarbose was fixed at a concentration of 7.7 µM and spiked with EGCG at concentrations 34, 136, 273 and 545 µM. Using the dose-response curve generated, the IC_{50} of the combinations of DFB/EGCG and acarbose/EGCG were calculated and shown in **Figure 30 (below)**. On its own, DFB gave an IC_{50} of 100 ± 7 µM, whereas EGCG alone gave a very high IC_{50} value of 539 ± 93 µM. With the DFB concentration fixed at 74 µM, the addition of EGCG at 22 and 44 µM would give an IC_{50} of 90 ± 2 and 83 ± 5 µM respectively, which is significantly different ($p < 0.05$) from DFB alone, but not significantly different ($p > 0.05$) among the EGCG cases themselves. Nevertheless, the subsequent increase in the concentration of EGCG, to 87 and 349 µM, significantly decreases ($p < 0.05$) the IC_{50}, to 71 ± 4 and 60 ± 4 µM respectively, compared to the IC_{50} of just DFB alone.

On its own, acarbose gave an IC_{50} value of 5.9 ± 2.3 µM. With the concentration of acarbose fixed, the addition of EGCG at a concentration of 34 µM lowered the IC_{50} slightly, although not significantly ($p > 0.05$), to 5.1 ± 1.9 µM. A subsequent increase in the concentration of EGCG to 136 µM decreased the IC_{50} to 3.7 ± 0.6 µM. Further additions, of 273 and 545 µM of EGCG, resulted in a significant decrease ($p < 0.05$) in IC_{50}, of 2.5 ± 0.2 and 1.4 ± 0.3 µM respectively, compared to acarbose alone.

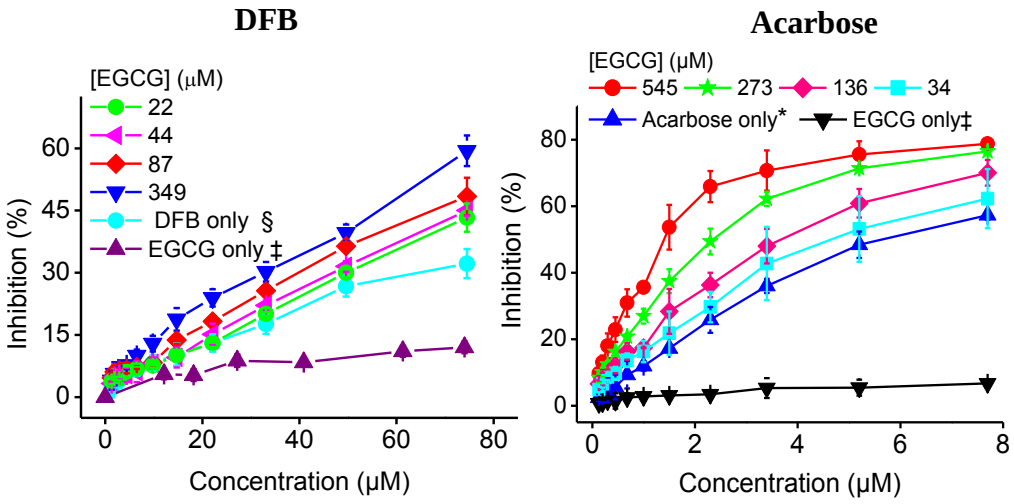

	EGCG (µM)	IC_{50} (µM)	P < 0.05
DFB §	22	90 ± 2	a
	44	83 ± 5	a
	87	71 ± 4	b
	349	60 ± 4	c
	DFB only §	100 ± 7	d
Acarbose *	34	5.1 ± 1.9	bc
	136	3.7 ± 0.6	abc
	273	2.5 ± 0.2	ab
	545	1.4 ± 0.3	a
	Acarbose only *	5.9 ± 2.3	c
	EGCG only ‡	247.5 ± 43	d

Figure 30. Dose-response curves of the % of inhibition of α-amylase by DFB spiked with different concentrations of EGCG (upper left), dose-response curves of the % of inhibition of α-amylase by acarbose spiked with different concentrations of EGCG (upper right), IC_{50} values of fixed DFB and acarbose combined with various concentrations of EGCG (below).

The different superscript symbols denote a fixed concentration of a compound: § 74 µM DFB, * 7.7 µM acarbose, Ø 2.3 µM acarbose, ǂ 700 µM EGCG. Significant difference between means were analysed using one-way ANOVA (Duncan test), where different alphabets represent significant differences at the p < 0.05 level.

6.3.2 Combination index plot of DFB/EGCG and acarbose/EGCG

In order to discern if the increase in the concentration of EGCG within media produced an additive or synergistic effect, we used the Combination Index (CI), which is a method of quantifying addition, synergism or antagonism between two drugs. The concept and equation **(Equation 12)** was introduced by Chou and Talalay (*270*). CI values will indicate synergism (<1), additive (=1) or antagonistic (>1) effects respectively. **Figure 31 (left)** shows the CI plot with all four combination ratios of a fixed concentration of DFB at 74 µM, spiked with 22, 44, 87 and 349 µM of EGCG. All the DFB/EGCG combinations gave CI values lesser than 1, which indicates synergistic interactions. In addition, our results also show that the strength of synergism is dependent on the concentration of EGCG within the system, and all the different concentrations tested gave a CI value that were significantly different ($p < 0.05$) from each other. Based on the classification developed by Chou (1991) (*267*), the addition of EGCG at 22 and 44 µM gave a CI value of 0.8 ± 0.05 and 0.7 ± 0.08 respectively, classifying it in the 'moderate synergism' category. A further addition of 87 and 349 µM of EGCG brings the system to the 'synergism' category, with a decrease in CI value to 0.63 ± 0.1 and 0.5 ± 0.07, respectively.

Similarly, **Figure 31 (right)** shows the CI plot with four combinations of acarbose and EGCG, with acarbose fixed at 7.7 µM and EGCG at concentrations 34, 136, 273 and 545 µM. All the different combinations gave CI values lesser than 1, which indicates synergistic interactions. Addition of 34 µM EGCG to acarbose gave an average CI value of 0.77 ± 0.08, which is in the 'moderate synergism' category. A further addition of 136 and 273 µM EGCG

into the system brings it to the 'synergism' category, with a CI value of 0.6 ± 0.04 and 0.41 ± 0.05 μM respectively. Finally, EGCG, at a concentration of 545 μM, gave the lowest CI value of 0.3 ± 0.06, under the 'strong synergism' category.

Our results indicate that EGCG works synergistically with DFB and acarbose to inhibit α-amylase. In addition, the extent of synergism is related to the amount of EGCG in the combination system; that is, the higher the concentration of EGCG in combination with acarbose and DFB, the stronger the synergistic effect.

6.3.3 Docking studies

Previous kinetic analysis revealed that DFB binds non-competitively to α-amylase (i.e. binding to a location on the enzyme that is different from the active site) with starch as the substrate, with a K_i value of 11.7 μM (results not published). Our results also seem to support the notion that EGCG may bind non-competitively to the enzyme, since the addition of a relatively high concentration of EGCG (700 μM) to the assay did not seem to affect the catalytic activity of the amylase to digest starch. In line with our findings, previous studies showed that EGCG binds non-competitively to human salivary α-amylase, with a calculated K_i value of 0.46 mM.

DFB **Acarbose**

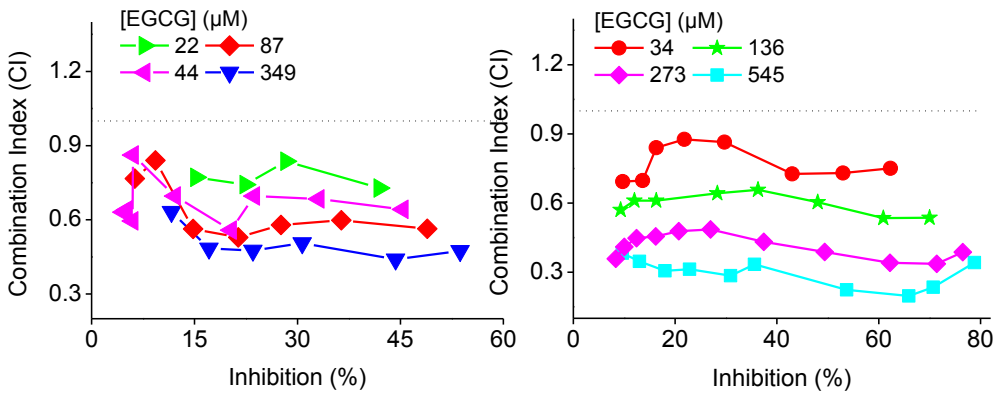

	[EGCG] (μM)	CI	P < 0.05	CI category
DFB §	22	0.8 ± 0.05	d	Moderate synergism
	44	0.7 ± 0.08	c	Moderate synergism
	87	0.63 ± 0.1	b	Synergism
	349	0.5 ± 0.07	a	Synergism

	[EGCG] (μM)	CI	P < 0.05	CI category
Acarbose *	34	0.77 ± 0.08	d	Moderate synergism
	136	0.6 ± 0.04	c	Synergism
	273	0.41 ± 0.05	b	Synergism
	545	0.3 ± 0.06	a	Strong synergism

Figure 31. Combination index plot of DFB-EGCG of the dose-response curve (upper left), combination index plot of acarbose-EGCG of the dose-response curve (upper right), combination index values and CI category of DFB and acarbose at different concentrations of EGCG (below).

The different superscript symbols denote a fixed concentration of a compound: § 74 μM DFB, * 7.7 μM acarbose. Significant differences between means were analysed using one-way ANOVA (Duncan test), where different alphabets represent significant differences at the $p < 0.05$ level.

In addition, EGCG was able to dock without affecting the binding to the catalytic sites of α-amylase. It was suggested that there are two types of docking machineries of EGCG on salivary α-amylase: the first is due to the hydrogen bonds between the hydroxyl groups of polyphenols and the amino acid residues, the other due to aromatic interactions of benzene rings between polyphenols and tryptophan residues of α-amylase (*75*). In light of this, EGCG was proposed to be able to dock at one or both of the secondary binding sites (SBSs).

Even though previous studies used human pancreatic α-amylase, the amino acid sequences for mammalian α-amylases have been shown to be similar in homology (*69*). In addition, the crystalline structure of α-amylases from human pancreases and saliva was shown to be similar to that of PPA. The comparisons revealed that the catalytic residues are not only similar, but most of the residues forming the substrate-binding site also have similar orientation (*271*). Hence, this assumes that the binding of EGCG to human pancreatic α-amylase and for PPA would be very similar.

In our DFB/EGCG system, both inhibitors are hypothetically non-competitive in nature, which raises the question of whether two non-competitive inhibitors, when applied together, can cause synergism to occur. In the simplest molecular case, if two non-competitive inhibitors target the same site on the enzyme, mutually exclusive binding would result, where, if one inhibitor is present, the addition of the second would only produce an additive effect. However, in our case, since two secondary binding sites exist on α-amylase (SBS1 and SBS2), it is possible that two inhibitors may bind

simultaneously, resulting in a case of "mutually non-exclusive" binding (*272*). Here, the two inhibitors would have specific and independent sites on the enzyme where the binding of one inhibitor would not prevent the binding of another to the enzyme, thus generating additional inhibited states of the enzyme **(Figure 32)**.

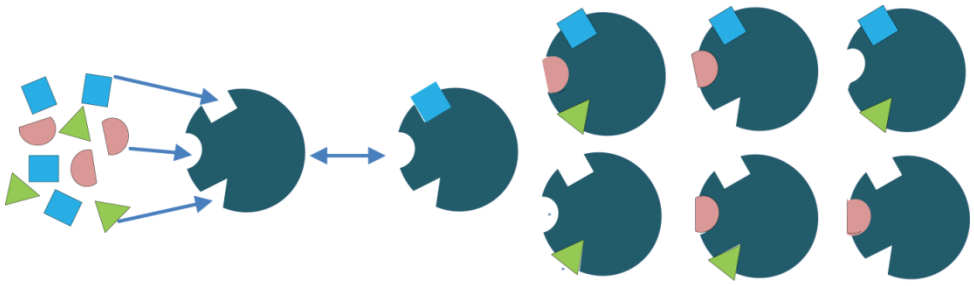

Figure 32. A schematic representation for two mutually non-exclusive, non-competitive inhibitors.

In order to gain a better understanding of its mechanism of inhibition, we applied molecular docking studies of the two ligands and the two secondary binding sites of α-amylase. Interestingly, MD simulations showed that both EGCG and DFB bind to the secondary binding sites of α-amylase, with one inhibitor having a preference towards one binding site over the other **(Table 7)**.

Table 7. Binding site energies of EGCG and DFB at secondary binding sites 1 and 2.

Protocol	**Binding location**	**EGCG Binding energy (kcal/mol)**	**DFB Binding energy (kcal/mol)**
Protocol 1: PB	SS1	-11.25	-7.98
	SS2	-4.83	-5.88
Protocol 2: GB	SS1	-8.11	-5.78
	SS2	-7.41	-10.10

Larger negative values suggest stronger binding energy between the enzyme and the ligand. Binding energy of EGCG to SBS1 was -11.25 kcal/mol, whereas DFB had a lower binding energy of -7.98 kcal/mol to SBS1. However, for SBS2, DFB revealed a larger binding energy of -5.88 kcal/mol as compared to the binding energy of EGCG, which was -4.83 kcal/mol. A similar trend was observed when a different protocol (protocol 2: GB) for energy calculations was used. The binding energies of EGCG and DFB at SBS1 were -8.11 kcal/mol and -5.78 kcal/mol respectively. For SBS2, DFB showed a higher binding energy compared to EGCG, which was -10.10 kcal/mol versus -7.41 kcal/mol respectively. Hence, EGCG was shown to have a preference of binding to SBS1, and DFB to SBS2. This explains the synergistic activity of EGCG and DFB towards the inhibition of α-amylase activity. We propose that there was 'Bliss Independence' occurring, where mutually non-exclusive binding results in cooperative inhibition of α-amylase. Since the two inhibitors each have a preference for an independent site, the inhibitors are able to bind, simultaneously and being mutually non-exclusive, through distinct mechanisms, without having to compete with one another for a specific binding site, thus resulting in synergistic inhibition against α-amylase. Since EGCG has relatively weak activity against α-amylase, it can be said that EGCG augments or potentiates the activity of DFB. It is possible that the binding of EGCG to α-amylase induces a conformational change that opens up the binding site for DFB for it to bind more strongly.

In the case of the acarbose/EGCG system, acarbose is a competitive inhibitor of α-amylase (*273*). Hence, this explains the synergistic activity of acarbose and EGCG against α-amylase, as a combination of both competitive

and non-competitive modes, which arise through binding at the active site, as well as a secondary site on the enzyme, resulting in a superadditive effect. Previous studies have also demonstrated that such synergistic activity is produced via the action of a competitive and a non-competitive inhibitor. For instance, chlorogenic acid (CGAs) and its derivatives (*274*), and finger millet phenolics (*275*), are shown to be non-competitive inhibitors. Berry components rich in CGAs and other phenolics are shown to potentiate the inhibition caused by acarbose (*262*).

6.3.4 3-D and 2-D interaction plot of EGCG, DFB to the secondary binding sites and acarbose to the catalytic site of α-amylase

Figure 33 shows a 3-D depiction of the three inhibitors binding to different sites of α-amylase, based on the binding energies in **Table 7**. DFB binds to SBS2, which is located between the interface of domains A and C of the free enzyme structure. EGCG has a binding preference towards SBS1, which is located near the catalytic site in domain A where acarbose binds to.

Figure 34 (a) shows a 2-D interaction plot between DFB and SBS2. The hydroxyl group at the 7^{th} position of the A-ring in flavan 1 displays H-bonding to the side chain of Arg343, and hydrophobic interaction with Val383. The methyl group in 6^{th} position of the A-ring in flavan 1 shows hydrophobic interaction with Phe315. The methoxy group in the 5^{th} position of the A-ring in flavan 1 has hydrophobic interaction with Ala318, negatively charged interaction with Glu484, and positively charged interaction with Lys322. In addition to hydrophobic interactions, ring B of flavan 1 has a multitude of interactions which includes polar interactions with Thr377 and

Thr376, positively charged interactions with Arg387 and 389, hydrophobic interaction with Trp388, and negatively charged interaction with Asp375.

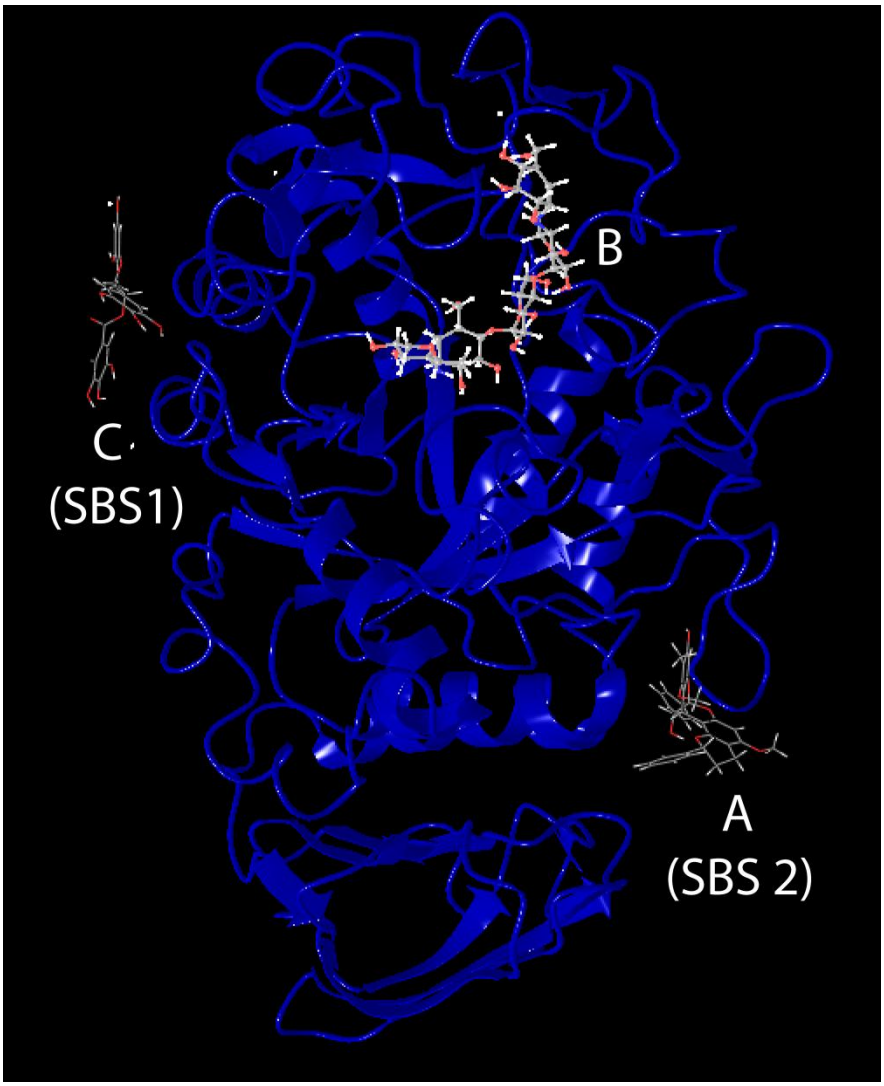

Figure 33. 3-D structure of PPA with three inhibitors: (a) DFB, (b) Acarbose and (c) EGCG at their proposed binding sites.

Figure 34 (b) shows the 2-D ligand interaction plot between EGCG and α-amylase. There were hydrophobic interactions between the catechin (A-C ring) moiety with Trp203 and Tyr155. The two hydroxyl groups in the gallate moiety (D-ring) were shown to have hydrogen-bonding interactions with the side chain of Gln243. In addition, the hydroxyl group in the epigallo

(B-ring) moiety at 3' forms hydrogen bonds with the side chain of Glu246. The hydroxyl group at 4' forms hydrogen bonds and hydrophobic interactions with the backbone of carboxyl oxygen of Ala241.

In all, hydrogen bonding and hydrophobic interactions play a significant role in the binding of EGCG and DFB to the secondary binding sites of α-amylase.

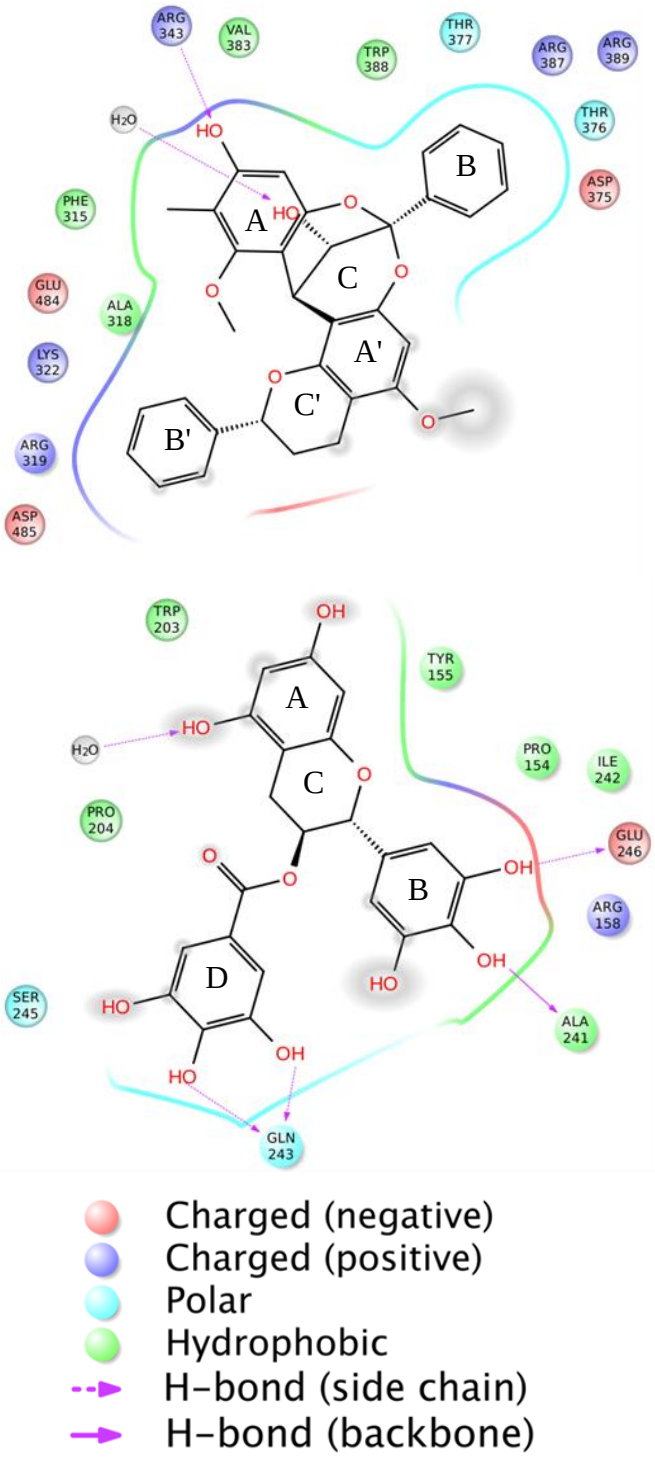

Figure 34. 2-D interaction plot of (a) DFB and (b) EGCG to their respective binding sites on α-amylase.

6.4 Conclusion

This study shows synergistic activity against α-amylase inhibition when EGCG was combined with conventional drugs, like DFB and acarbose. The extent of synergy was dependent on the amount of EGCG in the system, that is, the higher the concentration of EGCG in the system, the higher the potency of the combination towards inhibiting α-amylase (i.e. a lower IC_{50} value). Through MD simulation studies, EGCG was shown to have a binding preference for SBS1 and DFB to SBS2. The binding of the ligands to the binding sites are shown to be mainly through hydrogen bonding and hydrophobic interactions. 'Bliss independence', or mutually non-exclusive binding, was proposed to have occurred with the two inhibitors in their inhibition of α-amylase, which accounts for the synergistic activity observed. This study provides valuable implications for an alternative therapy for type 2 diabetics, using a combination of inhibitors. Furthermore, it also provides new insight into the use of naturally occurring enzyme inhibitors in foods rich in EGCG, like green tea, as a supplement to aid in the treatment of diabetes.

Chapter 7

Overall conclusions and future study

The number of type II diabetes cases is on the rise worldwide, and much research is focused on finding novel ways of mitigating this problem. A promising source for discovering new bioactive ingredients, which could be applied to treat diabetics, is the rich resource of tropical medicinal plants. There is a need for more specific inhibitors from natural sources to decrease undesirable side-effects like flatulence and diarrhoea that are frequently caused by conventional drugs. This work aims to tackle these two problems simultaneously and find potential solutions.

The first part of this project (Chapters 2 & 3) aims to validate the use of *in vitro* high-throughput colorimetric assays that are typically used to screen for starch hydrolase inhibitors. In chapter 2, a comparative study of native and artificial substrates was carried by measuring the K_i and K_i' of two known inhibitors (acarbose and 1-DNJ). Large differences were found between the K_i and $K_i^{'}$ of both inhibitors when different substrates were used. When *p*NPG was applied, the K_i of acarbose (130 ± 10 µM) and 1-DNJ (0.18 ± 0.04 µM) were shown to be consistently larger than when maltose was used as the substrate (K_i = 0.07 ± 0.01 and 0.01 ± 0.008 µM for acarbose and 1-DNJ, respectively). This chapter concludes that the use of native starch is vital in order to get an accurate indication of the interaction and potency of the inhibitors with the enzymes. Following this, chapter 3 shows the susceptibility of the GOP assay to interference by polyphenolic compounds that are

commonly found in botanicals. More specifically, this study found that compounds in the "high interference" group possess many OH groups that are in the *ortho* position. These findings from chapters 2 and 3 caution future research to first validate assays used for HTS of starch hydrolase inhibitors before their application. Furthermore, in order for the results to be relevant, assays should be accurately designed such that they mimic physiological reactions as closely as possible. The failure to validate assays before application may inadvertently lead to false results and wrong conclusions, which may mislead future work and result in a waste of resources.

The second part of this project involves applying the turbidity assay, which uses starch as the substrate, and to screen through a total of 298 botanicals for starch hydrolase inhibition. Out of the 298 samples tested, 71 showed activity, and were either edible and/or possessed medicinal value. Finally, 12 out of the 71 that showed activity stood out in terms of their starch hydrolase inhibition, as well as their historical use as medicinal herbs. A weak correlation was found between PAC and TPC contents with starch hydrolase inhibition, which indicates that there may be other specific inhibitors that may have contributed to its potency. This warrants further in-depth study to discover, characterise and isolate novel inhibitors. Although the correlation between TPC and starch hydrolase inhibition was low, plant extracts which have high TPC have potential for further development as anti-diabetic drugs, since these plants work through other mechanisms to control blood sugar levels. This research lays the important groundwork of screening for starch hydrolase inhibition, which is necessary for future in-depth studies of isolation and characterisation of novel compounds.

In line with this, a further step was taken and assay-guided fractionation and separation of the polyphenolic compounds from the ginger flower (*Etlingera elatior*) was conducted. Results show that proanthocyanidins in the flower were one of the main components for its high starch hydrolase inhibition. It is possible that other inhibitors besides PACs are present in the aqueous phase. Furthermore, it is also plausible that interactions between different groups of compounds can have a concerted action on the enzymes, to give synergistic inhibitory activity. Hence, further work could include identifying other active compounds within the ginger flower, as well as applying the ginger flower into a food system (e.g. bread or noodles) to create functional foods that are suitable for diabetics.

The final part of the project is to explore synergistic effects of tea catechins with acarbose (an anti-diabetic drug) and DFB, with the rationale of enhancing the effectiveness of conventional drugs through the use of commonly consumed foods like tea. Results indicate that acarbose and DFB are able to work together synergistically with EGCG to inhibit α-amylase. Through molecular docking studies, we suggest that the synergy occurs through the 'bliss independence' mechanism. In addition, this study also found that the extent of synergy is dependent on the amount of EGCG in the system - that is, the higher the concentration of EGCG in the system, the higher the synergy observed. This opens up a variety of possibilities for identifying synergistic reactions. For example, there are many other polyphenolic compounds (e.g. quercetin and kaempferol) present in many foods that can be studied and applied with conventional drugs. Their various interactions can

also be studied via molecular docking research to understand their structural activity.

Much work has been done on looking at individual inhibitors, but not on exploring the potential of synergism between drug combinations. This work shows that drug combination, coupled with everyday foods, is a plausible means of reducing undesirable side-effects, by decreasing the dosage of active inhibitors, while maintaining its efficacy for glycaemic control.

Bibliography

1. W.H.O. Definition and diagnosis of diabetes mellitus and intermediate hyperglycaemia.<http://www.who.int/diabetes/publications/diagnosis_diabetes 2006/en/> (accessed 1st June 2014).

2. A.D.A., Diagnosis and classification of diabetes mellitus. In *Diabetes Care*, American Diabetes Association: 2011; Vol. 34, pp 62-69.

3. Grundy, S. M.; Benjamin, I. J.; Burke, G. L.; Chait, A.; Eckel, R. H.; Howard, B. V.; Mitch, W.; Smith, S. C.; Sowers, J. R., Diabetes and cardiovascular disease: a statement for healthcare professionals from the american heart association. *Circulation* **1999,** *100*, 1134-1146.

4. Bhat, M.; Zinjarde, S. S.; Bhargava, S. Y.; Kumar, A. R.; Joshi, B. N., Antidiabetic Indian Plants: A good source of potent anylase inhibitors. *Evidence-Based Complementary and Alternative Medicine* **2008,** *2011*.

5. Campo, V. L.; Aragao-Leoneti, V.; Carvalho, I., Glycosidases and diabetes: Metabolic changes, mode of action and therapeutic perspectives. In *Carbohydrate Chemistry: Chemical and Biological Approaches, Vol 39*, Rauter, A. P.; Lindhorst, T. K., Eds. Royal Soc Chemistry, Thomas Graham House, Science Park, Cambridge Cb4 4wf, Cambs, Uk: 2013; Vol. 39, pp 181-203.

6. W.H.O. Global status report on noncommunicable diseases. <http://www.who.int/nmh/publications/ncd_report2010/en/>, (accessed 1st June 2014),

7. Sicree, R.; Shaw, J. E.; Baker, P. Z. *The global burden: Diabetes and impaired glucose tolerance*; International Diabetes Federation: **2009**.

8. Chan, J. C. N.; Malik, V.; Jia, W.; Kadowaki, T.; Yajnik, C. S.; Yoon, K.; Hu, F. B., Diabetes in asia: Epidemiology, risk factors and pathophysiology. *The Journal of American Medical Association* **2009,** *301*, 2129-2140.

9. W.H.O. Diabetes programme. <http://www.who.Int/diabetes/en/> (accessed 31st May 2014),

10. Canada, P. H. A. o., Diabetes in Canada: Facts and figures from a public health perspective. In Canada, P. H. A. o., Ed. Ottawa, 2011.

11. Yang, J.; Mao, Q. X.; Xu, H. X.; Ma, X.; Zeng, C. Y., Tea consumption and risk of type 2 diabetes mellitus: a systematic review and meta-analysis update. *BMJ Open* **2014,** *4*, e005632.

12. Liao, S.; Kao, Y. H.; Hiipakka, R. A., Green tea: biochemical and biological basis for health benefits. *Vitamins and hormones* **2001,** *62*, 1-94.

13. Yang, C. S.; Wang, Z.-Y., Tea and cancer. *Journal of the National Cancer Institute* **1993,** *85*, 1038-1049.

14. Mitscher, L. A.; Jung, M.; Shankel, D.; Dou, J. H.; Steele, L.; Pillai, S. P., Chemoprotection: A review of the potential therapeutic antioxidant properties of green tea (*Camellia sinensis*) and certain of its constituents. *Medicinal research reviews* **1997,** *17*, 327-65.

15. Lin, J. K.; Liang, Y. C.; Lin-Shiau, S. Y., Cancer chemoprevention by tea polyphenols through mitotic signal transduction blockade. *Biochemical pharmacology* **1999,** *58*, 911-5.

16. Ahmad, N.; Mukhtar, H., Green tea polyphenols and cancer: biologic mechanisms and practical implications. *Nutrition reviews* **1999,** *57*, 78-83.

17. Crespy, V.; Williamson, G., A review of the health effects of green tea catechins in in vivo animal models. *The Journal of nutrition* **2004,** *134*, 3431S-3440S.

18. Barbosa, D. S., Green tea polyphenolic compounds and human health. *Journal Fur Verbraucherschutz Und Lebensmittelsicherheit-Journal of Consumer Protection and Food Safety* **2007,** *2*, 407-413.

19. Cabrera, C.; Artacho, R.; Gimenez, R., Beneficial effects of green tea - A review. *Journal of the American College of Nutrition* **2006,** *25*, 79-99.

20. Yang, C. S.; Lambert, J. D.; Ju, J.; Lu, G.; Sang, S., Tea and cancer prevention: Molecular mechanisms and human relevance. *Toxicology and Applied Pharmacology* **2007,** *224*, 265-273.

21. Zaveri, N. T., Green tea and its polyphenolic catechins: Medicinal uses in cancer and noncancer applications. *Life Sciences* **2006,** *78*, 2073-2080.

22. Higdon, J. V.; Frei, B., Tea catechins and polyphenols: Health effects, metabolism, and antioxidant functions. *Critical Reviews in Food Science and Nutrition* **2003,** *43*, 89-143.

23. Stalmach, A.; Troufflard, S.; Serafini, M.; Crozier, A., Absorption, metabolism and excretion of Choladi green tea flavan-3-ols by humans. *Mol Nutr Food Res* **2009,** *53 Suppl 1*, S44-53.

24. Kao, Y. H.; Hiipakka, R. A.; Liao, S. S., Modulation of endocrine systems and food intake by green tea epigallocatechin gallate. *Endocrinology* **2000,** *141*, 980-987.

25. Han, M. K., Epigallocatechin gallate, a constituent of green tea, suppresses cytokine-induced pancreatic β-cell damage. *Experimental and Molecular Medicine* **2003,** *35*, 136-139.

26. Anderson, R. A.; Polansky, M. M., Tea enhances insulin activity. *Journal of agricultural and food chemistry* **2002,** *50*, 7182-7186.

27. Wu, L. Y.; Juan, C. C.; Ho, L. T.; Hsu, Y. P.; Hwang, L. S., Effect of green tea supplementation on insulin sensitivity in Sprague-Dawley rats. *Journal of agricultural and food chemistry* **2004,** *52*, 643-648.

28. Wu, L. Y.; Juan, C. C.; Hwang, L. S.; Hsu, Y. P.; Ho, P. H.; Ho, L. T., Green tea supplementation ameliorates insulin resistance and increases glucose transporter IV content in a fructose-fed rat model. *European Journal of Nutrition* **2004,** *43*, 116-124.

29. Kobayashi, Y.; Suzuki, M.; Satsu, H.; Arai, S.; Hara, Y.; Suzuki, K.; Miyamoto, Y.; Shimizu, M., Green tea polyphenols inhibit the sodium-dependent glucose transporter of intestinal epithelial cells by a competitive mechanism. *Journal of agricultural and food chemistry* **2000,** *48*, 5618-5623.

30. Matsui, T.; Tanaka, T.; Tamura, S.; Toshima, A.; Tamaya, K.; Miyata, Y.; Tanaka, K.; Matsumoto, K., α-glucosidase inhibitory profile of catechins and theaflavins. *Journal of Agricultural and Food Chemistry* **2007,** *55*, 99-105.

31. Liu, J.; Wang, M.; Peng, S.; Zhang, G., Effect of green tea catechins on the postprandial glycemic response to starches differing in amylose content. *Journal of agricultural and food chemistry* **2011,** *59*, 4582-4588.

32. Koh, L. W.; Wong, L. L.; Loo, Y. Y.; Kasapis, S.; Huang, D., Evaluation of different teas against starch digestibility by mammalian glycosidases. *Journal of agricultural and food chemistry* **2010,** *58*, 148-154.

33. Kamiyama, O.; Sanae, F.; Ikeda, K.; Higashi, Y.; Minami, Y.; Asano, N.; Adachi, I.; Kato, A., *In vitro* inhibition of α-glucosidases and glycogen phosphorylase by catechin gallates in green tea. *Food Chemistry* **2010,** *122*, 1061-1066.

34. Hara, Y.; Honda, M., The inhibition of α-amylase by tea polyphenols *Agricultural and Biological Chemistry* **1990,** *54*, 1939-1945.

35. Williamson, G.; Manach, C., Bioavailability and bioefficacy of polyphenols in humans. II. Review of 93 intervention studies. *American Journal of Clinical Nutrition* **2005,** *81*, 243S-255S.

36. Kao, Y. H.; Chang, H. H.; Lee, M. J.; Chen, C. L., Tea, obesity and diabetes. *Molecular Nutrition & Food Research* **2006,** *50*, 188-210.

37. Bandyopadhyay, P.; Ghosh, A. K.; Ghosh, C., Recent developments on polyphenol-protein interactions: effects on tea and coffee taste, antioxidant properties and the digestive system. *Food & Function* **2012,** *3*, 592-605.

38. Cai, K. H.; Bennick, A., Effect of salivary proteins on the transport of tannin and quercetin across intestinal epithelial cells in culture. *Biochemical pharmacology* **2006,** *72*, 974-980.

39. Record, I. R.; Lane, J. M., Simulated intestinal digestion of green and black teas. *Food Chemistry* **2001,** *73*, 481-486.

40. Lewandowska, U.; Szewczyk, K.; Hrabec, E.; Janecka, A.; Gorlach, S., Overview of metabolism and bioavailability enhancement of polyphenols. *Journal of agricultural and food chemistry* **2013,** *61*, 12183-12199.

41. Kuhnle, G.; Spencer, J. P. E.; Schroeter, H.; Shenoy, B.; Debnam, E. S.; Srai, S. K. S.; Rice-Evans, C.; Hahn, U., Epicatechin and catechin are *O*-methylated and glucuronidated in the small intestine. *Biochemical and Biophysical Research Communications* **2000,** *277*, 507-512.

42. Weinert, C. H.; Wiese, S.; Rawel, H. M.; Esatbeyoglu, T.; Winterhalter, P.; Homann, T.; Kulling, S. E., Methylation of catechins and procyanidins by rat and human catechol-*O*-methyltransferase: metabolite profiling and molecular modeling studies. *Drug Metabolism and Disposition* **2012,** *40*, 353-359.

43. Kay, C. D., Aspects of anthocyanin absorption, metabolism and pharmacokinetics in humans. *Nutrition Research Reviews* **2006,** *19*, 137-146.

44. Scalbert, A.; Williamson, G., Dietary intake and bioavailability of polyphenols. *The Journal of nutrition* **2000,** *130*, 2073S-2085S.

45. Philip, A. K.; Philip, B., Colon targeted drug delivery systems: A review on primary and novel approaches. *Oman Medical Journal* **2010,** *25*, 79-87.

46. Puls, W.; Keup, U.; Krause, H. P.; Thomas, G.; Hoffmeister, F., Glucosidase inhibition- new approach to treatment of diabetes, obesity, and hyperlipoproteinemia. *Naturwissenschaften* **1977,** *64*, 536-537.

47. Krentz, A. J.; Bailey, C. J., Oral antidiabetic agents - current role in type 2 diabetes mellitus. *Drugs* **2005,** *65*, 385-411.

48. Bischoff, H.; Puls, W.; Krause, H. P.; Schutt, H.; Thomas, G., Pharmacological properties of the novel glucosidase inhibitors BAY m 1099 (miglitol) and BAY o. *Diabetes Res Clin Pract* **1985,** *1*, 53-62.

49. Frandsen, T. P.; Lok, F.; Mirgorodskaya, E.; Roepstorff, P.; Svensson, B., Purification, enzymatic characterization, and nucleotide sequence of a high-isoelectric-point α-glucosidase from barley malt. *Plant physiology* **2000,** *123*, 275-86.

50. Schonert, S.; Buder, T.; Dahl, M. K., Identification and enzymatic characterization of the maltose-inducible α-glucosidase MalL (sucrase-isomaltase-maltase) of *Bacillus subtilis*. *J Bacteriol* **1998,** *180*, 2574-8.

51. Needleman, R. B.; Federoff, H. J.; Eccleshall, T. R.; Buchferer, B.; Marmur, J., Purification and characterization of an α-glucosidase from *Saccharomyces carlsbergensis*. *Biochemistry* **1978,** *17*, 4657-61.

52. Rudick, M. J.; Fitzgerald, Z. E.; Rudick, V. L., Intra- and extracellular forms of α-glucosidase from *Aspergillus niger*. *Arch Biochem Biophys* **1979,** *193*, 509-20.

53. Jones, K.; Sim, L.; Mohan, S.; Kumarasamy, J.; Liu, H.; Avery, S.; Naim, H. Y.; Quezada-Calvillo, R.; Nichols, B. L.; Pinto, B. M.; Rose, D. R., Mapping the intestinal α-glucogenic enzyme specificities of starch digesting maltase-glucoamylase and sucrase-isomaltase. *Bioorganic & medicinal chemistry* **2011,** *19*, 3929-34.

54. Yilmazer-Musa, M.; Griffith, A. M.; Michels, A. J.; Schneider, E.; Frei, B., Grape seed and tea extracts and catechin 3-gallates are potent inhibitors of α-amylase and α-glucosidase activity. *Journal of agricultural and food chemistry* **2012,** *60*, 8924-8929.

55. Li, T.; Liu, J.; Zhang, X.; Ji, G., Antidiabetic activity of lipophilic (-)-epigallocatechin-3-gallate derivative under its role of α-glucosidase inhibition. *Biomedicine & Pharmacotherapy* **2007,** *61*, 91-96.

56. Xu, Y.; Zhang, Z.; Li, L.; Joshi, M. K.; Huang, N.; Niu, J.; Lu, Y., Catechins play key role in green tea extract-induced postprandial hypoglycemic potential in vitro. *European Food Research and Technology* **2013,** *237*, 89-99.

57. Takahashi, T.; Miyazawa, M., Potent α-glucosidase inhibitors from safflower (*Carthamus tinctorius L.*) seed. *Phytotherapy Research* **2012,** *26*, 722-726.

58. Choi, C. W.; Choi, Y. H.; Cha, M.-R.; Yoo, D. S.; Kim, Y. S.; Yon, G. H.; Hong, K. S.; Kim, Y. H.; Ryu, S. Y., Yeast α-glucosidase inhibition by isoflavones from plants of leguminosae as an *in vitro* alternative to acarbose. *Journal of agricultural and food chemistry* **2010,** *58*, 9988-9993.

59. Ani, V.; Naidu, K. A., Antihyperglycemic activity of polyphenolic components of black/bitter cumin Centratherum anthelminticum (L.) Kuntze seeds. *European Food Research and Technology* **2008,** *226*, 897-903.

60. Oki, T.; Matsui, T.; Osajima, Y., Inhibitory effect of α-glucosidase inhibitors varies according to its origin. *Journal of agricultural and food chemistry* **1999,** *47*, 550-553.

61. Kim, M.-S.; Ahn, S.-M.; Jung, I.-C.; Kwon, G.-S.; Sohn, H.-Y., Screening of α-amylase and α-glucosidase inhibitor from nepalese plant extracts. *Korean Journal of Microbiology and Biotechnology* **2010,** *38*, 183-189.

62. Nichols, B. L.; Eldering, J.; Avery, S.; Hahn, D.; Quaroni, A.; Sterchi, E., Human small intestinal maltase-glucoamylase cDNA cloning - Homology to sucrase-isomaltase. *Journal of Biological Chemistry* **1998,** *273*, 3076-3081.

63. Rossi, E. J.; Sim, L.; Kuntz, D. A.; Hahn, D.; Johnston, B. D.; Ghavami, A.; Szczepina, M. G.; Kumar, N. S.; Sterchi, E. E.; Nichols, B. L.;

Pinto, B. M.; Rose, D. R., Inhibition of recombinant human maltase glucoamylase by salacinol and derivatives. *Febs J.* **2006,** *273*, 2673-2683.

64. Chiba, S., Molecular mechanism in α-glucosidase and glucoamylase. *Bioscience Biotechnology and Biochemistry* **1997,** *61*, 1233-1239.

65. Rempel, B. P.; Withers, S. G., Covalent inhibitors of glycosidases and their applications in biochemistry and biology. *Glycobiology* **2008,** *18*, 570-586.

66. Sim, L.; Quezada-Calvillo, R.; Sterchi, E. E.; Nichois, B. L.; Rose, D. R., Human intestinal maltase-glucoamylase: Crystal structure of the N-terminal catalytic subunit and basis of inhibition and substrate specificity. *Journal of Molecular Biology* **2008,** *375*, 782-792.

67. Robyt, J. F., Chapter 7 - enzymes and their action on starch. In *Starch (Third Edition)*, BeMiller, J.; Whistler, R., Eds. Academic Press: San Diego, **2009**; pp 237-292.

68. Cozzone, P.; Pasero, L.; Marchism.G, Characterization of porcine pancreatic isoamylase - Separation and amino acid composition *Biochimica Et Biophysica Acta* **1970,** *200*, 590-&.

69. Gilles, C.; Astier, J. P.; MarchisMouren, G.; Cambillau, C.; Payan, F., Crystal structure of pig pancreatic α-amylase isoenzyme II, in complex with the carbohydrate inhibitor acarbose. *European Journal of Biochemistry* **1996,** *238*, 561-569.

70. Qian, M. X.; Spinelli, S.; Driguez, H.; Payan, F., Structure of a pancreatic α-amylase bound to a substrate analogue at 2.03 angstrom resolution. *Protein Science* **1997,** *6*, 2285-2296.

71. Payan, F.; Qian, M. X., Crystal structure of the pig pancreatic α-amylase complexed with malto-oligosaccharides. *J. Protein Chem.* **2003,** *22*, 275-284.

72. Robyt, J. F.; French, D., Action pattern of porcine pancreatic α-amylase in relationship to substrate binding site of enzyme *Journal of Biological Chemistry* **1970,** *245*, 3917-&.

73. Brayer, G. D.; Luo, Y. G.; Withers, S. G., The structure of human pancreatic α-amylase at 1.8 angstrom resolution and comparisons with related enzymes. *Protein Science* **1995,** *4*, 1730-1742.

74. Svensson, B., Protein engineering in the α-amylase family- catalytic mechanism, substrate specificity and stability *Plant Molecular Biology* **1994,** *25*, 141-157.

75. Pasero, L.; Mazzeipierron, Y.; Abadie, B.; Chicheportiche, Y.; Marchismouren, G., Complete amino-acid sequence and location of the 5 disulfide bridges in porcine pancreatic α-amylase. *Biochimica Et Biophysica Acta* **1986,** *869*, 147-157.

76. Hakamata, W.; Kurihara, M.; Okuda, H.; Nishio, T.; Oku, T., Design and screening strategies for α-glucosidase inhibitors based on enzymological information. *Current Topics in Medicinal Chemistry* **2009,** *9*, 3-12.

77. Sim, L.; Willemsma, C.; Mohan, S.; Naim, H. Y.; Pinto, B. M.; Rose, D. R., Structural basis for substrate selectivity in human maltase-glucoamylase and sucrase-isomaltase N-terminal domains. *Journal of Biological Chemistry* **2010,** *285*, 17763-17770.

78. Breitmeier, D.; Gunther, S.; Heymann, H., Acarbose and 1-deoxynojirimycin inhibit maltose and maltooligosaccharide hydrolysis of human small intestinal glucoamylase-maltase in two different substrate-induced modes. *Archives of Biochemistry and Biophysics* **1997,** *346*, 7-14.

79. Osman, A. M., The advantages of using natural substrate-based methods in assessing the roles and synergistic and competitive interactions of barley malt starch-degrading enzymes. *Journal of the Institute of Brewing* **2002,** *108*, 204-214.

80. Breuil, C.; Mayers, P.; Saddler, J. N., Substrate conditions that infuence the assays used for determining the β-glucosidase activity of cellulolytic microorganisms *Biotechnology and Bioengineering* **1986,** *28*, 1653-1656.

81. van Diggelen, O. P.; Oemardien, L. F.; van der Beek, N.; Kroos, M. A.; Wind, H. K.; Voznyi, Y. V.; Burke, D.; Jackson, M.; Winchester, B. G.; Reuser, A. J. J., Enzyme analysis for Pompe disease in leukocytes; superior results with natural substrate compared with artificial substrates. *Journal of Inherited Metabolic Disease* **2009,** *32*, 416-423.

82. Miller, G. L., Use of dinitrosalicylic acid reagent for determination of reducing sugar *Analytical Chemistry* **1959,** *31*, 426-428.

83. Sumner, J. B.; Graham, V. A., Dinitrosalicylic acid: A reagent for the estimation of sugar in normal and diabetic urine. *Journal of Biological Chemistry* **1921,** *47*, 5-9.

84. Sumner, B., The estimation of sugar in diabetic urine, using dinitrosalicylic acid *J. Biol. Chem.* **1924,** *62*, 287-290.

85. Sumner, B., A more specific reagent for the determination of sugar in urine. *J. Biol. Chem.* **1925,** *65*, 51-54.

86. Teixeira, R. S. S.; da Silva, A. S.; Ferreira-Leitao, V. S.; Bon, E. P. D., Amino acids interference on the quantification of reducing sugars by the 3,5-dinitrosalicylic acid assay mislead carbohydrase activity measurements. *Carbohydrate Research* **2012,** *363*, 33-37.

87. Forouhi, E.; Gunn, D. J., Some effects of metal-ions of the estimation of reducing sugars in biological media *Biotechnology and Bioengineering* **1983,** *25*, 1905-1911.

88. Breuil, C.; Saddler, J. N., Comparison of the 3,5-dinitrosalicylic acid and nelson-somogyi methods of assaying for reducing sugars and determining cellulase activity *Enzyme and Microbial Technology* **1985,** *7*, 327-332.

89. Gusakov, A. V.; Kondratyeva, E. G.; Sinitsyn, A. P., Comparison of two methods for assaying reducing sugars in the determination of carbohydrase activities. *International Journal of Analytical Chemistry* **2011,** *2011*.

90. Robyt, J. F.; Whelan, W. J., Reducing value methods for maltodextrins. 1. chain-length dependence of alkaline 3,5-dinitrosalicylate and chain-length independence of alkaline copper. *Analytical Biochemistry* **1972,** *45*, 510.

91. Wong, A. I. C.; Huang, D., Tea and starch digestibility. In *Tea in health and disease prevention*, Preedy, V. R., Ed. Academic Press: **2013**.

92. Nelson, N., A photometric adaptation of the Somogyi method for the determination of glucose. *Journal of Biological Chemistry* **1944,** *153*, 375-380.

93. Somogyi, M., Notes on sugar determination *Journal of Biological Chemistry* **1952,** *195*, 19-23.

94. Morishita, Y.; Iinuma, Y.; Nakashima, N.; Majima, K.; Mizuguchi, K.; Kawamura, Y., Total and pancreatic amylase measured with 2-chloro-4-nitrophenyl-4-*O*-beta-D-galactopyranosylmaltoside. *Clinical chemistry* **2000,** *46*, 928-933.

95. Feng, Z.; Wang, Y.; Zheng, Y., A new microtiter plate-based screening method for microorganisms producing α-amylase inhibitors. *Biotechnology and Bioprocess engineering* **2011,** *16*, 894-900.

96. Hamdan, II; Afifi, F. U., Capillary electrophoresis as a screening tool for α-amylase inhibitors in plant extracts. *Saudi pharmaceutical journal : SPJ : the official publication of the Saudi Pharmaceutical Society* **2010,** *18*, 91-5.

97. Fontanini, D.; Capocchi, A.; Saviozzi, F.; Galleschi, L., Simplified electrophoretic assay for human salivary α-amylase inhibitor detection in cereal seed flours. *Journal of agricultural and food chemistry* **2007,** *55*, 4334-9.

98. Linscheid, M. W., Affinity capillary electrophoresis: DNA interactions with peptides, proteins, and modified DNA. In *Affinity Capillary Electrophoresis in Pharmaceutics and Biopharmaceutics*, Neubert, R. H. H., Ed. Mercel Dekker: New York, **2003**.

99. Fuwa, H., A new method for microdetermination of amylase activity by the use of amylose as the substrate *Journal of Biochemistry* **1954,** *41*, 583-603.

100. Lansky, S.; Kooi, M.; Schoch, T. J., Properties of the fractions and linear subfractions from various starches *Journal of the American Chemical Society* **1949,** *71*, 4066-4075.

101. Thomas, M.; Priest, F. G.; Stark, J. R., Characterization of an extracellular β-amylase from *Bacillus-megaterium*-sensu-stricto. *Journal of General Microbiology* **1980,** *118*, 67-72.

102. Gonzalez, C. F.; Farina, J. I.; Figueroa, L. I. C., A critical assessment of a viscometric assay for measuring *Saccharomycopsis fibuligera* α-amylase activity on gelatinised cassava starch. *Enzyme and Microbial Technology* **2002,** *30*, 169-175.

103. Wong, A. I. C.; Huang, D., Assessment of the degree of interference of polyphenolic compounds on glucose oxidation/peroxidase assay. *Journal of agricultural and food chemistry* **2014,** *62*, 4571-4576.

104. Kim, J. S.; Kwon, C. S.; Son, K. H., Inhibition of α-glucosidase and amylase by luteolin, a flavonoid. *Bioscience Biotechnology and Biochemistry* **2000,** *64*, 2458-2461.

105. Hagberg, S., A rapid method for determining α-amylase activity. *Cereal Chemistry* **1960,** *37*, 218- 222.

106. Ichiki, Y.; Tamura, H.; Ohtani, A.; Yoshikawa, H., An environmentally acceptable method of assaying the inhibition of α-amylase induction. *Journal of Pesticide Science* **2007,** *32*, 120-123.

107. Satoyama, T.; Nakai, Y.; Hirata, Y.; Tanno, K.; Hara, T.; Fujio, Y., Characteristics of a simple assay methods for α-amylase using microplates. *Nippon Nogeikagaku Kaishi* **1999,** *73*, 31-34.

108. Simpson, R., The measurement of turbidity and potential to predict some sugar quality parameters. *South African Sugar Technologist's Association* **1999,** *73*, 263-266.

109. Feng, S. B.; Song, L. X.; Liu, Y. C.; Lai, F. L.; Zuo, G.; He, G. Y.; Chen, M. J.; Huang, D. J., Hypoglycemic activities of commonly-used traditional chinese herbs. *American Journal of Chinese Medicine* **2013,** *41*, 849-864.

110. Lacroix, I. M. E.; Li-Chan, E. C. Y., Inhibition of dipeptidyl peptidase (DPP)-IV and α-glucosidase activities by pepsin-treated whey proteins. *Journal of agricultural and food chemistry* **2013,** *61*, 7500-7506.

111. Liu, T. T.; Yip, Y. M.; Song, L. X.; Feng, S. B.; Liu, Y. C.; Lai, F. L.; Zhang, D. W.; Huang, D. J., Inhibiting enzymatic starch digestion by the phenolic compound diboside A: A mechanistic and *in silico* study. *Food Research International* **2013,** *54*, 595-600.

112. Wang, H. Y.; Liu, T. T.; Song, L. X.; Huang, D. J., Profiles and α-amylase inhibition activity of proanthocyanidins in unripe *Manilkara zapota* (Chiku). *Journal of agricultural and food chemistry* **2012,** *60*, 3098-3104.

113. Wang, H. Y.; Song, L. X.; Feng, S. B.; Liu, Y. C.; Zuo, G.; Lai, F. L.; He, G. Y.; Chen, M. J.; Huang, D. J., Characterization of proanthocyanidins in stems of *Polygonum multiflorum* thunb as strong starch hydrolase inhibitors. *Molecules* **2013,** *18*, 2255-2265.

114. Pal, S. K., Complementary and alternative medicine: An overview. *Current Science* **2002,** *82*, 518-524.

115. Wang, Z.; Chan, P.; Wang, J., The preventive effect of traditional chinese medicinal herbs on type 2 diabetes mellitus. In *Traditional Chinese Medicine: Scientific Basis for ItsUse*, Adams Jr, J. D.; Lien, E. J., Eds. **2013;** pp 268-312.

116. Feng, S.; Song, L.; Liu, Y.; Lai, F.; Zuo, G.; He, G.; Chen, M.; Huang, D., Hypoglycemic Activities of Commonly-Used Traditional Chinese Herbs. *American Journal of Chinese Medicine* **2013,** *41*, 849-864.

117. Mukherjee, A.; Sengupta, S., Indian medicinal plants known to contain intestinal glucosidase inhibitors also inhibit pancreatic lipase activity-an ideal situation for obesity control by herbal drugs. *Indian Journal of Biotechnology* **2013,** *12*, 32-39.

118. Bhat, M.; Zinjarde, S. S.; Bhargava, S. Y.; Kumar, A. R.; Joshi, B. N., Antidiabetic indian plants: A good source of potent amylase inhibitors. *Evidence-Based Complementary and Alternative Medicine* **2011**, 1-6.

119. Marrelli, M.; Loizzo, M. R.; Nicoletti, M.; Menichini, F.; Conforti, F., Inhibition of key enzymes linked to obesity by preparations from Mediterranean dietary plants: effects on α-amylase and pancreatic lipase activities. *Plant Foods for Human Nutrition* **2013,** *68*, 340-346.

120. de Souza, P. M.; de Sales, P. M.; Simeoni, L. A.; Silva, E. C.; Silveira, D.; Magalhaes, P. d. O., Inhibitory activity of α-amylase and α-glucosidase by plant extracts from the brazilian cerrado. *Planta Medica* **2012,** *78*, 393-399.

121. Kasabri, V.; Afifi, F. U.; Hamdan, I., *In vitro* and *in vivo* acute antihyperglycemic effects of five selected indigenous plants from Jordan used in traditional medicine. *Journal of Ethnopharmacology* **2011,** *133*, 888-896.

122. Jemain, M. R. M.; Musa'adah, M. N.; Rohaya, A.; Rashid, L. A.; Hadiani, I. N., *In vitro* antihyperglycaemic effects of some Malaysian plants. *Journal of Tropical Forest Science* **2011,** *23*, 467-472.

123. Ali, H.; Houghton, P. J.; Soumyanath, A., α-amylase inhibitory activity of some malaysian plants used to treat diabetes; with particular reference to *Phyllanthus amarus*. *Journal of Ethnopharmacology* **2006,** *107*, 449-455.

124. Bhandari, M. R.; Jong-Anurakkun, N.; Hong, G.; Kawabata, J., α-Glucosidase and α-amylase inhibitory activities of nepalese medicinal herb pakhanbhed (*Bergenia ciliata*, Haw.). *Food Chemistry* **2008,** *106*, 247-252.

125. Shai, L. J.; Masoko, P.; Mokgotho, M. P.; Magano, S. R.; Mogale, A. M.; Boaduo, N.; Eloff, J. N., Yeast α-glucosidase inhibitory and antioxidant activities of six medicinal plants collected in Phalaborwa, South Africa. *South African Journal of Botany* **2010,** *76*, 465-470.

126. Gurib-Fakim, A., Medicinal plants: traditions of yesterday and drugs of tomorrow. *Molecular Aspects of Medicine* **2006,** *27*, 1-93.

127. Cragg, G. M.; Newman, D. J., Drugs from nature: past achievements, future prospects In *Ethnomedicine and drug discovery*, Iwu, M. M.; Wootton, J., Eds. Elsevier: **2002**; pp 23-37.

128. Truscheit E; Hillebrand I; Junge, B.; Muller, L.; Puls, W.; Schmidt, D., Microbial α-glucosidase inhibitors: Chemistry, biochemistry and therapeutic potential. *Progress in Clinical Biochemistry and Medicine* **1988,** *7*, 17-99.

129. Parenti, F.; Coronelli, C., Members of the genus actinoplanes and their antibiotics *Annual Review of Microbiology* **1979,** *33*, 389-411.

130. Bischoff, H., Pharmacology of α-glucosidase inhibition. *European Journal of Clinical Investigation* **1994,** *24*, 3-10.

131. Hummer, W.; Schreier, P., Analysis of proanthocyanidins. *Mol Nutr Food Res* **2008,** *52*, 1381-98.

132. Souquet, J.-M.; Cheynier, V.; Brossaud, F.; Moutounet, M., Polymeric proanthocyanidins from grape skins. *Phytochemistry* **1996,** *43*, 509-512.

133. Shahat, A. A.; Cos, P.; De Bruyne, T.; Apers, S.; Hammouda, F. M.; Ismail, S. I.; Azzam, S.; Claeys, M.; Goovaerts, E.; Pieters, L.; Vanden Berghe, D.; Vlietinck, A. J., Antiviral and antioxidant activity of flavonoids and proanthocyanidins from *Crataegus sinaica*. *Planta Med* **2002,** *68*, 539-41.

134. Esquenazi, D.; Wigg, M. D.; Miranda, M. M.; Rodrigues, H. M.; Tostes, J. B.; Rozental, S.; da Silva, A. J.; Alviano, C. S., Antimicrobial and antiviral activities of polyphenolics from *Cocos nucifera* Linn. (Palmae) husk fiber extract. *Research in microbiology* **2002,** *153*, 647-52.

135. Tanaka, A.; Ohnishi, M.; Hiromi, K.; Miyata, S.; Murao, S., Static and kinetic- studies on the binding of *Streptomyces trehalase* inhibitor SGI and *Rhizopus* glucoamylase- comparison with glucose and gluconolactone *Journal of Biochemistry* **1982,** *91*, 1-9.

136. Semenza, G.; Balthaza.Ak, Steady-state kinetics of rabbit-intestinal sucrase - kinetic mechanism, Na+ activation, inhibition by tris(hydroxymethyl)aminomethane at glucose subsite *European Journal of Biochemistry* **1974,** *41*, 149-162.

137. Cogoli, A.; Semenza, G., Probable oxocarbonium ion in reaction-mechanism of small intestinal sucrase and isomaltase. *Journal of Biological Chemistry* **1975,** *250*, 7802-7809.

138. Witczak, Z. J., Glycoscience- Chemistry and chemical biology. In *Monosaccharides- properties*, Fraser-Reid, B. O.; Tatsuta, K.; Thiem, J., Eds. Springer: Berlin, **2001**; Vol. 2, pp 885-902.

139. Witczak, Z. J., Thio sugars: Biological relevance as potential new therapeutics. *Current Medicinal Chemistry* **1999,** *6*, 165-178.

140. Sim, L.; Jayakanthan, K.; Mohan, S.; Nasi, R.; Johnston, B. D.; Pinto, B. M.; Rose, D. R., New glucosidase inhibitors from an ayurvedic herbal treatment for type 2 diabetes: structures and inhibition of human intestinal maltse-glucoamylase with compounds from *Salacia reticulata*. *Biochemistry* **2010,** *49*, 443-451.

141. Mohan, S.; Pinto, B. M., Zwitterionic glycosidase inhibitors: salacinol and related analogues. *Carbohydrate Research* **2007,** *342*, 1551-1580.

142. Nasi, R.; Patrick, B. O.; Sim, L.; Rose, D. R.; Pinto, B. M., Studies directed toward the stereochemical structure determination of the naturally occurring glucosidase inhibitor, kotalanol: synthesis and inhibitory activities against human maltase glucoamylase of seven-carbon, chain-extended homologues of salacinol. *Journal of Organic Chemistry* **2008,** *73*, 6172-6181.

143. Li, C. M.; Begum, A.; Numao, S.; Park, K. H.; Withers, S. G.; Brayer, G. D., Acarbose rearrangement mechanism implied by the kinetic and structural analysis of human pancreatic α-amylase in complex with analogues and their elongated counterparts. *Biochemistry* **2005,** *44*, 3347-3357.

144. Mohan, S.; Pinto, B. M., Towards the elusive structure of kotalanol, a naturally occurring glucosidase inhibitor. *Natural Product Reports* **2010,** *27*, 481-488.

145. Cheng, Y. C.; Prusoff, W. H., Relationship between the inhibition constant (Ki) and the concentration of inhibitor which causes 50% Inhibition (IC_{50}) of an enzymatic reaction. *Biochemical pharmacology* **1973,** *22*, 3099-3108.

146. Copeland, R. A., Enzymes: a practical introduction to structure, mechanism and data analysis. In second ed.; Wiley-VCH, Ed. New York, 2000.

147. Chapdelaine, P.; Tremblay, R. R.; Dube, J. Y., *p*-Nitrophenol-α-D-glucopyranoside as substrate for measurement of maltase activity in human semen. *Clinical chemistry* **1978,** *24*, 208-211.

148. Bailey, C. J.; Aschner, P.; Del Prato, S.; LaSalle, J.; Ji, L.; Matthaei, S.; Global Partnership Effective, D., Individualized glycaemic targets and pharmacotherapy in type 2 diabetes. *Diabetes & Vascular Disease Research* **2013,** *10*, 397-409.

149. Wardrop, D. J.; Waidyarachchi, S. L., Synthesis and biological activity of naturally occurring α-glucosidase inhibitors. *Natural Product Reports* **2010,** *27*, 1431-1468.

150. Xiao, J.; Kai, G.; Yamamoto, K.; Chen, X., Advance in dietary polyphenols as α-glucosidases inhibitors: a review on structure-activity relationship aspect. *Critical Reviews in Food Science and Nutrition* **2013,** *53*, 818-836.

151. Williamson, G., Possible effects of dietary polyphenols on sugar absorption and digestion. *Molecular Nutrition & Food Research* **2013,** *57*, 48-57.

152. Huggett, A. S. G.; Nixon, D. A., Use of glucose oxidase, peroxidase and *o*-dianisidine in determination of blood and urinary glucose *Lancet* **1957,** *2*, 368-370.

153. Conyers, S. M.; Kidwell, D. A., Chromogenic substrates for horseradish-peroxidase. *Analytical Biochemistry* **1991,** *192*, 207-211.

154. Cooper, G. R., Methods for determining the amount of glucose in blood. *CRC critical reviews in clinical laboratory sciences* **1973,** *4*, 101-45.

155. Kaufmann-Raab, I.; Jonen, H. G.; Jahnchen, E.; Kahl, G. F.; Groth, U., Interference by acetaminophen in the glucose oxidase-peroxidase method for blood glucose determination. *Clinical chemistry* **1976,** *22*, 1729-31.

156. Nakashima, E.; Nakamura, J.; Hamada, Y.; Koh, N.; Sakakibara, F.; Hotta, N., Interference by gliclazide in the glucose oxidase/peroxidase method for glucose assay. *Diabetes Research and Clinical Practice* **1995,** *30*, 149-152.

157. Fales, F. W., *Glucose (Enzymatic)*. Academic press: New York, **1963**.

158. Shaukat, S.; Waqar, M. A., Green tea phenols interference in the glucose oxidase/peroxidase test *Journal of Food Biochemistry* **2011,** *35*, 1170-1185.

159. Xu, H.; Leng, X.; Wang, M.; Zhang, G., Glucose measurement in the presence of tea polyphenols. *Food Analytical Methods* **2012,** *5*, 1027-1032.

160. Fatmawati, S.; Shimizu, K.; Kondo, R., Ganoderol B: A potent α-glucosidase inhibitor isolated from the fruiting body of *Ganoderma lucidum*. *Phytomedicine : international journal of phytotherapy and phytopharmacology* **2011,** *18*, 1053-5.

161. Brand-Williams, W.; Cuvelier, M. E.; Berset, C., Use of free radical method to evaluate antioxidant activity. *Lebensm Wiss Technology* **1995,** *28*, 25-30.

162. Claiborne, A.; Fridovich, I., Chemical and enzymatic intermediates in the peroxidation of o-dianisidine by horseradish peroxidase. 1. Spectral

properties of the products of dianisidine oxidation. *Biochemistry* **1979,** *18*, 2324-9.

163. Kireyko, A. V.; Veselova, I. A.; Shekhovtsova, T. N., Mechanisms of peroxidase oxidation of *o*-dianisidine, 3,3 ',5,5 '-tetramethylbenzidine, and *o*-phenylenediamine in the presence of sodium dodecyl sulfate. *Russian Journal of Bioorganic Chemistry* **2006,** *32*, 71-77.

164. Miyake, Y.; Yamamoto, K.; Tsujihara, N.; Osawa, T., Protective effects of lemon flavonoids on oxidative stress in diabetic rats. *Lipids* **1998,** *33*, 689-695.

165. Jeon, S. M.; Bok, S. H.; Jang, M. K.; Kim, Y. H.; Nam, K. T.; Jeong, T. S.; Park, Y. B.; Choi, M. S., Comparison of antioxidant effects of naringin and probucol in cholesterol-fed rabbits. *Clinica Chimica Acta* **2002,** *317*, 181-190.

166. Soobrattee, M. A.; Neergheen, V. S.; Luximon-Ramma, A.; Aruoma, O. I.; Bahorun, T., Phenolics as potential antioxidant therapeutic agents: Mechanism and actions. *Mutation Research-Fundamental and Molecular Mechanisms of Mutagenesis* **2005,** *579*, 200-213.

167. Pannala, A. S.; Chan, T. S.; O'Brien, P. J.; Rice-Evans, C. A., Flavonoid B-ring chemistry and antioxidant activity: Fast reaction kinetics. *Biochemical and Biophysical Research Communications* **2001,** *282*, 1161-1168.

168. Seyoum, A.; Asres, K.; El-Fiky, F. K., Structure-radical scavenging activity relationships of flavonoids. *Phytochemistry* **2006,** *67*, 2058-2070.

169. Amic, D.; Davidovic-Amic, D.; Beslo, D.; Trinajstic, N., Structure-radical scavenging activity relationships of flavonoids. *Croatica Chemica Acta* **2003,** *76*, 55-61.

170. Van Acker, S. A. B. E.; De Groot, M. J.; Van Den Berg, D.-J.; Tromp, M. N. J. L.; Den Kelder, G. D.-O.; Van Der Vijgh, W. J. F.; Bast, A., A quantum chemical explanation of the antioxidant activity of flavonoids. *Chemical Research in Toxicology* **1996,** *9*, 1305-1312.

171. Riceevans, C. A.; Miller, N. J.; Bolwell, G. P.; Bramley, P. M.; Pridham, J. B., The relative antioxidant activities of plant-derived polyphenolic flavonoids *Free Radical Research* **1995,** *22*, 375-383.

172. Rasulev, B. F.; Abdullaev, N. D.; Syrov, V. N.; Leszczynski, J., A quantitative structure-activity relationship (QSAR) study of the antioxidant activity of flavonoids. *Qsar & Combinatorial Science* **2005,** *24*, 1056-1065.

173. Cao, G. H.; Sofic, E.; Prior, R. L., Antioxidant and prooxidant behavior of flavonoids: Structure-activity relationships. *Free Radical Biology and Medicine* **1997,** *22*, 749-760.

174. Thavasi, V.; Leong, L. P.; Bettens, R. P., Investigation of the influence of hydroxy groups on the radical scavenging ability of polyphenols. *The journal of physical chemistry A* **2006,** *110*, 4918-23.

175. Liu, T.; Song, L.; Wang, H.; Huang, D., A high-throughput assay for quantification of starch hydrolase inhibition based on turbidity measurement. *Journal of agricultural and food chemistry* **2011,** *59*, 9756-62.

176. Xu, L. W.; Jia, M.; Salchow, R.; Kentsch, M.; Cui, X. J.; Deng, H. Y.; Sun, Z. J.; Kluwe, L., Efficacy and side effects of chinese herbal medicine for menopausal symptoms: a critical review. *Evidence-based complementary and alternative medicine : eCAM* **2012,** *2012*, 568106.

177. Grover, J. K.; Yadav, S.; Vats, V., Medicinal plants of India with anti-diabetic potential. *J Ethnopharmacol* **2002,** *81*, 81-100.

178. Alarcon-Aguilara, F. J.; Roman-Ramos, R.; Perez-Gutierrez, S.; Aguilar-Contreras, A.; Contreras-Weber, C. C.; Flores-Saenz, J. L., Study of the anti-hyperglycemic effect of plants used as antidiabetics. *J Ethnopharmacol* **1998,** *61*, 101-10.

179. Myer, N., The primary source: tropical forests and our future. In 2nd edn ed.; W.W. Norton and Company: New York, **1992**.

180. Bahadoran, Z.; Mirmiran, P.; Azizi, F., Dietary polyphenols as potential nutraceuticals in management of diabetes: a review. *Journal of diabetes and metabolic disorders* **2013,** *12*, 43.

181. Ainsworth, E. A.; Gillespie, K. M., Estimation of total phenolic content and other oxidation substrates in plant tissues using Folin-Ciocalteu reagent. *Nature Protocols* **2007,** *2*, 875-877.

182. Singleton, V. L.; Orthofer, R.; Lamuela-Raventos, R. M., Analysis of total phenols and other oxidation substrates and antioxidants by means of Folin-Ciocalteu reagent. In *Oxidants and Antioxidants, Pt A*, Packer, L., Ed. Elsevier Academic Press Inc: San Diego, **1999**; Vol. 299, pp 152-178.

183. Prior, R. L.; Fan, E.; Ji, H.; Howell, A.; Nio, C.; Payne, M. J.; Reed, J., Multi-laboratory validation of a standard method for quantifying proanthocyanidins in cranberry powders. *Journal of the Science of Food and Agriculture* **2010,** *90*, 1473-1478.

184. Wibowo, A.; Ahmat, N.; Hamzah, A. S.; Sufian, A. S.; Ismail, N. H.; Ahmad, R.; Jaafar, F. M.; Takayama, H., Malaysianol A, a new trimer resveratrol oligomer from the stem bark of Dryobalanops aromatica. *Fitoterapia* **2011,** *82*, 676-681.

185. Syah, Y. M.; Aminah, N. S.; Hakim, E. H.; Aimi, N.; Kitajima, M.; Takayama, H.; Achmad, S. A., Two oligostilbenes, cis- and trans-diptoindonesin B, from Dryobalanops oblongifolia. *Phytochemistry* **2003,** *63*, 913-917.

186. Cheung, H. T.; Wong, C. S., Structures of triterpenes from Dryobalanops aromatica. *Phytochemistry* **1972,** *11*, 1771-1780.

187. Dennis, T. J.; Akshaya Kumar, K., Constituents of *Mesua ferrea*. *Fitoterapia* **1998,** *69*, 291-304.

188. Verotta, L.; Lovaglio, E.; Vidari, G.; Finzi, P. V.; Neri, M. G.; Raimondi, A.; Parapini, S.; Taramelli, D.; Riva, A.; Bombardelli, E., 4-Alkyl- and 4-phenylcoumarins from *Mesua ferrea* as promising multidrug resistant antibacterials. *Phytochemistry* **2004,** *65*, 2867-2879.

189. Govindac.Tr; Pai, B. R.; Subraman.Ps; Rao, U. R.; Muthukum.N, Constituents of *Mesua ferrea* L. 2. ferruol A A new 4-alkylcoumarin *Tetrahedron* **1967,** *23*, 4161.

190. Govindac.Tr; Pai, B. R.; Subraman.Ps; Rao, U. R.; Muthukum.N, Constituents of *Mesua ferrea* L.I. mesuaxanthone A and mesuaxanthone B *Tetrahedron* **1967,** *23*, 243.

191. Chow, Y. L.; Quon, H. H., Chemical constituents of heartwood of *Mesua ferrea*. *Phytochemistry* **1968,** *7*, 1871.

192. Walia, S.; Mukerjee, S. K., Ferrxanthone, A 1,3,5,6- tetraoxygenated xanthone from *Mesua ferrea Phytochemistry* **1984,** *23*, 1816-1817.

193. Pedraza-Chaverri, J.; Cardenas-Rodriguez, N.; Orozco-Ibarra, M.; Perez-Rojas, J. M., Medicinal properties of mangosteen (*Garcinia mangostana*). *Food and chemical toxicology : an international journal published for the British Industrial Biological Research Association* **2008,** *46*, 3227-39.

194. Balasubramanian, K.; Rajagopalan, K., Novel xanthones from *Garcinia mangostana*, structures of BR-xanthone-A and BR-xanthone-B. **1988,** *27*, 1554.

195. Garnett, M.; Sturton, S. D., *Garcinia Mangostana* in the treatment of amoebic dysentery. **1932,** *XLVI*, 973.

196. Mahabusarakam, W.; Wiriyachitra, P.; Taylor, W. C., Chemical constituents of *Garcinia mangostana*. **1987,** *50*, 478.

197. Loo, A. E. K.; Huang, D., Assay-guided fractionation study of α-amylase inhibitors from *Garcinia mangostana* pericarp. *Journal of agricultural and food chemistry* **2007,** *55*, 9805-9810.

198. Ryu, H. W.; Cho, J. K.; Curtis-Long, M. J.; Yuk, H. J.; Kim, Y. S.; Jung, S.; Kim, Y. S.; Lee, B. W.; Park, K. H., α-Glucosidase inhibition and antihyperglycemic activity of prenylated xanthones from *Garcinia mangostana*. *Phytochemistry* **2011,** *72*, 2148-2154.

199. Ross, I. A., Chemical constituents, traditional and modern medicinal uses. In *Medicinal plants of the world*, 2 ed.; Humana Press Inc.: Totowa, NJ, **2005**; Vol. 1.

200. Kumar, A.; Ilavarasan, R.; Jayachandran, T.; Deecaraman, M.; Aravindan, P.; Padmanabhan, N.; Krishan, M. R. V., Anti-diabetic activity of *Syzygium cumini* and its isolated compound against streptozotocin-induced diabetic rats. *Journal of Medicinal Plants Research* **2008,** *2*, 246-249.

201. Alagesan, K.; Thennarasu, P.; Kumar, V.; Sankarnarayanan, S.; Balsamy, T., Identification of α-glucosidase inhibitors from Psidium guajava leaves and *Syzygium cumini* linn. seeds. *International Journal of Pharma Sciences and Research* **2012,** *3*, 316-322.

202. Karthic, K.; Kirthiram, K. S.; Sadasivam, S.; Thayumanavan, B.; Palvannan, T., Identification of α-amylase inhibitors from *Syzygium cumini* Linn seeds. *Indian Journal of Experimental Biology* **2008,** *46*, 677-680.

203. Lim, T. K., *Pachira aquatica* In *Edible medicinal and non-medicinal plants: volume 1, fruits*, Springer Science: **2012**; Vol. 1.

204. Belina-Aldemita, M. D.; Sabularse, V. C.; Dizon, E. I.; Hurtada, W. A.; Torio, M. A. O., Antioxidant properties of bignay *Antidesma bunius* (L.) Spreng. wine at different stages of processing. *Philipp. Agric. Sci.* **2013,** *96*, 308-313.

205. Lawag, I. L.; Aguinaldo, A. M.; Naheed, S.; Mosihuzzaman, M., α-Glucosidase inhibitory activity of selected Philippine plants. *Journal of Ethnopharmacology* **2012,** *144*, 217-219.

206. Samappito, S.; Butkhup, L., An analysis on flavonoids, phenolics and organic acids contents in brewed red wines of both non-skin contact and skin contact fermentation techniques of mao luang ripe fruits (*Antidesma bunius*) harvested from Phupan Valley in Northeast Thailand. *Pakistan Journal of Biological Sciences* **2008,** *11*, 1654-1661.

207. Hui, W. H.; Sung, M. L., An examination of the Euphorbiaceae of Hong Kong. II. The occurrence of epitaraxerol and other triterpenoids. *Australian Journal of Chemistry* **1968,** *21*, 2137-2140.

208. Elya, B.; Malik, A.; Septimahanani, P. I.; Loranza, B., Anti-diabetic activity test by inhibition of α-glucosidase and phytochemical screening from the most active fraction of Buni (*Antidesma bunius* L.) stem, barks and leaves. *International Journal of PharmTech Research* **2012,** *4*, 1667-1671.

209. Prance, G. T., The uses of Atuna racemosa Raf. (Chrysobalanaceae) in Samoa. *Economic Botany* **2004,** *58*, 470-475.

210. Buenz, E. J.; Tillner, J. E., Jr.; Limburg, P.; Bauer, B. A., Antibacterial properties and toxicity of Atuna racemosa extract depend on kernel maturity. *Journal of Ethnopharmacology* **2007,** *111*, 592-597.

211. Sunita, M.; Sarojini, P., *Madhuca Longifolia* (Sapotaceae): a review of its traditional uses and nutritional properties. *International Journal of Humanities and Social Science Invention* **2013,** *2*, 30-36.

212. Dahake, A. P.; Chakma, C. S.; Chakma, R. C.; Bagherwal, P., Antihyperglycemic activity of methanolic extract of *Madhuca longifolia* bark *Diabetologia Croatica* **2010,** *39*, 3-8.

213. Chen, C.-C.; Liu, I. M.; Cheng, J.-T., Improvement of insulin resistance by miracle fruit (*Synsepalum dulcificum*) in fructose-rich chow-fed rats. *Phytotherapy Research* **2006,** *20*, 987-992.

214. Wang, H.-M.; Chou, Y.-T.; Hong, Z.-L.; Chen, H.-A.; Chang, Y.-C.; Yang, W.-L.; Chang, H.-C.; Mai, C.-T.; Chen, C.-Y., Bioconstituents from stems of *Synsepalum dulcificum Daniell* (Sapotaceae) inhibit human melanoma proliferation, reduce mushroom tyrosinase activity and have antioxidant properties. *Journal of the Taiwan Institute of Chemical Engineers* **2011,** *42*, 204-211.

215. Chen, C. Y.; Wang, Y. D.; Wang, H. M., Chemical constituents from the leaves of *Synsepalum dulcificum*. *Chemistry of Natural Compounds* **2010,** *46*, 495-495.

216. Bhadoriya, S. S.; Ganeshpurkar, A.; Narwaria, J.; Gopal, R.; Jain, A. P., *Tamarindus indica* : Extent of explored potential. *Pharmacogn Rev.* **2011,** *5*, 73-81.

217. Maiti, R.; Das, U. K.; Ghosh, D., Attenuation of hyperglycemia and hyperlipidemia in streptozotocin-induced diabetic rats by aqueous extract of seed of *Tamarindus indica*. *Biological & Pharmaceutical Bulletin* **2005,** *28*, 1172-1176.

218. Maiti, R.; Jana, D.; Das, U. K.; Ghosh, D., Antidiabetic effect of aqueous extract of seed of *Tamarindus indica* in streptozotocin-induced diabetic rats. *Journal of Ethnopharmacology* **2004,** *92*, 85-91.

219. Ramchander, T.; Rajkumar, D.; Sravanprasad, M.; Venkateshwarlu, G.; Dhanalakshmi, C. H.; Arjun, Antidiabetic activity of aqueous methanolic extracts of leaf of *Tamarindus indica*. *International Journal of Pharmacognosy and Phytochemical Research* **2012,** *4*, 5-7.

220. Funke, I.; Melzig, M. F., Traditionally used plants in diabetes therapy: Phytotherapeutics as inhibitors of α-amylase activity fitomedicamentos como inibidores da atividade alfa-amilase. *Revista Brasileira de Farmacognosia* **2006,** *16*, 1-5.

221. Khan, A.; Zaman, G.; Anderson, R. A., Bay leaves improve glucose and lipid profile of people with type 2 diabetes. *Journal of Clinical Biochemistry and Nutrition* **2009,** *44*, 52-56.

222. Basak, S. S.; Candan, F., *In vitro* α-amylase inhibition of essential oil obtained from Laurel (*Laurus nobilis L.*) leaves. *Hacettepe Journal of Biology and Chemistry* **2009,** *37*, 41-46.

223. Basak, S. S.; Candan, F., Effect of *Laurus nobilis* L. essential oil and its main components on α-glucosidase and reactive oxygen species scavenging activity. *Iranian Journal of Pharmaceutical Research* **2013,** *12*, 367-379.

224. Luo, X. D.; Wu, S. H.; Ma, Y. B.; Wu, D. G., A new triterpenoid from *Azadirachta indica*. *Fitoterapia* **2000,** *71*, 668-672.

225. Dixit, V. P.; Sinha, R.; Tank, R., Effect of neem seed oil on the blood-glucose concentration of normal and alloxan diabetic rats *Journal of Ethnopharmacology* **1986,** *17*, 95-98.

226. Gupta, S.; Kataria, M.; Gupta, P. K.; Murganandan, S.; Yashroy, R. C., Protective role of extracts of neem seeds in diabetes caused by streptozotocin in rats. *Journal of Ethnopharmacology* **2004,** *90*, 185-189.

227. Perez-Gutierrez, R. M.; Damian-Guzman, M., Meliacinolin: A potent α-glucosidase and α-amylase inhibitor isolated from *Azadirachta indica* leaves and in vivo antidiabetic property in streptozotocin-nicotinamide-induced type 2 diabetes in mice. *Biological & Pharmaceutical Bulletin* **2012,** *35*, 1516-1524.

228. Patil, P. C.; Jadhav, V. D.; Mahadkar, S. D., Pharmacognostical studies on leaf of *Antidesma ghaesembilla* Gaertn, a promising wild edible plant. *Der Pharmacia Sinica* **2013,** *4*, 136-142.

229. Lim, T. K., *Lepisanthes alata*. In *Edible medicinal and non-medicinal plants: volume 6, fruits*, Springer Science: **2013**; Vol. 6.

230. Lim, C. K., Taxonomic notes on *Etlingera Giseke* (Zingiberaceae) in Peninsular Malaysia: the "chasma" taxa and supplementary notes on the "Nicolaia" taxa. *Folia Malaysiana* **2001,** *2*, 141-78.

231. Larsen, K.; Ibrahim, H.; Khaw, S. H.; Saw, L. G., *Gingers of Peninsular Malaysia and Singapore*. Kota Kinabalu: Natural History Publications (Borneo): **1999**; p 135.

232. Noweg, T.; Abdullah, A. R.; Nidang, D., Forest plants as vegetables for communities bordering the Crocket Range National Park. *ASEAN Review of Biodiversity and Environmental Conservation (ARBEC) (January-March)* **2003**, 1-18.

233. Andarwulan, N.; Batari, R.; Sandrasari, D. A.; Bolling, B.; Wijaya, N., Flavonoid content and antioxidant activity of vegetables from Indonesia. *Food Chemistry* **2010,** *121*, 1231-1235.

234. Ibrahim, H.; Setyowati, F. M., *Etlingera*, Plant resources of South-East Asia. **1999,** *13*, 123-26.

235. Williams, C. A.; Harborne, J. B., The leaf flavonoids of the zingiberales. *Biochemical Systematics and Ecology* **1977,** *5*, 221-229.

236. Miean, K. H.; Mohamed, S., Flavonoid (myricetin, quercetin, kaempferol, luteolin, and apigenin) content of edible tropical plants. *Journal of agricultural and food chemistry* **2001,** *49*, 3106-3112.

237. Chan, E. W. C.; Lim, Y. Y.; Wong, S. K.; Lim, K. K.; Tan, S. P.; Lianto, F. S.; Yong, M. Y., Effects of different drying methods on the antioxidant properties of leaves and tea of ginger species. *Food Chemistry* **2009,** *113*, 166-172.

238. Lachumy, S. J. T.; Sasidharan, S.; Sumathy, V.; Zuraini, Z., Pharmacological activity, phytochemical analysis and toxicity of methanol extract of *Etlingera elatior* (torch ginger) flowers. *Asian Pacific Journal of Tropical Medicine* **2010,** *3*, 769-774.

239. Habsah, M.; Ali, M.; Lajis, N. H.; Sukari, M. A.; Yap, Y. H.; Kikuzaki, H.; Nakatani, N., Antitumor promoting and cytotoxic constituents of *Etlingera Elatior*. *Malaysian J Med Sci* **2005,** *12*, 6-12.

240. Haleagrahara, N.; Jackie, T.; Chakravarthi, S.; Rao, M.; Pasupathi, T., Protective effects of Etlingera elatior extract on lead acetate-induced changes in oxidative biomarkers in bone marrow of rats. *Food and chemical toxicology : an international journal published for the British Industrial Biological Research Association* **2010,** *48*, 2688-2694.

241. Jackie, T.; Haleagrahara, N.; Chakravarthi, S., Antioxidant effects of *Etlingera elatior* flower extract against lead acetate - induced perturbations in free radical scavenging enzymes and lipid peroxidation in rats. *BMC Research Notes* **2011,** *4*, 67.

242. Chan, E. W. C.; Lim, Y. Y.; Wong, L. F.; Lianto, F. S.; Wong, S. K.; Lim, K. K.; Joe, C. E.; Lim, T. Y., Antioxidant and tyrosinase inhibition properties of leaves and rhizomes of ginger species. *Food Chemistry* **2008,** *109*, 477-483.

243. Mackeen, M. M.; Ali, A. M.; El-Sharkawy, S. H.; Manap, M. Y.; Salleh, K. M.; Lajis, N. H.; Kawazu, K., Antimicrobial and cytotoxic properties of some Malaysian traditional vegetables (ulam). *International Journal of Pharmacognosy* **1997,** *35*, 174-178.

244. Schafer, A.; Hogger, P., Oligomeric procyanidins of french maritime pine bark extract (Pycnogenol (R)) effectively inhibit α-glucosidase. *Diabetes Research and Clinical Practice* **2007,** *77*, 41-46.

245. Kajdžanoska, M.; Gjamavski, V.; Stefova, M., HPLC-DAD-ESI-MS^n identification of phenolic compounds in cultivated strawberries from Macedonia. *Macedonian Journal of Chemistry and Chemical Engineering* **2010,** *29*, 181-194.

246. Venter, A.; Joubert, E.; de Beer, D., Characterisation of phenolic compounds in South african plum fruits (*Prunus salicina* Lindl.) using HPLC coupled with diode-array, fluorescence, mass spectrometry and on-line antioxidant detection. *Molecules* **2013,** *18*, 5072-5090.

247. Shui, G.; Leong, L. P., Analysis of polyphenolic antioxidants in star fruit using liquid chromatography and mass spectrometry. *Journal of chromatography A* **2004,** *1022*, 67-75.

248. Harbaum, B.; Hubbermann, E. M.; Wolff, C.; Herges, R.; Zhu, Z.; Schwarz, K., Identification of flavonoids and hydroxycinnamic acids in pak choi varieties (*Brassica campestris* L. ssp chinensis var. communis) by HPLC-ESI-MS^n and NMR and their quantification by HPLC-DAD. *Journal of agricultural and food chemistry* **2007,** *55*, 8251-8260.

249. Simirgiotis, M., Antioxidant capacity and HPLC-DAD-MS profiling of Chilean peumo (*Cryptocarya alba*) fruits and comparison with German peumo (*Crataegus monogyna*) from Southern Chile. *Molecules* **2013,** *18*, 2061-2080.

250. Pereira-Caro, G.; Borges, G.; Nagai, C.; Jackson, M. C.; Yokota, T.; Crozier, A.; Ashihara, H., Profiles of phenolic compounds and purine alkaloids during the development of seeds of *Theobroma cacao cv. Trinitario*. *Journal of agricultural and food chemistry* **2012,** *61*, 427-434.

251. Ye, M.; Yang, W.-Z.; Liu, K.-D.; Qiao, X.; Li, B.-J.; Cheng, J.; Feng, J.; Guo, D.-A.; Zhao, Y.-Y., Characterization of flavonoids in *Millettia nitida* var. hirsutissima by HPLC/DAD/ESI-MS^n. *Journal of Pharmaceutical Analysis* **2012,** *2*, 35-42.

252. Clifford, M. N.; Johnston, K. L.; Knight, S.; Kuhnert, N., Hierarchical scheme for LC-MS^n identification of chlorogenic acids. *Journal of agricultural and food chemistry* **2003,** *51*, 2900-11.

253. Parveen, I.; Threadgill, M. D.; Hauck, B.; Donnison, I.; Winters, A., Isolation, identification and quantitation of hydroxycinnamic acid conjugates, potential platform chemicals, in the leaves and stems of *Miscanthus x giganteus* using LC-ESI-MS^n. *Phytochemistry* **2011,** *72*, 2376-84.

254. Wang, H.; Liu, T.; Huang, D., Starch hydrolase inhibitors from edible plants. In *Advances in Food and Nutrition Research, Vol 70*, Henry, J., Ed. **2013**; Vol. 70, pp 103-136.

255. Manach, C.; Williamson, G.; Morand, C.; Scalbert, A.; Remesy, C., Bioavailability and bioefficacy of polyphenols in humans. I. review of 97 bioavailability studies. *American Journal of Clinical Nutrition* **2005,** *81*, 230S-242S.

256. Williamson, G.; Clifford, M. N., Colonic metabolites of berry polyphenols: the missing link to biological activity? *British Journal of Nutrition* **2010,** *104*, S48-S66.

257. Rosak, C.; Mertes, G., Critical evaluation of the role of acarbose in the treatment of diabetes: patient considerations. *Diabetes, metabolic syndrome and obesity : targets and therapy* **2012,** *5*, 357-367.

258. Li, S. J.; Wu, C. H.; Chen, J. X.; Lu, P.; Chen, C.; Fu, M. H.; Fang, J.; Gao, J.; Zhu, L.; Liang, R. X.; Shen, X.; Yang, H. J., An effective solution to discover synergistic drugs for anti-cerebral ischemia from traditional chinese medicinal formulae. *Plos One* **2013,** *8*.

259. Yao, Y.; Zhang, X. D.; Wang, Z. Z.; Zheng, C. L.; Li, P.; Huang, C.; Tao, W. Y.; Xiao, W.; Wang, Y. H.; Huang, L. Q.; Yang, L., Deciphering the combination principles of traditional chinese medicine from a systems pharmacology perspective based on Ma-huang Decoction. *Journal of Ethnopharmacology* **2013,** *150*, 619-638.

260. Akkarachiyasit, S.; Charoenlertkul, P.; Yibchok-anun, S.; Adisakwattana, S., Inhibitory activities of cyanidin and its glycosides and synergistic effect with acarbose against intestinal α-glucosidase and pancreatic α-amylase. *International Journal of Molecular Sciences* **2010,** *11*, 3387-3396.

261. Gao, J.; Xu, P.; Wang, Y.; Wang, Y.; Hochstetter, D., Combined effects of green tea extracts, green tea polyphenols or epigallocatechin gallate with acarbose on inhibition against α-amylase and α-glucosidase *in vitro*. *Molecules* **2013,** *18*, 11614-23.

262. Boath, A. S.; Stewart, D.; McDougall, G. J., Berry components inhibit α-glucosidase in vitro: Synergies between acarbose and polyphenols from black currant and rowanberry. *Food Chemistry* **2012,** *135*, 929-936.

263. Adisakwattana, S.; Lerdsuwankij, O.; Poputtachai, U.; Minipun, A.; Suparpprom, C., Inhibitory activity of cinnamon bark species and their combination effect with acarbose against intestinal α-glucosidase and pancreatic α-amylase. *Plant Foods for Human Nutrition* **2011,** *66*, 143-148.

264. Adisakwattana, S.; Ruengsamran, T.; Kampa, P.; Sompong, W., In vitro inhibitory effects of plant-based foods and their combinations on intestinal α-glucosidase and pancreatic α-amylase. *BMC Complement Altern Med* **2012,** *12*, 110.

265. Vuong, Q. V., Epidemiological evidence linking tea consumption to human health: a review. *Critical Reviews in Food Science and Nutrition* **2014,** *54*, 523-536.

266. Gupta, D.; Bleakley, B.; Gupta, R. K., Dragon's blood: Botany, chemistry and therapeutic uses. *Journal of Ethnopharmacology* **2008,** *115*, 361-380.

267. Chou, T. C., The median-effect principle and the combination index for quantitation of synergism and antagonism in *Synergism and antagonism in chemotherapy*; Academic press; San Diego **1991**; p 61-102.

268. Chou, T.-C., Theoretical basis, experimental design, and computerized simulation of synergism and antagonism in drug combination studies. *Pharmacological Reviews* **2006,** *58*, 621-681.

269. Chou, T. C., Derivation and properties of Michaelis-Menten type and Hill type equations for reference ligands. *Journal of Theoretical Biology* **1976,** *59*, 253-276.

270. Chou, T. C.; Talalay, P., Analysis of combined drug effects - A new look at a very old problem. *Trends in Pharmacological Sciences* **1983,** *4*, 450-454.

271. Qian, M. X.; Haser, R.; Buisson, G.; Duee, E.; Payan, F., The active-center of mammalian α-amylase- structure of the complex of a pancreatic α-amylase with a carbohydrate inhibitor refined to 2.2-angstrom resolution *Biochemistry* **1994,** *33*, 6284-6294.

272. Bliss, C. I., The toxicity of poisons applied jointly. *Annals of Applied Biology* **1939,** *26*, 585-615.

273. Sales, P. M.; Souza, P. M.; Simeoni, L. A.; Silveira, D., α-Amylase inhibitors: a review of raw material and isolated compounds from plant source. *Journal of pharmacy & pharmaceutical sciences : a publication of the Canadian Society for Pharmaceutical Sciences, Societe canadienne des sciences pharmaceutiques* **2012,** *15*, 141-83.

274. Matsui, T.; Ebuchi, S.; Fujise, T.; Abesundara, K. J. M.; Doi, S.; Yamada, H.; Matsumoto, K., Strong antihyperglycemic effects of water-soluble fraction of Brazilian propolis and its bioactive constituent, 3,4,5-tri-*O*-caffeoylquinic acid. *Biological & Pharmaceutical Bulletin* **2004,** *27*, 1797-1803.

275. Shobana, S.; Sreerama, Y. N.; Malleshi, N. G., Composition and enzyme inhibitory properties of finger millet (*Eleusine coracana* L.) seed coat phenolics: Mode of inhibition of α-glucosidase and pancreatic amylase. *Food Chemistry* **2009,** *115*, 1268-1273.

Appendix 1

Table 8. Inhibition activities (IC_{50}) of flavonoids on α-amylase and α-glucosidase by various researchers.

Compound	Reference	Enzyme source	IC_{50} (μM)	Method
Epigallocatechin 3-gallate (EGCG)	**α-glucosidase**			
	Kamiyama *et.al.* (2010)	rat intestine	16	GOP
	Tadera *et.al.*(2006)	rat intestine	(32 %)	GOP (2 % maltose)
	Matsui *et. al.* (2007)	rat intestine	40	GOP/ iAGH assay
	Xu *et.al.*(2013)	rat intestine	914	*p*NPG
	Gamberucci *et.al.*(2006)	rat liver	47.72	*p*NPG
	Yilmazer-musa *et.al.* (2012)	yeast (0.02 U/mL)	0.65	*p*NPG (0.045 mM)
	Li *et. al.* (2007)	yeast (0.2 U/mL)	537.9	*p*NPG (0.3125 mM)
	Gao *et.al.*(2013)	yeast (1 U/mL)	11.5	*p*NPG G (1.25 mM)
	Tadera *et.al.*(2006)	yeast (0.01 mg/mL)	2	*p*NPG (0.147 mM)
	Deng *et.al.* (2014)	yeast (immobilized)	0.67	UHPLC-QTOF MS
	Gamberucci *et.al.*(2006)	rat liver	50.92	4-methylumbelliferyl α-D-glucopyranoside (MUG)
	α-amylase			
	Yilmazer-musa *et.al.* (2012)	Human saliva (0.0025 U/mL)	52.4	DQ starch substrate from enzchek ultra amylase assay kit (5 μg/mL)
	Hara (2001)	Human saliva	260	colorimetric method

	Miao *et.al.*(2014)	Human pancreas	2300	Nelson-Somogyi
	Gao *et.al.*(2013)	Porcine pancreas (0.125 mg/mL)	4033	DNSA (1 % starch)
	Xu *et.al.*(2013)	Porcine pancreas (0.00165 U/mL)	278	Gal-G2-alpha-CNP (1.25 mM)
	Tadera *et.al.*(2006)	Porcine pancreas (0.03 mg/mL)	> 500	*p*-nitrophenyl maltoheptaoside (BPNPG7)
Epicatechin 3-gallate (ECG)	**α-glucosidase**			
	Kamiyama *et.al.* (2010)	rat intestine	40	GOP
	Matsui *et. al.* (2007)	rat intestine	53	GOP/ iAGH assay
	Yilmazer-musa *et.al.* (2012)	yeast (0.02 U/mL)	7.9	*p*NPG (0.045 mM)
	Xu *et.al.*(2013)	rat intestine	1487	*p*NPG
	Deng *et.al.* (2014)	yeast (immobilized)	0.48	UHPLC-QTOF MS
	Gamberucci *et.al.*(2006)	rat liver	15.14	4-methylumbelliferyl α-D-glucopyranoside (MUG)
	Gamberucci *et.al.*(2006)	rat liver	19.06	*p*NPG
	α-amylase			
	Yilmazer-musa *et.al.* (2012)	Human saliva (0.0025 U/mL)	61.03	DQ starch substrate from enzchek ultra amylase assay kit (5 µg/mL)
	Miao *et.al.*(2014)	Human pancreas	1400	Nelson-Somogyi
	Hara (2001)	Human saliva	130	colorimetric method
	Xu *et.al.*(2013)	Porcine pancreas (0.00165 U/mL)	72	Gal-G2-alpha-CNP (1.25 mM)

Gallocatechin 3-gallate (GCG)	**α-glucosidase**			
	Kamiyama *et.al.* (2010)	rat intestine	67	GOP
	Yilmazer-musa *et.al.* (2012)	yeast (0.02 U/mL)	3.1	*p*NPG (0.045 mM)
	Xu *et.al.*(2013)	rat intestine	29	*p*NPG
	Deng *et.al.* (2014)	immobilized yeast AGH	0.59	UHPLC-QTOF MS
	Gamberucci *et.al.*(2006)	Glucosidase II from rat liver	3.5	4-methylumbelliferyl α-D-glucopyranoside (MUG)
	Gamberucci *et.al.*(2006)	Glucosidase II from rat liver	3.7	*p*NPG
	α-amylase			
	Yilmazer-musa *et.al.* (2012)	Human saliva (0.0025 U/mL)	37.1	DQ starch substrate from enzchek ultra amylase assay kit (5 µg/mL)
	Miao *et.al.*(2014)	Human pancreas	1100	Nelson-Somogyi
	Hara (2001)	Human saliva	55	colorimetric method
	Xu *et.al.*(2013)	Porcine pancreas (0.00165 U/mL)	1831	Gal-G2-alpha-CNP (1.25 mM)
Catechin 3-gallate (CG)	**α-glucosidase**			
	Kamiyama *et.al.* (2010)	rat intestine	62	GOP
	α-amylase			
	Hara (2001)	Human saliva	20	Colorimetric method
Epigallocatechin (EGC)	**α-glucosidase**			
	Kamiyama *et.al.* (2010)	rat intestine	120	GOP
	Matsui *et. al.* (2007)	rat intestine	1260	GOP/ iAGH assay
	Yilmazer-musa *et.al.* (2012)	yeast (0.02 U/mL)	ND	*p*NPG (0.045 mM)
	Xu *et.al.*(2013)	rat intestine	ND	*p*NPG
	Deng *et.al.* (2014)	immobilized yeast AGH	560	UHPLC-QTOF MS

	Tadera *et.al.*(2006)	yeast (0.01 mg/mL)	75	*p*NPG (0.147 mM)
	Tadera *et.al.*(2006)	rat intestine	(7 %)	GOP
	Gamberucci *et.al.*(2006)	Glucosidase II from rat liver	117.7	4-methylumbelliferyl α-D-glucopyranoside (MUG)
	Gamberucci *et.al.*(2006)	Glucosidase II from rat liver	110.7	*p*NPG
	α-amylase			
	Yilmazer-musa *et.al.* (2012)	Human saliva (0.0025 U/mL)	ND	DQ starch substrate from enzchek ultra amylase assay kit (5 µg/mL)
	Miao *et.al.*(2014)	Human pancreas	38200	Nelson-Somogyi
	Hara (2001)	Human saliva	>1000	colorimetric method
	Xu *et.al.*(2013)	Porcine pancreas (0.00165 U/mL)	562	Gal-G2-alpha-CNP (1.25 mM)
	Tadera *et.al.*(2006)	Porcine pancreas	> 500	BPNPG7
(-)-Epicatechin (EC)	**α-glucosidase**			
	Kamiyama *et.al.* (2010)	rat intestine	290	GOP
	Matsui *et. al.* (2007)	rat intestine	770	GOP/ iAGH assay
	Yilmazer-musa *et.al.* (2012)	yeast (0.02 U/mL)	>1000	*p*NPG (0.045 mM)
	Xu *et.al.*(2013)	rat intestine	ND	*p*NPG
	Deng *et.al.* (2014)	immobilized yeast AGH	526	UHPLC-QTOF MS
	Tadera *et.al.*(2006)	yeast (0.01 mg/mL)	>200	*p*NPG (0.147 mM)
	Tadera *et.al.*(2006)	rat intestine	(5 %)	GOP
	α-amylase			
	Yilmazer-musa *et.al.* (2012)	Human saliva (0.0025 U/mL)	ND	DQ starch substrate from enzchek ultra amylase assay kit

	Miao *et.al.*(2014)	Human pancreas	40500	Nelson-Somogyi
	Hara (2001)	Human saliva	>1000	colorimetric method
	Xu *et.al.*(2013)	Porcine pancreas (0.00165 U/mL)	314	Gal-G2-alpha-CNP (1.25 mM)
	Tadera *et.al.*(2006)	Porcine pancreas	> 500	BPNPG7
Gallocatechin (GC)	**α-glucosidase**			
	Kamiyama *et.al.* (2010)	rat intestine	320	GOP
	Xu *et.al.*(2013)	rat intestine	ND	*p*NPG
	Gamberucci *et.al.*(2006)	Glucosidase II from rat liver	136.3	4-methylumbelliferyl α-D-glucopyranoside (MUG)
	Gamberucci *et.al.*(2006)	Glucosidase II from rat liver	102.7	*p*NPG
	α-amylase			
	Hara (2001)	Human saliva	>1000	colorimetric method
	Xu *et.al.*(2013)	Porcine pancreas (0.00165 U/mL)	473	Gal-G2-alpha-CNP (1.25 mM)
Catechin (C)	**α-glucosidase**			
	Yilmazer-musa *et.al.* (2012)	yeast (0.02 U/mL)	107	*p*NPG (0.045 mM)
	Xu *et.al.*(2013)	rat intestine	ND	*p*NPG
	Tadera *et.al.*(2006)	yeast (0.01 mg/mL)	>200	*p*NPG (0.147 mM)
	Tadera *et.al.*(2006)	rat intestine	(1 %)	GOP
	Oki *et.al.*(1999)	yeast α-glucosidase	130	*p*NPG
	Oki *et.al.*(1999)	rat intestine	2700	Maltose
	α-amylase			
	Yilmazer-musa *et.al.* (2012)	Human saliva (0.0025 U/mL)	551	DQ starch substrate from enzchek ultra amylase

				assay kit (5 µg/mL)
	Miao *et.al.*(2014)	Human pancreas	45900	Nelson-Somogyi
	Hara (2001)	Human saliva	>1000	colorimetric method
	Xu *et.al.*(2013)	Porcine pancreas (0.00165 U/mL)	637	Gal-G2-alpha-CNP (1.25 mM)
	Tadera *et.al.*(2006)	Porcine pancreas	> 500	BPNPG7
Theaflavins	**α-glucosidase**			
	Matsui *et. al.* (2007)	rat intestine	500	GOP/ iAGH assay
	Hara (2001)	Human saliva	18	colorimetric method
Theaflavin-3-O-gallate	Matsui *et. al.* (2007)	rat intestine	10	GOP/ iAGH assay
	Hara (2001)	Human saliva	1.0	colorimetric method
Theaflavin-3'O-gallate	Matsui *et. al.* (2007)	Rat intestine	136	GOP/ iAGH assay
	Hara (2001)	Human saliva	1.7	colorimetric method
Theaflavin-3,3'-di-O-gallate	Matsui *et. al.* (2007)	Rat intestine	58	GOP/ iAGH assay
	Hara (2001)	Human saliva	0.6	colorimetric method
Theasinensin A	Matsui *et. al.* (2007)	rat intestine	142	GOP/ iAGH assay
Acarbose	**α-glucosidase**			
	Matsui *et. al.* (2007)	rat intestine	0.43	GOP/ iAGH assay
	Ani & Naidu (2008)	rat intestine	0.0003	GOP (6 mM)
	Ani & Naidu (2008)	rat intestine	0.18	*p*NPG (0.35 mM)
	Oki *et.al.* (1999)	rat intestine (0.032 U/mL)	63	*p*NPG (1.2 mM)
	Kim *et. al.* (2010)	Bacterial (*B. stearothermopillus*) (0.025 U/mL)	3.25	*p*NPG (0.3 mM)
	Yilmazer-musa *et.al.* (2012)	yeast (0.02 U/mL)	141	*p*NPG (0.045 mM)
	Li *et. al.* (2007)	yeast (0.2 U/mL)	242	*p*NPG (0.3125 mM)

Wu *et. al.* (2013)	yeast (0.6 U/mL)	217	*p*NPG (7.8 mM)
Takahashi & Miyazawa (2012)	yeast (0.02 U/mL)	907.5	*p*NPG (0.25 mM)
Choi *et. al.* (2010)	yeast (0.32 U/mL)	9110	*p*NPG (2.3 mM)
Oki *et.al.* (1999)	pig intestine	87	*p*NPG (1.2 mM)
Oki *et.al.* (1999)	rabbit intestine	62	*p*NPG (1.2 mM)
α-amylase			
Piparo *et.al.*(2008)	Human saliva (0.18 µM)	0.996	Nelson-Somogyi (0.15 µg)
Yilmazer-musa *et.al.* (2012)	Human saliva (0.0025 U/mL)	10.7	DQ starch substrate from enzchek ultra amylase assay kit (5 µg/mL)
Grussu *et. al.* (2011)	Porcine pancreas (0.38 mg/mL)	1.24	DNSA (0.3 %)
Sudha *et. al.* (2011)	Porcine pancreas (0.01 U/mL)	15.8	DNSA (0.25 %)
Funke & Melzig (2005)	Porcine pancreas (25 U/mL)	23	p-Nitrophenyl-α-d-maltopentaoside (PNPG5) (18.75 mM)

Appendix 2

Kaempferol-3-*O*-glucoside (1)

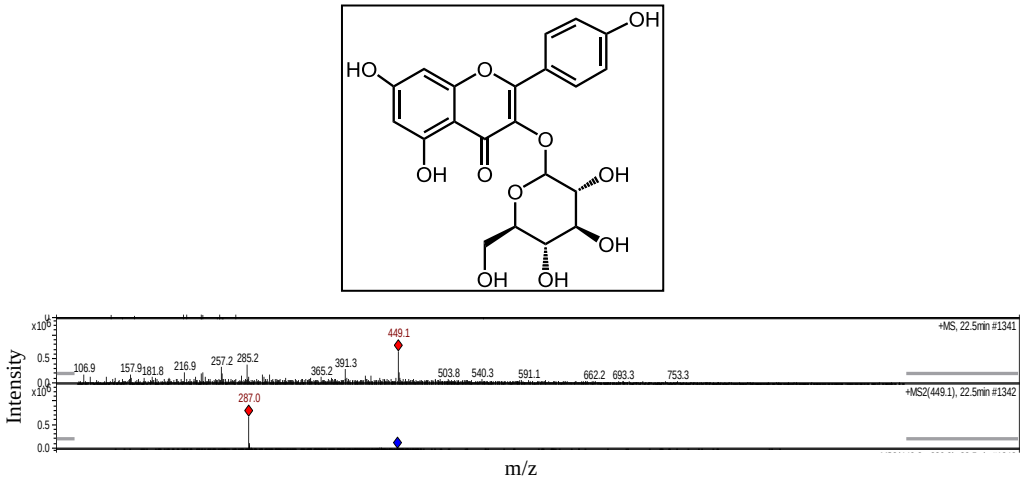

Figure 35. Mass spectra from LC-MS analysis of peak 1 of fraction 10 (kaempferol-3-*O*-glucoside).

Procyanidin B1 (2)

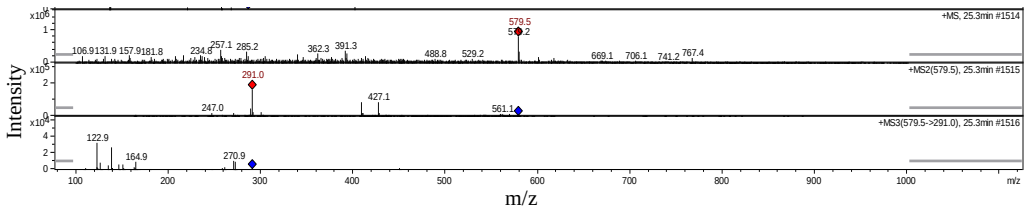

Figure 36. Mass spectra from LC-MS analysis of peak 2 of fraction 10 (procyanidin B1).

Epi(catechin) (3)

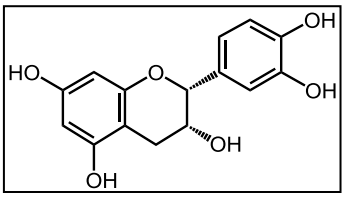

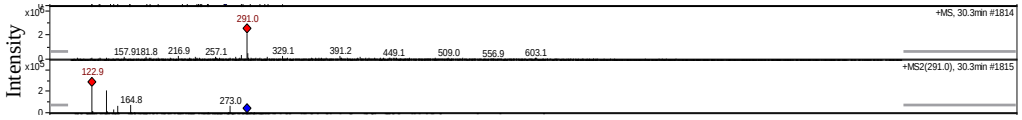

Figure 37. Mass spectra from LC-MS analysis of peak 3 of fraction 10 (possibly epi(catechin)).

Quercetin-3,4'-O-di-beta-glucopyranoside (4)

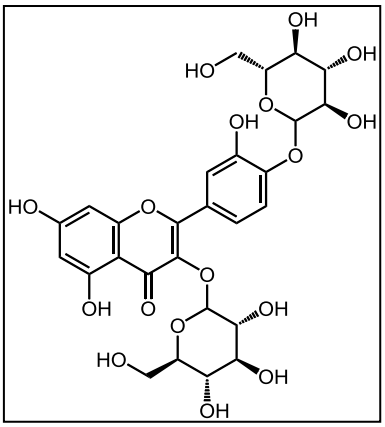

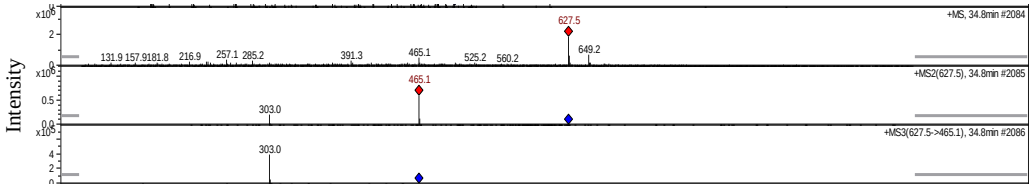

Figure 38. Mass spectra from LC-MS analysis of peak 4 of fraction 10 (Quercetin-3,4'-O-di-beta-glucopyranoside).

Monocaffeoylquinic acid (5)

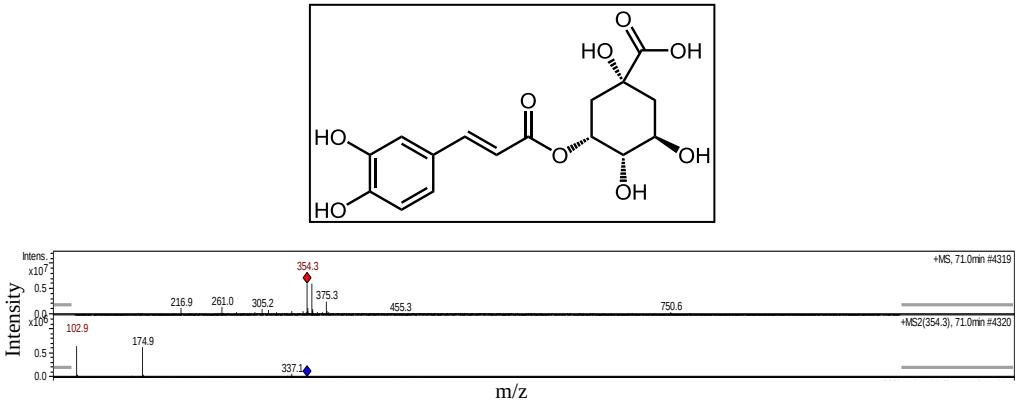

Figure 39. Mass spectra from LC-MS analysis of peak 5 of fraction 10 (monocaffeoylquinic acid).

Diconiferyl alcohol glucoside/ alaschanioside C (6)

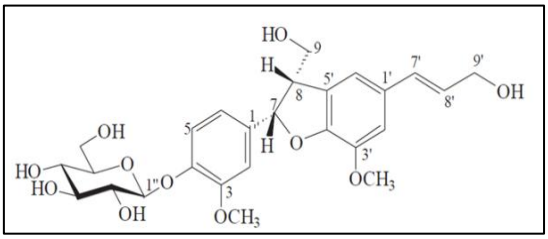

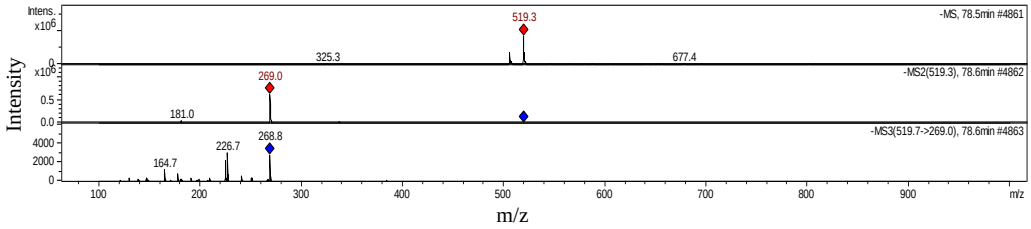

Figure 40. Mass spectra from LC-MS analysis of peak 6 of fraction 10 (diconiferyl alcohol glucoside/ alaschanioside C).

Feruloyl quinate (7)

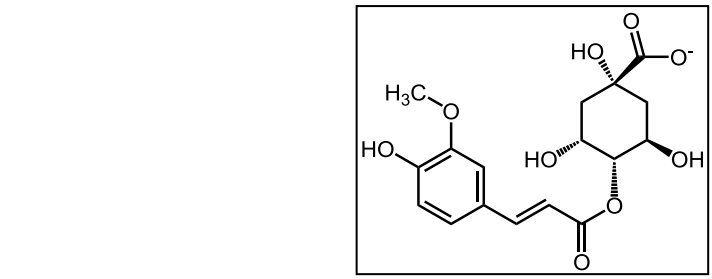

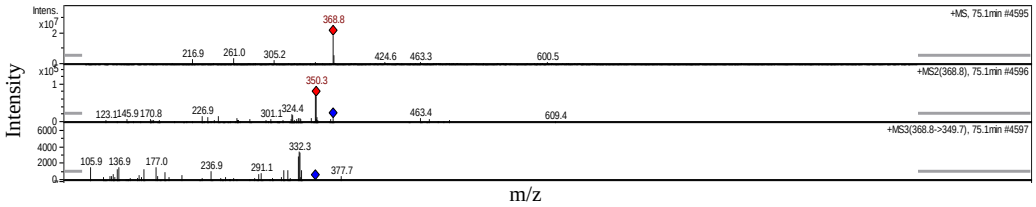

Figure 41. Mass spectra from LC-MS analysis of peak 7 of fraction 10 (feruloyl quinate).

Feruloyl malate (4-O-8 coupled) coniferyl alcohol (8)

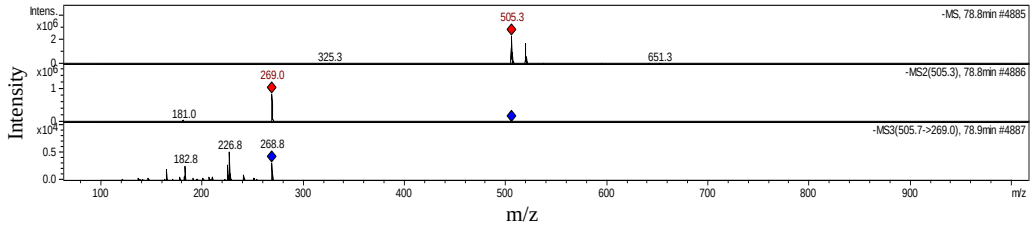

Figure 42. Mass spectra from LC-MS analysis of peak 8 of fraction 10 (possibly feruloyl malate (4-O-8 coupled) coniferyl alcohol).

Appendix 3

Coumaroyl aspartate (9)

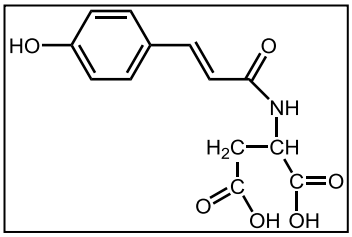

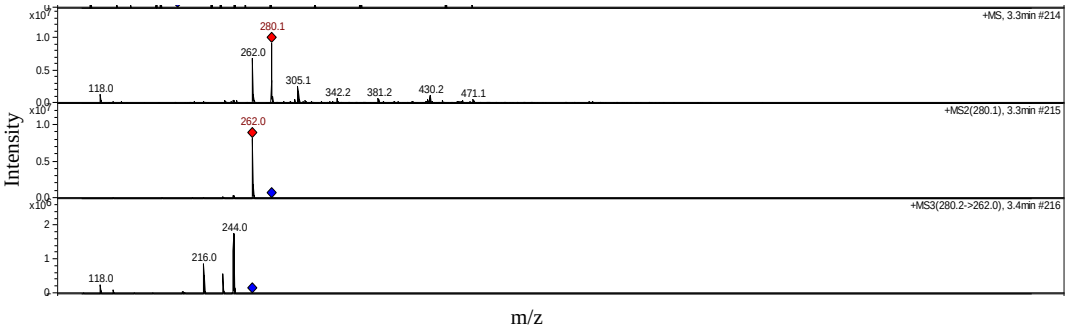

Figure 43. Mass spectra from LC-MS analysis of peak 9 of fraction 12 (coumaroyl aspartate).

1,7-bis (4-hydroxyphenyl)-1,4,6-heptatrien-3-one (10)

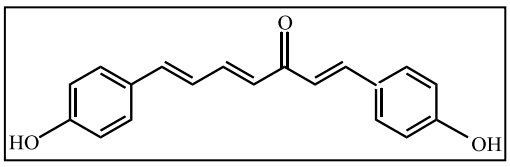

Figure 44. Mass spectra from LC-MS analysis of peak 10 of fraction 12 (1,7-bis (4-hydroxyphenyl)-1,4,6-heptatrien-3-one).

Genistein (11)

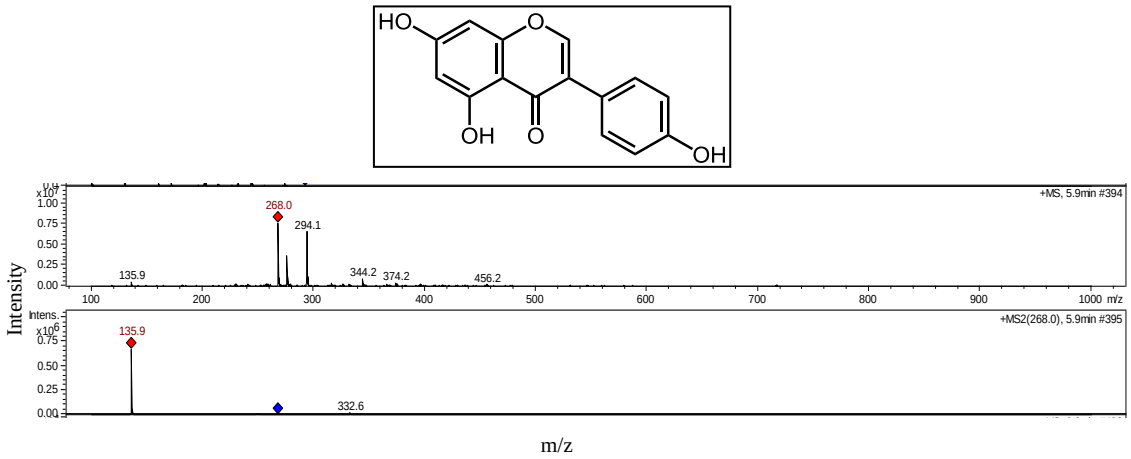

Figure 45. Mass spectra from LC-MS analysis of peak 11 of fraction 12 (genistein).

Dicaffeoylquinic acid (14)

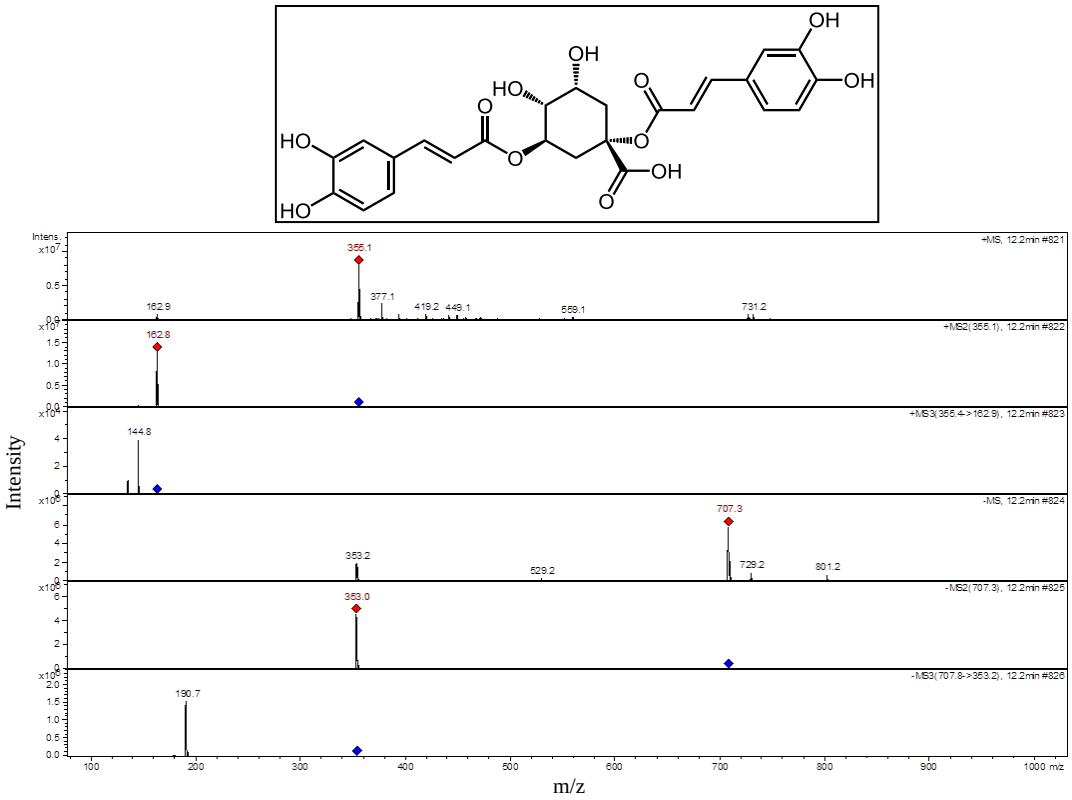

Figure 46. Mass spectra from LC-MS analysis of peak 14 of fraction 12 (dicaffeoylquinic acid).

β-stigmasterol (15)

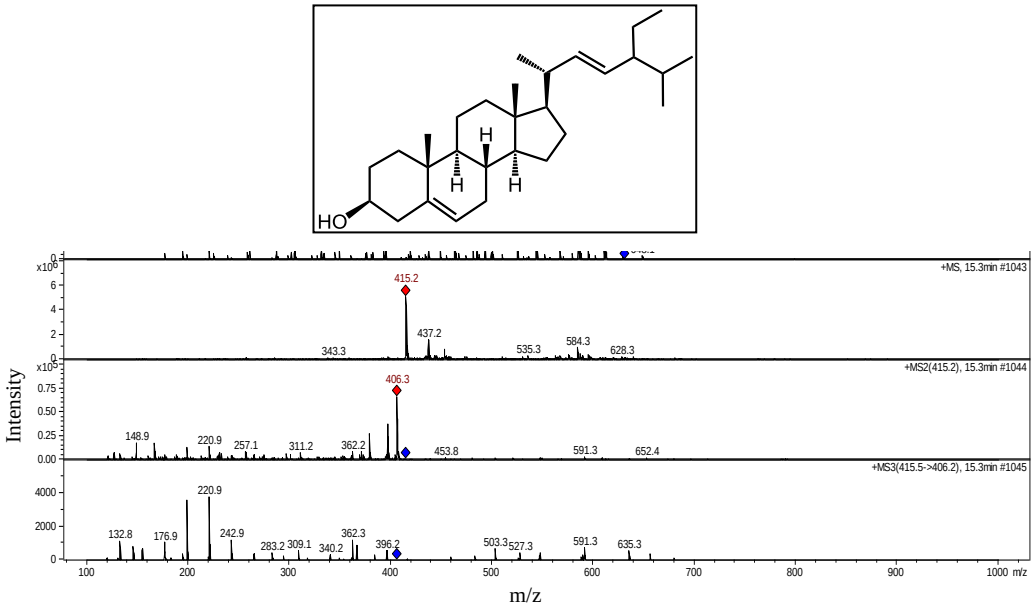

Figure 47. Mass spectra from LC-MS analysis of peak 15 of fraction 12 (β-stigmasterol).